

**ANKARA YILDIRIM BEYAZIT UNIVERSITY**  
**GRADUATE SCHOOL OF NATURAL AND APPLIED SCIENCES**



**THE EFFECTS OF CUTTING CONDITIONS ON CUTTING  
TEMPERATURE AND HOLE QUALITY IN DRILLING OF  
INCONEL 718 USING SOLID CARBIDE DRILLS**

**M.Sc. Thesis by**

**Necati UÇAK**

**Department of Mechanical Engineering**

**July, 2017**

**ANKARA**

**THE EFFECTS OF CUTTING CONDITIONS ON  
CUTTING TEMPERATURE AND HOLE QUALITY IN  
DRILLING OF INCONEL 718 USING SOLID CARBIDE  
DRILLS**

**A Thesis Submitted to**

**The Graduate School of Natural and Applied Sciences of**

**Ankara Yıldırım Beyazıt University**

**In Partial Fulfillment of the Requirements for the Degree of Master of Science  
in Mechanical Engineering, Department of Mechanical Engineering**

**by**

**Necati UÇAK**

**July, 2017**

**ANKARA**

## M.Sc. THESIS EXAMINATION RESULT FORM

We have read the thesis entitled “**THE EFFECTS OF CUTTING CONDITIONS ON CUTTING TEMPERATURE AND HOLE QUALITY IN DRILLING OF INCONEL 718 USING SOLID CARBIDE DRILLS**” completed by **NECATİ UÇAK** under the supervision of **PROF. DR. ADEM ÇİÇEK** and we certify that in our opinion it is fully adequate, in scope and in quality, as a thesis for the degree of Master of Science.

Prof. Dr. Adem ÇİÇEK

Supervisor

Prof. Dr. Kubilay ASLANTAŞ

Jury Member

Asst. Prof. Dr. İhsan TOKTAŞ

Jury Member

Prof. Dr. Fatih V. ÇELEBİ

Director

Graduate School of Natural and Applied Sciences

## ETHICAL DECLARATION

I hereby declare that, in this thesis which has been prepared in accordance with the Thesis Writing Manual of Graduate School of Natural and Applied Sciences,

- All data, information and documents are obtained in the framework of academic and ethical rules,
- All information, documents and assessments are presented in accordance with scientific ethics and morals,
- All the materials that have been utilized are fully cited and referenced,
- No change has been made on the utilized materials,
- All the works presented are original,

and in any contrary case of above statements, I accept to renounce all my legal rights.

21.07.2017

Necati UÇAK

## **ACKNOWLEDGMENTS**

First and foremost, I would like to express my sincere gratitude to my supervisor Prof. Dr. Adem ÇİÇEK for his guidance and encouragement throughout this study. At all stages of this research work I benefited from his immense knowledge and valuable advice. His positive outlook and confidence in my research inspired me and gave me confidence.

I also would like to thank Gazi University, Technology Faculty, Department of Manufacturing Engineering for providing me the laboratory facilities and equipment to perform my study. Also, many thanks to Dr. Gültekin UZUN for his guidance during experimental tests. Besides, I am grateful to Ermaksan Dişli Co. for their technical support during hole diameter measurements.

Also, I am grateful to my dear friends Polat KURT, Ahmet Yasin SEDEF, Gökan YİĞİT and Semih AĞCA for their excellent contributions and technical helps during the tests and measurements.

I also would like to thank Ankara Yıldırım Beyazıt University Scientific Research Project Division for financial support to the Project No: 3578.

Finally, I would especially want to thank my family for their endless love and understanding over the years. This accomplishment would not have been possible without them. Thank you.

**2017, 21 July**

**Necati UÇAK**

# **THE EFFECTS OF CUTTING CONDITIONS ON CUTTING TEMPERATURE AND HOLE QUALITY IN DRILLING OF INCONEL 718 USING SOLID CARBIDE DRILLS**

## **ABSTRACT**

In this study, the drillability of Inconel 718, a nickel-based superalloy, which is frequently used in aerospace industry due to its superior mechanical and physical properties, was experimentally investigated under different cutting and cooling/lubrication conditions. Drilling tests were performed at 2 different cutting speeds (10, 15 m/min) and a constant feed (0.02 mm/rev) using TiAlN coated and uncoated solid carbide twist drills with diameter of 5 mm. The effects of cooling/lubricating conditions and coating material on drillability of Inconel 718 were evaluated in terms of the generated thrust force, torque, cutting temperature, hole quality (including surface roughness, hole diameter and roundness error, burr formation at the entrance and the exit of the hole, machined subsurface changes) and tool wear. Experimental results showed that different cooling/lubrication conditions have significant effects on all performance criteria. Cryogenic cooling significantly reduced the cutting temperatures. Generally, cryogenic drilling exhibited better performance on hole quality and surface integrity with less burr formation at the entrance and the exit of the hole, more accurate hole diameter, less roundness error, better machined subsurface quality, etc. However, it was determined that cryogenic conditions increased the thrust force and significantly reduced the tool life due to excessive chippings. Experiments under dry conditions did not show any superior performance to other conditions. Good surface roughness values and tool life were achieved in drilling test under wet conditions. The increased cutting speed improved the cutting performance, especially in cryogenic conditions. The use of the coating material (TiAlN) also reduced the tool wear dramatically.

**Keywords:** Inconel 718, cryogenic drilling, cutting temperature, hole quality, tool wear, thrust force.

# INCONEL 718'İN KARBÜR MATKAPLAR KULLANILARAK DELİNMESİNDE KESME ŞARTLARININ KESME SICAKLIĞINA VE DELİK KALİTESİNE ETKİLERİ

## ÖZ

Bu çalışmada, üstün mekanik ve fiziksel özellikleri nedeniyle özellikle havacılık endüstrisinde sıklıkla kullanılan, bir nikel bazlı süper alaşım olan Inconel 718'in farklı kesme ve soğutma/yağlama koşullarında delinebilirliği deneysel olarak araştırılmıştır. Delme deneyleri, 5 mm çapındaki TiAlN kaplamalı ve kaplamasız karbür matkap uçları kullanılarak 2 farklı kesme hızı (10, 15 m/min) ve sabit bir ilerleme (0.02 mm/dev) değerinde gerçekleştirilmiştir. Soğutma/yağlama şartlarının ve kaplama malzemesinin Inconel 718'in delinebilirliği üzerine etkileri, aksel kuvvet, tork, kesme sıcaklığı, delik kalitesi (yüzey pürüzlülüğü, delik çapı ve yuvarlaklık hatası, delik girişinde ve çıkışında çapak oluşumu, işlenmiş yüzey altı değişimlerini kapsayan) ve takım aşınması açısından değerlendirilmiştir. Deney sonuçları farklı soğutma/yağlama ortamlarının tüm performans kriterleri üzerinde önemli bir etkisi olduğunu göstermiştir. Kriyojenik soğutma ile kesme sıcaklıkları önemli ölçüde azalmıştır. Genel olarak kriyojenik delik delmenin, delik girişinde ve çıkışında çapak oluşumunu azalttığı, nominal çapa daha yakın çap değerleri verdiği, deliklerin yuvarlaklık hatasını azalttığı, deliğin yüzey altı kalitesini arttırdığı, vb. ile daha iyi delik kalitesi ve yüzey bütünlüğü sağladığı tespit edilmiştir. Ancak kriyojenik şartların aksel kuvveti arttırdığı ve takım ömrünü önemli ölçüde düşürdüğü belirlenmiştir. Kuru şartlarda gerçekleştirilen deneyler diğer şartlara göre performans kriterleri bakımından herhangi bir üstünlük gösterememiştir. İyi yüzey pürüzlülüğü değerleri ve düzenli takım aşınması ıslak şartlarda gerçekleştirilen delme deneylerinde elde edilmiştir. Kesme hızının artması özellikle kriyojenik şartlarda delme performansını arttırmıştır. Kaplama malzemesinin kullanımı takım aşınmasını önemli derecede azaltmıştır.

**Anahtar Kelimeler:** Inconel 718, kriyojenik delme, kesme sıcaklığı, delik kalitesi, takım aşınması, aksel kuvvet.

## CONTENTS

M.Sc. THESIS EXAMINATION RESULT FORM .....	ii
ETHICAL DECLARATION .....	iii
ACKNOWLEDGMENTS .....	iv
ABSTRACT .....	v
ÖZ .....	vi
NOMENCLATURE .....	ix
LIST OF TABLES .....	xi
LIST OF FIGURES .....	xii
<b>CHAPTER 1 - INTRODUCTION.....</b>	<b>1</b>
1.1 Superalloys .....	3
1.1.1 Classification of Superalloys .....	4
1.2 General Properties of Inconel 718.....	7
1.2.1 Machinability of Inconel 718 .....	8
1.3 Metal Cutting Processes .....	9
1.3.1 Drilling Operation.....	9
1.4 Literature Review .....	26
1.5 Aim of The Study .....	36
<b>CHAPTER 2 - EXPERIMENTAL SETUP AND PROCEDURE .....</b>	<b>37</b>
2.1 Workpiece Material .....	38
2.2 Cutting Tools .....	38
2.3 Experimental Setup and Cutting Conditions .....	39
2.4 Cutting Force and Torque .....	42
2.5 Cutting Temperature .....	43
2.6 Surface Roughness .....	45
2.7 Hole Diameter and Roundness Error.....	46
2.8 Burr Formation .....	48
2.9 Microstructural Examination and Microhardness .....	49
2.10 Tool Wear.....	52
<b>CHAPTER 3 - RESULTS AND DISCUSSION .....</b>	<b>53</b>
3.1 Cutting Force and Torque .....	53
3.2 Cutting Temperature .....	56



3.3 Surface Roughness .....	58
3.4 Hole Diameter and Roundness Error.....	60
3.5 Burr Formation .....	62
3.6 Microstructural Examination and Microhardness .....	64
3.7 Tool Wear.....	68
<b>CHAPTER 4 - CONCLUSION AND FUTURE WORK.....</b>	<b>74</b>
4.1 Summary of The Present Study.....	74
4.2 Future Work.....	75
<b>REFERENCES.....</b>	<b>77</b>
<b>APPENDIX .....</b>	<b>87</b>
Appendix A – Certificate of the workpiece material Inconel 718.....	88
<b>CURRICULUM VITAE .....</b>	<b>93</b>

## NOMENCLATURE

### Roman Letter Symbols

$A_c$	Chip cross-sectional area, $\text{mm}^2$
$b$	Thickness of cut chip, mm
$D$	Diameter of the drill, mm
$f$	Feed, mm/rev
$F_a$	Thrust force, N
$f_r$	Feed rate, mm/min
$F_r$	Radial force, N
$F_v$	Circumferential force, N
$h$	Width of cut chip, mm
$k_s$	Specific cutting resistance, $\text{N}/\text{mm}^2$
$l$	Cutoff length, $\mu\text{m}$
$M$	Drilling torque, N mm
$M_r$	Drilling torque due to the radial force, N mm
$M_v$	Drilling torque due to the circumferential force, N mm
$n$	Number of deviations
$N$	Spindle speed, rev/min
$N_c$	Main drilling power, kW
$N_{fd}$	Feed power, kW
$N_m$	Motor power, kW
$n_m$	Mechanical efficiency of employed drilling machine
$N_t$	Total drilling power, kW
$R_a$	Average surface roughness, $\mu\text{m}$
$R_{MR}$	Material removal rate, $\text{mm}^3/\text{min}$
$v$	Cutting speed, m/min
$w$	Half of the web thickness, mm
$y$	Vertical deviations, $\mu\text{m}$

### **Greek Letter Symbols**

$\beta_o$	Helix angle, °
$\kappa_t$	Taper angle, °
$\chi$	Lip angle, °

### **Acronyms**

BUE	Built-up Edge
CF	Catastrophic Failure
CMM	Coordinate Measuring Machine
CNC	Computer Numerical Control
HRB	Hardness Rockwell measured on the B scale
HV	Hardness Vickers
GW	Gradual Wear
LN <sub>2</sub>	Liquid Nitrogen
LSC	Least Square Circle
MCC	Minimum Circumscribed Circle
MIC	Maximum Inscribed Circle
MQL	Minimum Quantity Lubrication
MZC	Minimal Zone Circle
SEM	Scanning Electron Microscope
TiAlN	Titanium Aluminum Nitride

## LIST OF TABLES

<b>Table 1.1</b> Chemical compositions limits of Inconel 718 and functions of some notable elements.....	7
<b>Table 2.1</b> Chemical composition of the Inconel 718.....	38
<b>Table 2.2</b> Some mechanical and physical properties of the Inconel 718 .....	38
<b>Table 2.3</b> Selected properties of the twist drills .....	39
<b>Table 2.4</b> Technical specifications of the CNC vertical machining center .....	39
<b>Table 2.5</b> Cutting conditions for the drilling tests.....	40
<b>Table 2.6</b> Technical specifications of Kistler 9272 4-component dynamometer.....	42
<b>Table 2.7</b> Technical specifications of Kistler 5070A01100 multichannel charge amplifier.....	43
<b>Table 2.8</b> Technical properties of Elimko E-PR-110 data logger .....	44

## LIST OF FIGURES

<b>Figure 1.1</b> A typical aero-engine with component materials and working temperatures. ....	3
<b>Figure 1.2</b> Some typical superalloys .....	5
<b>Figure 1.3</b> Components and materials of Rolls-Royce XWB Turbofan engine.....	6
<b>Figure 1.4</b> Comparison of the machinability ratings of some materials .....	8
<b>Figure 1.5</b> Geometry of a twist drill.....	10
<b>Figure 1.6</b> Cutting actions along the diameter of a twist drill.....	11
<b>Figure 1.7</b> Cutting force components in the drilling process .....	13
<b>Figure 1.8</b> Factors affecting the drill forces .....	15
<b>Figure 1.9</b> Characteristic wear types and wear regions of a twist drill.....	16
<b>Figure 1.10</b> The different wear types on the carbide drills .....	18
<b>Figure 1.11</b> The flank wear measurement on a twist drill.....	19
<b>Figure 1.12</b> The common cutting temperature measurement methods in drilling operation a) thermocouple insertion into the workpiece, b) thermocouple insertion into the cutting tool .....	20
<b>Figure 1.13</b> Impacts of coolants on a cutting process .....	21
<b>Figure 1.14</b> Cryogenic cooling strategies.....	22
<b>Figure 1.15</b> Cryogenic cooling setup for a milling operation .....	22
<b>Figure 1.16</b> Error types in drilling operations .....	24
<b>Figure 1.17</b> The average surface roughness .....	24
<b>Figure 1.18</b> a) uniform burr with drill cap b) crown burr .....	25
<b>Figure 1.19</b> Subsurface microstructures resulting from a) drilling b) mill boring....	27
<b>Figure 1.20</b> Tool life performance of different type coating materials.....	28
<b>Figure 1.21</b> Wear progress in drilling Inconel 718 .....	28
<b>Figure 1.22</b> Effects of coating material and cutting fluid on drill life in drilling of Inconel 718.....	29
<b>Figure 1.23</b> Machined subsurface microstructures under a) dry, b) wet, and c) cryogenic milling conditions.....	31
<b>Figure 1.24</b> Cryogenic cooling application of the study .....	33
<b>Figure 1.25</b> Experimental setup of the study.....	34
<b>Figure 1.26</b> Tool wear examination of the study .....	35
<b>Figure 1.27</b> Temperature distribution under $v_c=10$ m/min, $f=0.11$ mm cutting conditions a) wet , b) LN <sub>2</sub> .....	36

<b>Figure 2.1</b> Schematic representation of examination and measurement methods in the study. ....	37
<b>Figure 2.2</b> The dimensions of the tungsten carbide twist drills. ....	39
<b>Figure 2.3</b> Experimental setup. ....	41
<b>Figure 2.4</b> Positions of the test holes and thermocouple holes on the specimen. ....	41
<b>Figure 2.5</b> Measurement setup for cutting temperature. ....	44
<b>Figure 2.6</b> SEM and digital microscope images of the cross section of the workpiece showing positions and dimensions of thermocouple holes. ....	45
<b>Figure 2.7</b> Surface roughness measurement. ....	46
<b>Figure 2.8</b> Hole diameter and roughness error measurement. ....	47
<b>Figure 2.9</b> LSC method for roundness error measurement. ....	48
<b>Figure 2.10</b> Burr height measurement. ....	48
<b>Figure 2.11</b> Grinding and polishing equipment. ....	49
<b>Figure 2.12</b> Optical microscope. ....	50
<b>Figure 2.13</b> Microstructure of Inconel 718 used in the tests. ....	50
<b>Figure 2.14</b> Vickers hardness tester. ....	51
<b>Figure 2.15</b> Microhardness measurements. ....	51
<b>Figure 2.16</b> Measurement of the tool wear on a digital microscope. ....	52
<b>Figure 3.1</b> Thrust force values at cutting speeds of a) 10 m/min, and b) 15 m/min. ....	54
<b>Figure 3.2</b> Torque values at a) 10 m/min, and b) 15 m/min cutting speeds. ....	55
<b>Figure 3.3</b> Cutting temperature values under different machining conditions at 10 m/min. ....	56
<b>Figure 3.4</b> Cutting temperature values under different machining conditions at 15 m/min. ....	57
<b>Figure 3.5</b> Surface roughness values at a) 10 m/min and b) 15 m/min cutting speeds. ....	59
<b>Figure 3.6</b> Cross-sectional SEM images of the holes under different cutting conditions. ....	60
<b>Figure 3.7</b> Hole diameter values at a) 10 m/min and b) 15 m/min cutting speeds. ....	60
<b>Figure 3.8</b> Roundness error values at a) 10 m/min and b) 15 m/min cutting speeds. ....	61
<b>Figure 3.9</b> Burr height values at the entrance at a) 10 m/min and b) 15 m/min cutting speeds. ....	63
<b>Figure 3.10</b> Burr height values at the exit at a) 10 m/min and b) 15 m/min cutting speeds. ....	63
<b>Figure 3.11</b> The most common burr types at the exit surface of the holes: a) uniform burr and b) uniform burr with drill cap. ....	64

<b>Figure 3.12</b> Plastic deformation zone beneath the hole surface at 10 m/min with uncoated twist drill under different cutting environments. ....	65
<b>Figure 3.13</b> Plastic deformation zone beneath the hole surface at 15 m/min with uncoated twist drill under different cutting environments. ....	65
<b>Figure 3.14</b> Plastic deformation zone beneath the hole surface at 10 m/min with TiAlN coated twist drill under different cutting environments.....	66
<b>Figure 3.15</b> Plastic deformation zone beneath the hole surface at 15 m/min with TiAlN coated twist drill under different cutting environments.....	66
<b>Figure 3.16</b> Microhardness values beneath the hole surface under different cooling/lubricating environments with uncoated twist drill at 10 m/min. ....	67
<b>Figure 3.17</b> Microhardness values beneath the hole surface under different cooling/lubricating environments with uncoated twist drill at 15 m/min. ....	67
<b>Figure 3.18</b> Microhardness values beneath the hole surface under different cooling/lubricating environments with TiAlN coated twist drill at 10 m/min.....	68
<b>Figure 3.19</b> Microhardness values beneath the hole surface under different cooling/lubricating environments with TiAlN coated twist drill at 15 m/min.....	68
<b>Figure 3.20.</b> Tool wear types on uncoated twist drill after three holes at 10 m/min under dry conditions.....	69
<b>Figure 3.21</b> Tool wear types on uncoated twist drill after two holes at 10 m/min under cryogenic conditions. ....	70
<b>Figure 3.22</b> Tool wear types on uncoated twist drill after three holes at 10 m/min under wet conditions. ....	70
<b>Figure 3.23</b> Tool wear types on TiAlN coated twist drill after three holes at 15 m/min under dry conditions. ....	71
<b>Figure 3.24</b> Tool wear types on TiAlN coated twist drill after three holes at 15 m/min under cryogenic conditions.....	71
<b>Figure 3.25</b> Tool wear types on TiAlN coated twist drill after three holes at 15 m/min under wet conditions.....	72
<b>Figure 3.26</b> Comparison of tool performances under different cutting conditions...	73
<b>Figure 3.27</b> Tool wear types on uncoated twist drill after fifty holes under wet conditions. ....	73
<b>Figure 3.28</b> Tool wear types on TiAlN coated twist drill after fifty holes under wet conditions. ....	73

# CHAPTER 1

## INTRODUCTION

Technology can be described as application of science to obtain needed or desired things for human civilization. At this point, manufacturing is one of the essential factors that make technology feasible [1]. Thus, it is possible to obtain desired parts using necessary machining techniques such as turning, milling, drilling, etc. Economically, machining operations consume a great quantity of money worldwide. Besides, this quantity is greater for machining of difficult-to-cut materials such as superalloys. However, it is proposed that it is possible to save this consumption up to 20 % by choosing the suitable cutting tool and machining conditions for related machining operations [2].

Nowadays, nickel-based superalloys have a great importance in critical applications such as aerospace, nuclear, marine, chemical, and medical industries thanks to their superior mechanical and physical properties such as ideal toughness, hot hardness, thermal expansion, ductility, melting point, resistance to corrosion, thermal shock resistance, and thermal fatigue strength. They can maintain their outstanding properties at even elevated temperatures, thus, the desired service performance of the parts can be achieved by using these superalloys in industries mentioned above, in especially aerospace industry [3, 4].

Inconel 718 is one of the most common nickel-based superalloys in industrial area [5]. It is developed to meet very demanding requirements of aerospace turbines. As well as its application in hot section parts of gas turbine engines in aerospace industry [6], thanks to its outstanding mechanical and physical properties, it is also preferred in various industries such as automotive, chemical and medical industries for high-performance applications [5]. When the application fields of Inconel 718 are considered, high surface quality and close tolerances are needed. However, it is difficult to plastically deform and to provide high product quality during machining of Inconel 718 due to its high ductility, strength, and hot hardness. Drilling is one of



common machining operations in aerospace industry where the Inconel 718 is employed frequently [7]. Besides, due to its high corrosion resistance, Inconel 718 is often preferred as the workpiece materials for valves, gas wells and safety equipment in oil and gas industry [5]. Drilling operations are also common in these processes. Thus, it has a great importance to perform drilling operations under optimal machining conditions.

The drilling operations differ from the other machining operations because cutting process occurs inside the hole and chip evacuation is more difficult. Therefore, higher cutting temperatures are generated due to high friction and inadequate cooling and lubrication [1]. This situation leads to undesirable hole quality and tool life when machining the materials with low thermal conductivity such as Inconel 718. Besides, high temperatures lead to some variations in hole subsurface microstructure and some modes of thermal failure on a cutting tool, thus resulting in undesirable hole quality and limited cutting tool life. In addition, Inconel 718 has strong chemical affinity to most of the cutting materials [6], thus increased cutting temperatures will substantially affect the tool life in drilling of Inconel 718 due to diffusion wear mechanism.

It is desired to perform drilling operations under optimal machining conditions to prevent secondary operations such as grinding, reaming, deburring. Besides, it is important to achieve appropriate limits on power consumption in drilling. However, when drilling Inconel 718, higher thrust force values can be monitored due to its work hardening tendency and ability to maintain its mechanical properties at elevated temperatures. Secondary operations are generally used because of its ductile characteristic. Therefore, it is essential to determine optimal cutting parameters and effective cooling environments when drilling Inconel 718.

The rest of this chapter presents general information about superalloys and its subgrades, Inconel 718, and drilling operation. In addition, a review of some related works is given in this section. The rest of the thesis is organized as follows:

- Chapter two presents experimental setup and procedure of the study. The materials, instruments and experimental and assessment procedures used in this thesis study are also described.
- Chapter three discusses the test results for each cutting condition.
- Chapter four presents concluding remarks of the study and some recommendations for future works.

## 1.1 Superalloys

Superalloys are a technologically important group and high-performance alloys maintaining the superior mechanical and physical properties at elevated temperatures and severe working conditions. The primary reason for development of these alloys is a need for high-performance materials to withstand elevated operating temperatures and high stresses components in gas turbine engines [8]. Working temperatures of these alloys are usually around 1100 °C. Superior properties of the superalloys make them an important group of engineering materials. In addition, they are also commercially remarkable materials because they are very expensive. These materials are widely preferred in the systems in which higher temperatures are needed to improve operational efficiency. Jet and rocket engines, steam turbines, and nuclear power plants can be examples for these systems. [1]. Figure 1.1 shows a typical aero-engine with approximate operating temperatures and relevant material usage.

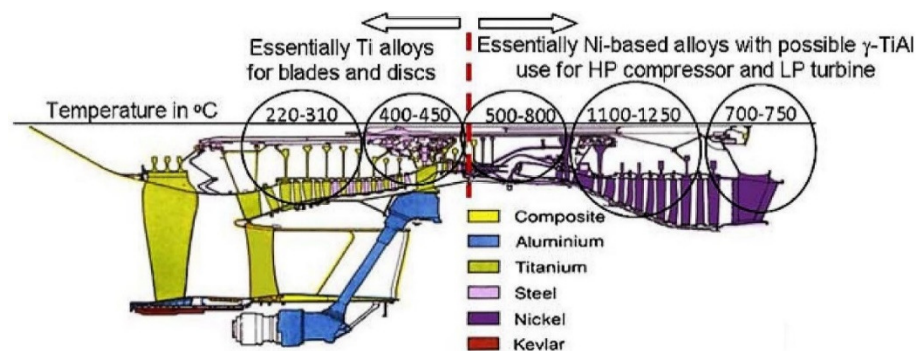


**Figure 1.1** A typical aero-engine with component materials and working temperatures [9].

Typical superalloys contain high content nickel, cobalt, iron, molybdenum, and chromium, in combination with up to fourteen elements. They are regarded as the most advanced alloys currently. The development and widespread applications of superalloys started with the development of gas turbine engines in the late of 1940s. Nowadays, they are preferred for aircrafts, power generation systems, nuclear reactors, chemical and petrochemical applications, medical devices, rocket engine components, cryogenic applications, etc. [9].

In fact, new classes of superalloys are investigated by gas turbine manufacturers and researchers around the world for applications in the engine parts exposed to high temperatures. The reason is that higher temperatures result in the enhancements in the efficiency of the engine and thus lower fuel consumption. Engine performance is a major factor in any power plant system. This can be a reason for spending so much money to development of future generations of superalloys [10]. From this viewpoint, it is considered that near future studies on any enhancement in the machinability of these high-performance engineering materials always are one of the most popular research topics.

### **1.1.1 Classification of Superalloys**

The superalloys are based on iron, cobalt, or nickel and many of them comprises of considerable amounts of three or more elements. They are divided into three categories according to the main elements as:

- Iron-based superalloys
- Cobalt-based superalloys
- Nickel-based superalloys

Figure 1.2 indicates some typical superalloys examples for these three categories and their compositions and tensile strength properties at room and high temperatures.

Superalloy	Chemical Analysis, % <sup>a</sup>							Tensile Strength at Room Temperature		Tensile Strength at 870°C (1600°F)	
	Fe	Ni	Co	Cr	Mo	W	Other <sup>b</sup>	MPa	lb/in <sup>2</sup>	MPa	lb/in <sup>2</sup>
Iron-based											
Incoloy 802	46	32		21			<2	690	100,000	195	28,000
Haynes 556	29	20	20	22	3		6	815	118,000	330	48,000
Nickel-based											
Incoloy 807	25	40	8	21		5	1	655	95,000	220	32,000
Inconel 718	18	53		19	3		6	1435	208,000	340	49,000
Rene 41		55	11	19	1		5	1420	206,000	620	90,000
Hastelloy S	1	67		16	15		1	845	130,000	340	50,000
Nimonic 75	3	76		20			<2	745	108,000	150	22,000
Cobalt-based											
Stellite 6B	3	3	53	30	2	5	4	1010	146,000	385	56,000
Haynes 188	3	22	39	22		14		960	139,000	420	61,000
L-605		10	53	20		15	2	1005	146,000	325	47,000

**Figure 1.2** Some typical superalloys [1].

### 1.1.1.1 Iron-Based Superalloys

Iron-based superalloys are used in applications where high toughness and ductility are required. Turbine discs and forged rotors are two application examples for these superalloys. They are used only wrought condition to obtain desirable grain size and morphology. Owing to high Fe % content in their chemical composition, their cost is lower than the other superalloys [8].

### 1.1.1.2 Cobalt-Based Superalloys

High melting temperatures (due to cobalt) and superior thermal fatigue and corrosion resistance properties are the main reasons to usage of cobalt-based superalloys. They can be used as cast form (such as X40) or wrought form (such as L-605). Vanes and stationary components of a gas turbine engine are application examples of these superalloys [8].

### 1.1.1.3 Nickel-Based Superalloys

Among all superalloys, nickel-based superalloys have the highest temperature/strength combination. This superior property makes them optimal materials for very challenging applications such as turbine blades. The wrought manufacturing method is preferred if high toughness is necessary. Turbine discs and forged blades are two applications of wrought nickel-based superalloys. On the other

hand, casting manufacturing method is chosen if high strength and creep resistance are required for high- temperature applications such as investment-cast turbine blades and wheels [8].

Thanks to their superior properties, nickel-based superalloys have a wide range of applications, especially in aerospace industry. For instance, Figure 1.3 shows the components of an aero-engine and their materials. As shown in the figure, most of the components (about 50%) of an aero-engine are made of nickel-based superalloys [11]. They also play a significant role in other high-temperature applications such as space vehicles, rocket engines, nuclear reactors, submarines, steam power plants, petrochemical equipment, etc. [3]. However, machinability of these advanced engineering materials is regarded as difficult-to-cut materials. Some properties of these materials such as low thermal conductivity, high chemical reactivity with cutting tools, high work hardening tendency, high shear strength properties, and presence of hard carbide particles in the microstructure, etc. cause to high machining costs, poor part quality, cutting tool life and productivity [4, 11–14]. An enhancement in the machinability and a reduction in machining cost of these superalloys are popular problems that must be overcome.

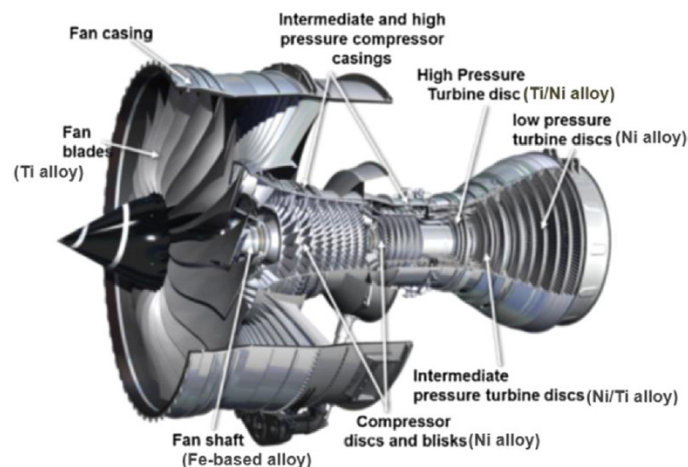


**Figure 1.3** Components and materials of Rolls-Royce XWB Turbofan engine [11, 14].

Due to critical applications of these advanced engineering materials, there are many studies in the literature on surface integrity, power consumption, and tool wear.

## 1.2 General Properties of Inconel 718

Among nickel-based alloys, Inconel 718 is the most widely used superalloy [15]. It constitutes 35 % of total wrought superalloy production worldwide [8]. It was developed for applications in aerospace turbines [5]. Inconel 718 is used for aircraft gas turbine engine components such as the compressor, turbine discs, compressor blades, casings, and fasteners [8]. It has superior mechanical properties at low and high working temperatures (-250 to 700°C), thus it is widely preferred in aerospace, petroleum and nuclear energy industries [7].

The main purpose in superalloy development is to achieve an alloy with optimal mechanical properties under severe working conditions. Therefore, composition elements of a superalloy determine the mechanical properties, surface stability, and cost of this alloy. Thus, important properties such as yield strength, ductility, toughness, fatigue strength and creep resistance can be rearranged with modification of compositions [8]. Table 1.1 indicates typical chemical compositional limits of Inconel 718 and effects of some notable elements [1, 8, 16].

**Table 1.1** Chemical compositions limits of Inconel 718 and functions of some notable elements.

Element	Weight %	Function
Nickel	50-55	Increase strength and toughness, Face-centered cubic (fcc) matrix stabilizer
Chromium	17-21	Improves corrosion and oxidation resistance, strength, wear resistance and hot hardness. Solid-solution hardening
Iron	Balance	
Niobium	4.75-5.50	
Molybdenum	2.80-3.90	Improves hot hardness and toughness, hardenability, and wear resistance
Titanium	0.65-1.15	$\gamma'$ , TiC carbide precipitation
Aluminum	0.2-0.8	$\gamma'$ precipitation
Cobalt	1.00 max.	
Carbon	0.08 max.	Forms MC, $M_7C_3$ , $M_6C$ and $M_{23}C_6$ carbides
Manganese	0.35 max.	
Silicon	0.35 max.	
Phosphorus	0.015 max.	
Sulfur	0.015 max.	
Boron	0.006 max.	Improves creep strength and ductility
Copper	0.30 max.	

### 1.2.1 Machinability of Inconel 718

Inconel 718 is known as one of the difficult-to-machine materials. Figure 1.4 indicates a comparison between some common engineering materials according to machinability ratings. As shown in the figure, Inconel 718 has the machinability rating of about 15% when compared to an AISI 1018 low carbon steel (reference steel) [17].

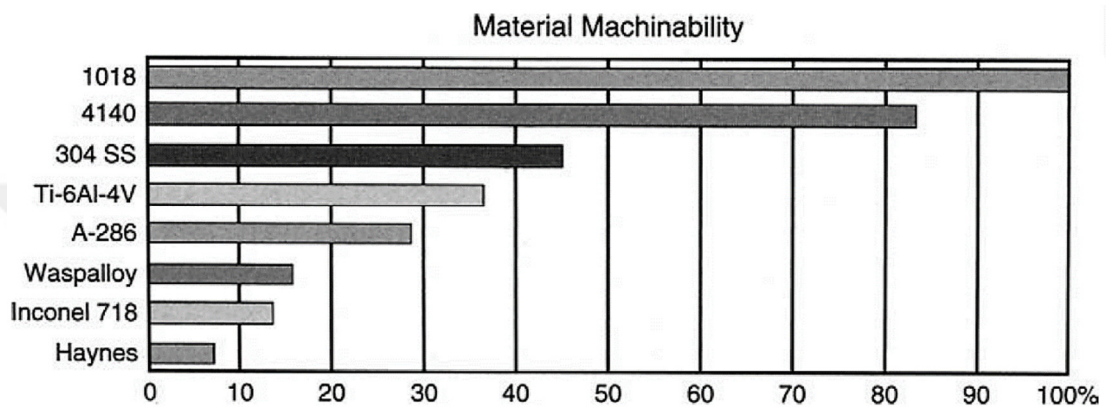


**Figure 1.4** Comparison of the machinability ratings of some materials [17].

The reasons for poor machinability of Inconel 718 can be listed as follows [3, 6, 18]:

- Due to good thermal properties, its strength is considerably maintained during cutting and thus, high cutting forces occur,
- Work hardening causes excessive tool wear (notch wear),
- The abrasive carbide particles in its microstructure lead to abrasive wear,
- Low thermal conductivity (11.4 W/mK) causes high cutting temperatures,
- High chemical affinity with some tool materials cause diffusion wear,
- Adhesions of Inconel 718 onto the cutting tool (BUE) occur due to its high ductility during machining.

These reasons lead to undesirable product quality, poor tool life, and high manufacturing costs when machining of Inconel 718. In order to increase machining performance of Inconel 718, it is crucial to determine optimal tool and coating

material, tool geometry, cooling and lubrication conditions and cutting parameters (cutting speed, feed rate and depth of cut).

### 1.3 Metal Cutting Processes

The desired final geometries of most mechanical parts are obtained by metal cutting processes via removing excess material from a starting work part. After bulk deformation processes, such as forging, casting and rolling processes, for desired shapes, dimensions, tolerances and surface quality, material removal operations are employed. In general, the most common operations in machining processes are turning, milling and drilling [19]. The significant benefits of metal cutting processes can be given as follows [2]:

- In general, they are accepted as the optimal way to machine limited number of prototypes or components.
- They have minimal effects on the features of materials.
- They can be used to produce the most imaginable surface geometries, dimensional tolerances, and surface qualities.
- They can be applied to all types of materials.

#### 1.3.1 Drilling Operation

Drilling is one of the most common and basic operations in machining processes. Different cutting tools are available to perform hole making process, but twist drills are the most common. In this process, a drill is used to make cylindrical holes in parts by rotational motion of tool or workpiece. A twist drill has a chisel edge at the center and two or more helical cutting lips with a taper angle ( $\kappa_t$ ) that meet with the flutes with a helix angle ( $\beta_0$ ). Basically, a twist drill consists of the shank, drilling body and the drill point as shown in Figure 1.5. The shank of the drill is required to clamp the drill to tool holder. Point of the drill cuts the excess material from workpiece and conveys the chips out of the cutting zone through the flutes. The flutes, ground on the drill body, have no contributions to cutting but have the responsibility to evacuate the chip to outside the hole and bring the coolant to the cutting zone. The helix angle, the most important factor regarding the flutes of the



drill, affects the efficiency of drilling by influencing the rake angle distribution along cutting edges and also chip evacuation time. Additionally, the drill point and the point angle are the most important parts in drill bit design, because the drilling process occurs at these parts [19].

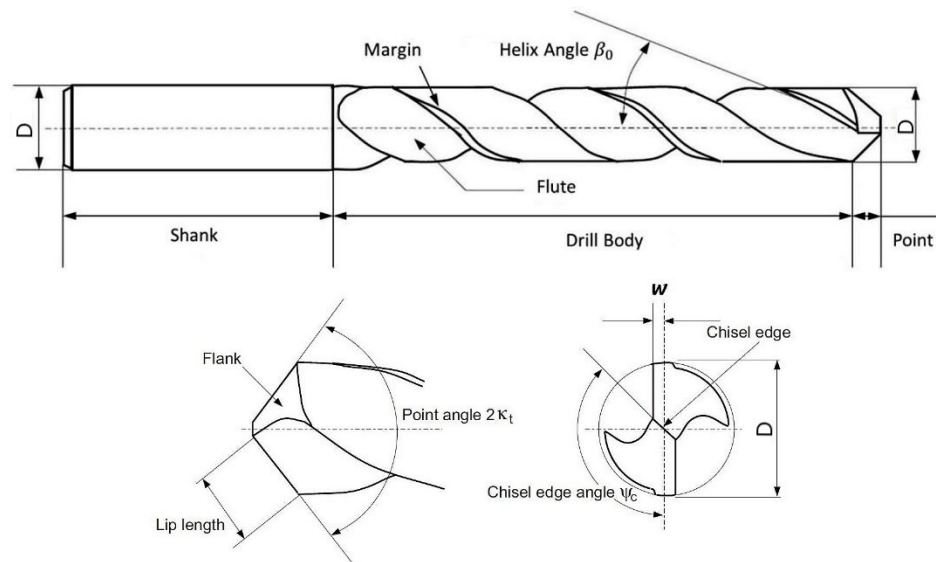


**Figure 1.5** Geometry of a twist drill [19].

The cutting action during drilling is complicated. The relative motion between cutting edges of the drill bit and the workpiece occurs with the rotational motion and the feed of the drill. Thus, chip forms. The cutting speed varies along the cutting edges during drilling operation. Accordingly, maximum cutting speed takes place at the outer diameter of the drill and therefore, most effective cutting action appears at these points. On the other hand, no cutting action takes place at the drill point, because relative velocity is zero at the chisel edge. This part penetrates into the workpiece and thrusts aside the material at the center. A great quantity of thrust force is required to perform this motion. Because of that, the thrust force value is higher during the penetration of the twist drill into the material at the beginning of the operation. The material removal action along the cutting lips of a twist drill are given in Figure 1.6. During penetration of chisel edge into the material, positional accuracy errors can take place because of rotational motion of spindle. Several

research works are conducted to address this problem such as changing of chisel edge geometry [1].

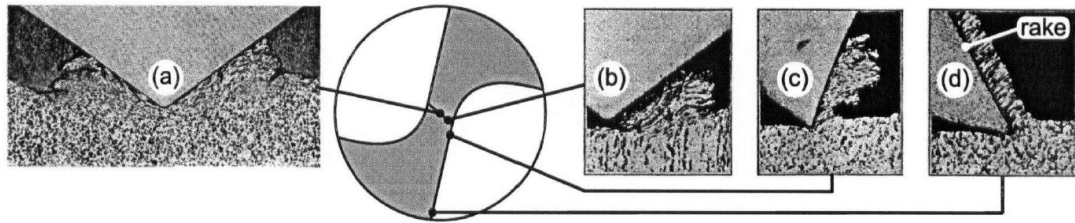


**Figure 1.6** Cutting actions along the diameter of a twist drill [20].

Due to the fact that cutting action occurs inside the hole in drilling operations, chip evacuation is a serious problem. The flutes of the drill must ensure adequate clearance along the length of the drill to provide chip flow to outside the hole. As the chip forms with the motion of the drill, it is forced to out of the hole through the flutes. In metal cutting, the main friction occurs between the rake face of the cutting tool and the chip. In drilling operations, in addition to the main friction, secondary friction also takes place between the new machined surface and the outer surface of the drill due to rubbing motion. This situation leads to the increases in temperatures of both the twist drill and the workpiece. The cutting fluids used for the purpose of decreasing friction and cutting temperatures cannot be met efficient cooling and lubrication requirements in drilling. Since chips flow in opposite direction according to feed direction and thus, cutting fluids cannot reach to the chisel edge sufficiently. This situation limits the hole length of a drilling operation [1]. In drilling operation, it is recommended that the drilling depth should be maximum three times of the diameter of the drill [21]. Insufficient chip clearance, tool deflection, and failure problems can take place if drilling depth exceeds. If deeper holes are necessary, in general, peck drilling method or custom designed drills must be used.

#### *1.3.1.1 Cutting Conditions in Drilling*

In drilling operation, cutting speed is described as the surface speed at the outside diameter of the twist drill. It is described in this way for convenience, although nearly all of the cutting process is essentially carried out at a lower speed closer to

axis of the rotation. Determination of the rotational speed of the drill is necessary to set the required cutting speed [1]. The spindle speed  $N$  (rev/min), can be calculated as follows:

$$N = \frac{v}{\pi D} \quad (1.1)$$

Where,  $v$  is cutting speed (m/min), and  $D$  is diameter of the drill (m). This formula can be also used if the workpiece is rotated and the drill is fixed in the drilling operation.

Feed  $f$  in drilling is stated in mm/rev. The feed values increase in proportion with drill diameter, thus higher feed values are used in larger hole making operations. In general, a typical twist drill has two cutting edges. Therefore, uncut chip thickness (chip load) removed by each cutting edge is half of the feed value. Feed can be converted to feed rate  $f_r$  (mm/min), as follows:

$$f_r = Nf \quad (1.2)$$

The material removal rate  $R_{MR}$  (mm<sup>3</sup>/min) in drilling is calculated as follows:

$$R_{MR} = \frac{\pi D^2 f_r}{4} \quad (1.3)$$

### 1.3.1.2 Cutting Forces and Power Consumption

Figure 1.7 shows the main components of the drilling forces on a twist drill. As shown in this figure, they are positioned at a distance ( $D/4$ ) from the drill center. Each force component is subdivided into three components. Where,  $F_{a1}$  and  $F_{a2}$  represent the thrust force components. They are parallel to the drill axis and in the same direction with feed.  $F_{v1}$  and  $F_{v2}$  represent the circumferential (cutting) force components. They are perpendicular to the drill axis at the cutting lips. Finally,  $F_{r1}$  and  $F_{r2}$  represent the radial force components. They are parallel to the drill axis at the cutting lips.

The resultant axial drilling force  $F_a$  (N) is obtained as:

$$F_a = F_{a1} + F_{a2} \quad (1.4)$$

The torque of the components  $M_v$  and  $M_r$  (Nmm) can be calculated as follows:

$$M_v = F_{v1} \frac{D}{2} = F_{v2} \frac{D}{2} \quad (1.5)$$

$$M_r = F_{r1} 2w = F_{r2} 2w \quad (1.6)$$

Thus, the resultant torque  $M$  (Nmm) is computed as:

$$M = M_v - M_r \quad (1.7)$$

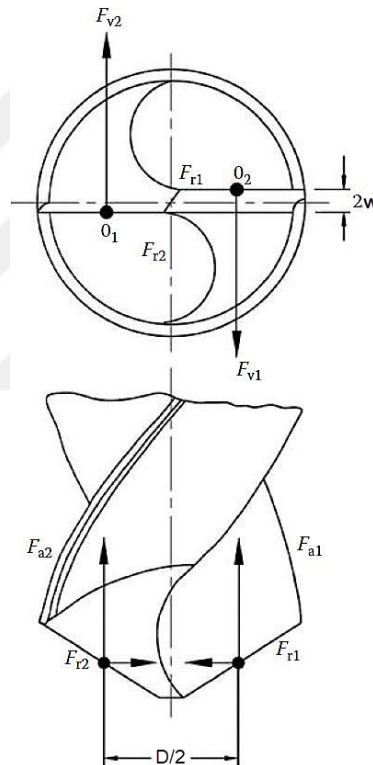


**Figure 1.7** Cutting force components in the drilling process [22].

If two cutting edges of a drill are properly sharpened, then it is possible to suppose that

$$F_{v1} = F_{v2} = F_v \quad (1.8)$$

and

$$F_{a1} = F_{a2} = F_a \quad (1.9)$$

If the drill is not sharpened properly, lateral forces can affect the drill and result in nonlinear holes due to lateral drift of the drill.

The main cutting force  $F_v$  acting on each cutting lip of the drill can be determined using following formula:

$$F_v = k_s A_c \quad (1.10)$$

Where,  $k_s$  (N/mm<sup>2</sup>) is the specific cutting resistance and  $A_c$  (mm) is the chip cross-sectional area. This formula can be also expressed as follows:

$$F_v = k_s \frac{fD}{4} = k_s b h \quad (1.11)$$

$$b = \frac{D}{2\sin(\chi)} \quad (1.12)$$

Where  $f$  (mm/rev) is feed,  $D$  (mm) is the drill diameter,  $b$  (mm) is the chip thickness to be cut by each cutting lip of the drill and  $\chi$  (°) is the drill lip angle.

In most of the cases, radial force components  $F_{r1}$  and  $F_{r2}$  are assumed to counterbalance each other. Thus, according to Equation (1.8),  $M_r$  is equal to zero, and

$$M = M_v = F_v \frac{D}{2} \quad (1.13)$$

$$M = k_s \left(\frac{fD}{4}\right) \left(\frac{D}{2}\right) = k_s \frac{fD^2}{8} \quad (1.14)$$

The total drilling power,  $N_t$  (kW) can be determined as follows:

$$N_t = N_c + N_{fd} \quad (1.15)$$

Where,  $N_c$  (kW) is the main drilling power and  $N_{fd}$  (kW) is the feed power. If the  $N_{fd}$  is assumed to equal to zero,  $N_t$  is equal to  $N_c$ .  $N_t$  (kW) can be also expressed as:

$$N_t = N_c = \frac{F_v v}{60 \times 10^3} = \frac{k_s f D v}{4 \times 60 \times 10^3} \quad (1.16)$$

Here,  $v$  (m/min) is the cutting speed.

The motor power  $N_m$  (kW) can be calculated as follows:

$$N_m = \frac{k_s f D v}{4 \times 60 \times 10^3 \eta_m} \quad (1.17)$$

$\eta_m$  is the mechanical efficiency of a drill press [22].

In a drilling operation, the torque  $M$  and the thrust force  $F_a$  values have a great importance. These parameters directly affect the hole quality, the surface integrity of the machined surface and the tool life. These values change according to cutting conditions. Figure 1.8 shows the factors affecting the drilling forces.

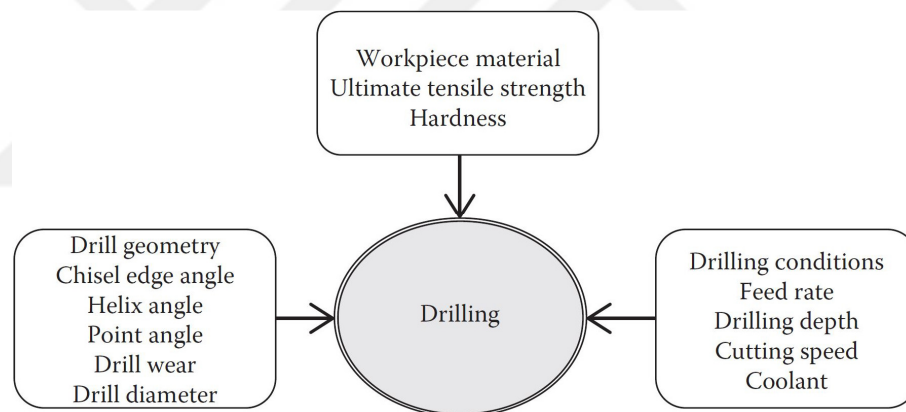


**Figure 1.8** Factors affecting the drill forces [22].

### 1.3.1.3 Tool wear

It is important to employ optimal cutting conditions and cutting tool material in a drilling operation because high heat generation and excessive cutting forces lead to very hard cutting conditions for a twist drill. If the cutting temperature is too high, thermal failure occurs due to softening of the tool point, and losing its cutting edge geometry. If the thrust force and the torque are too high, this situation leads to

fracture failure. On the other hand, gradual wear, the desired wear mode, provides as long as possible tool life [1].

Characteristic wear forms for a traditional twist drill are indicated in Figure 1.9. Chisel edge wear takes place at the tip of the drill and arises from abrasion or plastic deformation of the chisel edge. This type of wear causes the increases in the thrust forces two or three times and also leads to centering errors.

Flank wear takes place through the flank face of the drill and arises from abrasion. Increasing flank wear leads to the increases in the thrust force, the power consumption and the cutting temperature. Elevated temperatures accelerate the flank wear due to thermal softening effect. In addition, flank wear causes the increases in the burr heights at the exit of the hole when drilling through holes.

Margin wear takes place at the outer corner of the drill or land of the drill which is contacted with machined surface, and arises from abrasion, thermal softening, or diffusion. Increasing margin wear leads to hole diameter errors and undesirable hole surface roughness.

Crater wear takes place at the rake face of the drill and arises from abrasion and/or diffusion. Excessive crater wear may cause cutting edge deformation, chipping or failure of the drill.

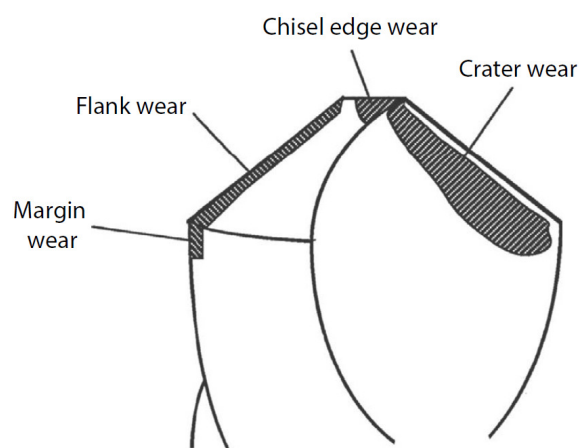


**Figure 1.9** Characteristic wear types and wear regions of a twist drill [23].

Cutting speed is directly affect the tool life. At low to medium cutting speeds, abrasive wears occur mostly on outer corner of the drill. On the other hand, at higher cutting speeds, abrasive wear and adhesive wear mechanisms can be observed. Overall, higher cutting speeds negatively affect the tool life.

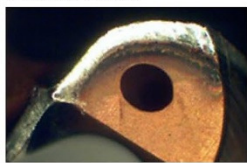
In general, instead of changing the cutting parameters (cutting speed and feed rate), changing of the tool material with another having higher hot hardness will improve the cutting tool performance. Because of that, a significant increase in tool life can be obtained by using coated drills.

The failure of the drill and chipping can be resulted from several reasons such as overloading, chip packing, vibrations, hard points in workpiece material, misalignment and tool defects, etc. [23].

The wear types occurred on the solid carbide drills in a drilling operation are given in Figure 1.10 with causes and solution suggestions to reduce the related tool wear.



### Flank wear



Flank wear on main edge



Flank wear on circular land

**Cause**

1. Total indicator run-out too large
2. Cutting speed too high
3. Feed too low
4. Grade too soft
5. Insufficient cutting fluid

**Action**

1. Check radial run-out
2. Decrease cutting speed
3. Increase feed
4. Use a harder grade
5. Increase cutting fluid pressure

### Chisel edge wear



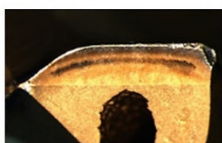
**Cause**

1. Total indicator run-out too large
2. Cutting speed too low
3. Feed too high

**Action**

1. Check radial run-out
2. Increase cutting speed
3. Decrease feed

### Chipping



Chipping on periphery



Chipping on main edge

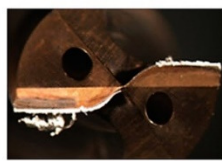
**Cause**

1. Unstable conditions
2. Total indicator run-out too large
3. Insufficient cutting fluid
4. Maximum allowed wear exceeded

**Action**

1. Check set-up
2. Check radial run-out
3. Check cutting fluid supply
4. Adjust cutting data

### Built-up edge (BUE)



**Cause**

1. Cutting speed and edge temperature too low
2. Negative land too large
3. No coating

**Action**

- 1.1. Increase cutting speed when BUE in centre
- 1.2. Decrease cutting speed when BUE in periphery
2. Sharper cutting edge
3. Coating on the edge

### Drill breakage



**Cause**

1. Total indicator run-out too large
2. Unstable conditions
3. Insufficient spindle power
4. Chip jamming
5. Feed too high
6. Excessive wear

**Action**

1. Check radial run-out
2. Check set-up
3. Check cutting data
4. Check cutting fluid supply
5. Decrease feed
6. Check wear more frequently

### Corner wear



### Margin / periphery wear



- Wear starts as notch  
- Grows towards corner

Figure 1.10 The different wear types on the carbide drills [24].

In general, one of the performance criteria of a twist drill is flank wear. It is measured from the wear band on the flank face [1]. The measurement method of the flank wear on a twist drill is indicated in Figure 1.11.

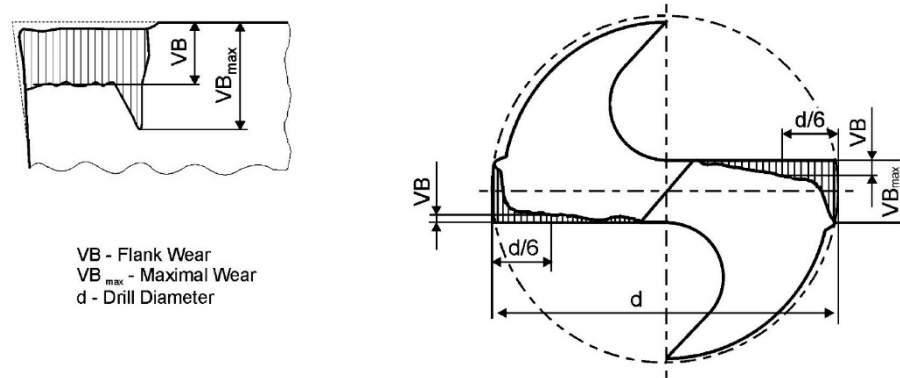


**Figure 1.11** The flank wear measurement on a twist drill [25].

#### 1.3.1.4 Cutting Temperature

During the machining operations, large amount of energy is spent for material removal. It is known that virtually all of this energy is transformed to heat, and leads to high temperatures at cutting zone. These high temperatures affect the machining performance directly. For instance, workpiece and cutting tool materials properties, cutting forces, tool life, chip formation, and machined surface quality are affected greatly by cutting temperatures.

In drilling, thermal conditions differ from the other machining operations such as turning, boring, etc. because chip formation occurs inside the hole and the chip keeps being in contact with the drill for a long time, which results in an increase in tool temperatures. Because of that, the cutting temperatures are further increased with the motion of the cutting tool. In general, cutting temperatures do not become a steady state in drilling, and increase with increasing hole depth. This situation limits the maximum hole depth for particularly difficult-to-cut materials such as Inconel 718. Lastly, the temperatures vary along cutting edges of the drill, because the cutting speed is lower at the cutting edges close to center of the drill. Therefore, outer corners or margin of the drill has higher rotational speed and cutting temperatures during a drilling operation [23].

Cutting temperatures in drilling operations have been worked both as experimentally and theoretically for many years. The widely used temperature measurement

methods in drilling operation are thermocouples inserted into the workpiece [26, 27] (Figure 1.12a) or the twist drill [28–30] (Figure 1.12b).

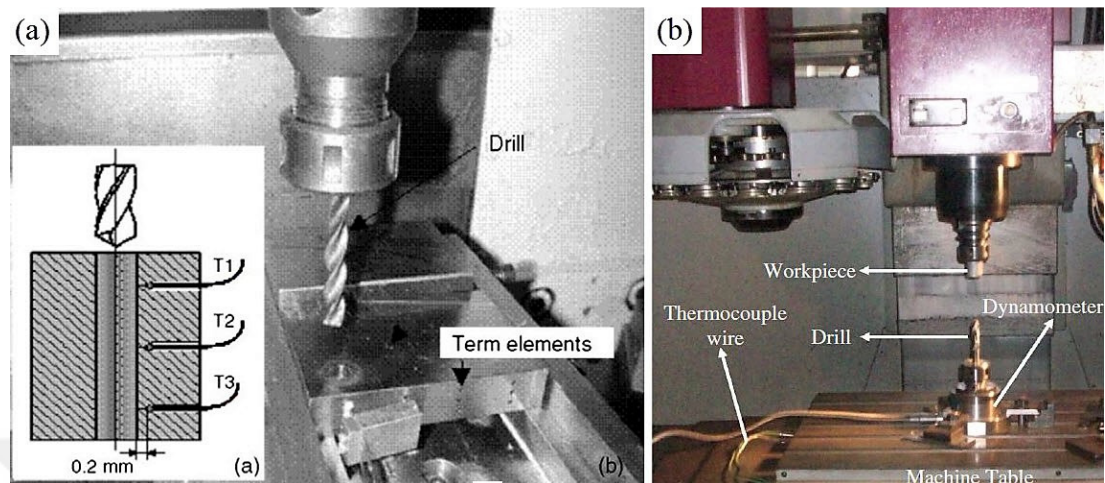


**Figure 1.12** The common cutting temperature measurement methods in drilling operation a) thermocouple insertion into the workpiece [26], b) thermocouple insertion into the cutting tool [30].

### 1.3.1.5 Cryogenic Cooling

In cutting of difficult to cut materials such as Inconel 718, the main goals are minimization of the machining costs and time, energy and required resources while improving the machining efficiency [31]. For the purpose of an improvement in the cutting performance, coolants and lubricants are applied directly to drilling processes with different coolant types and application methods. Usage of cutting fluids helps to removing heat from the cutting zone, reducing friction at tool-workpiece and tool-chip interfaces, removing chips from cutting region, improving finished product quality and decreasing cutting forces and power requirements required for the metal cutting process [1]. However, usage of cutting fluids cause some environmental and human health problems. The impacts of coolants are shown in Figure 1.13.

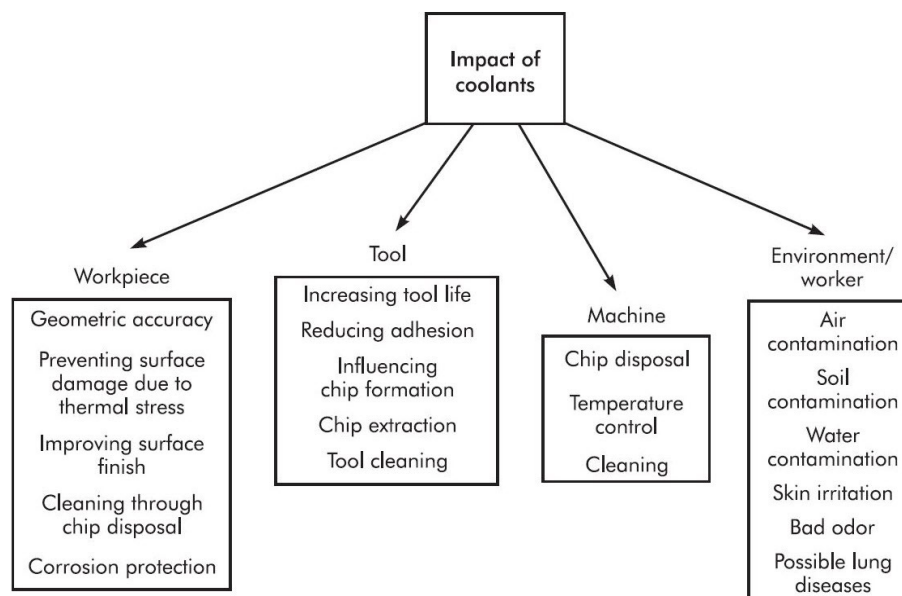


**Figure 1.13** Impacts of coolants on a cutting process [17].

Different cooling methods such as high-pressure water-oil based cutting fluid application [32], minimum quantity lubrication (MQL) [26] and hybrid cooling/lubrication systems [33] etc. have been trying by researchers in order to enhance machining performance and/or eliminate health problems and environmental pollutions. One of the cooling methods is cryogenic cooling. In this method, cryogenic coolants with boiling points under  $-150^{\circ}\text{C}$ , are used. Liquid nitrogen ( $\text{LN}_2$ ) (melting point:  $-210^{\circ}\text{C}$ , boiling point:  $-195.798^{\circ}\text{C}$ ) is the most common cryogenic coolant in drilling of various engineering materials [27, 34–38]. However, liquid  $\text{CO}_2$  is also used [39]. Besides, when used  $\text{LN}_2$  as a cryogenic coolant, it is not needed to coolant disposal and cleaning after operation, because  $\text{LN}_2$  will evaporate and return back to atmosphere rapidly after applied into the cutting zone. Because of that, this process called environmentally friendly when compared to conventional cutting fluids [40].

Cryogenic drilling is especially efficient for drilling of difficult-to-cut materials due to high cutting temperatures during cutting. With proper utilization of the cryogenic cooling, both tool life and material removal rate can enhance. In general, cryogenic cooling is applied to cemented carbide cutting tools and pre-cooling of the cutting tool can be performed to prevent thermal shocks [23].

There are several strategies for usage of cryogenic cooling in machining. They are the cooling the workpiece or both, the cooling the chip, the freezing the workpiece and the cooling the cutting zone [41]. Basically, application methods can be divided into three categories as pre-cooling, spray cooling and indirect cooling [42]. Their schematic application strategies are given in Figure 1.14. Literature survey showed that in general, spray cooling method is used in cryogenic machining of nickel-based superalloys.

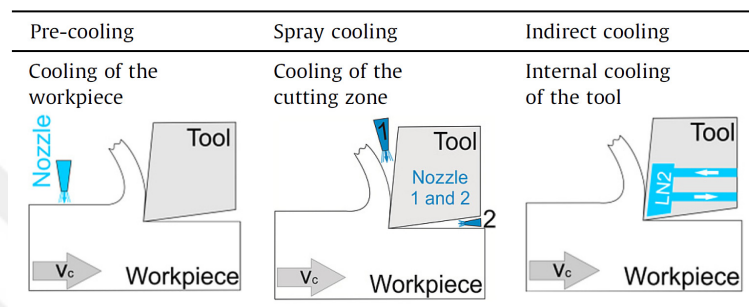
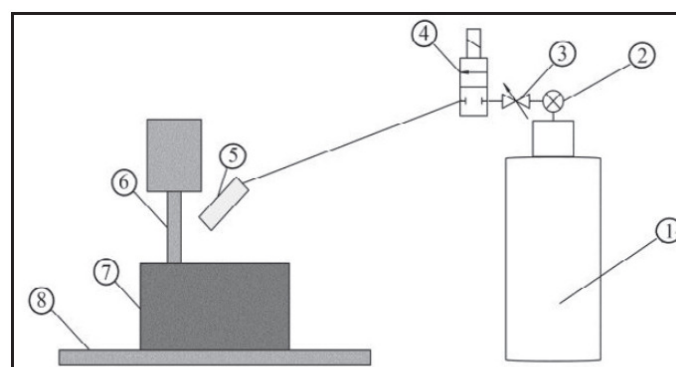


**Figure 1.14** Cryogenic cooling strategies [35].

Generally, a cryogenic cooling setup consist of a cryogenic tank to store LN<sub>2</sub> (or different kind of cryogen); a pressure gage, a gate valve and a solenoid valve to control cryogen flow; cryogenic hose and nozzle to deliver the cryogen to the cutting zone. Figure 1.15 indicates a schematic representation of a cryogenic cooling setup.



(1) Cryogenic dewar; (2) pressure gauge; (3) gate valve; (4) solenoid valve; (5) specially designed nozzle; (6) cutting tool; (7) workpiece; (8) machine tool table.

**Figure 1.15** Cryogenic cooling setup for a milling operation [43].

### *1.3.1.6 Hole Quality*

Holes with the desired accuracy can be drilled with a single pass and without the need for any second operation like reaming, if a suitable drill geometry, tool material and cutting conditions are used. Generally, in an ordinary drilling operation, the diametrical tolerance of the drilled holes ranges between 0.05 and 0.13 mm. However, it is possible to obtain more precise tolerances up to 0.015 mm with properly designed drill geometry, tool holder and machine. One of the criteria to control the accuracy of the hole is roundness error. It should be less than or equal to 0.005 mm. The other is lip height error. The height differences between two cutting lips for a feed should be less than 20%. The symmetry of the cutting edges also critically affects the accuracy of the hole [23].

During drilling operation, a combination of cutting and rubbing actions occurs. Initially, the cutting edges which are close to the drill point remove material from the surface and then, drill enters the hole with rubbing and burnishing action of margins and lands. Thus, machined surface quality is directly affected by feed per revolution and hardness and ductility of the workpiece material. BUE formation also deteriorates the surface quality and increases dimensional errors [23].

The accuracy of the holes is a critical issue and associated with the hole quality. The types of the errors that can occur in drilling operations are given in Figure 1.16. These errors are associated with non-uniform drill geometry, location, roundness, and dimensional errors.

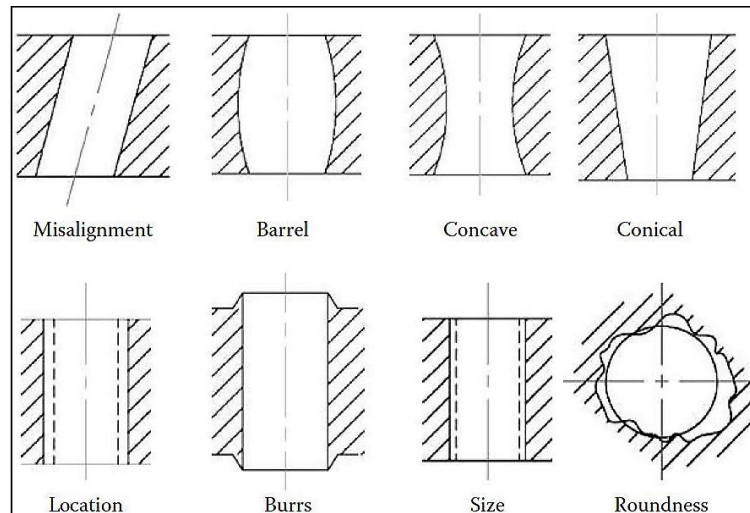


**Figure 1.16** Error types in drilling operations [22].

### 1.3.1.7 Surface Roughness

Surface roughness consists of tiny and fine surface deviations that can be led by a cutting tool making small grooves on the machined surface. It can be defined as the average of the roughness deviations in the vertical direction from the nominal surface on a determined surface length (cutoff length). Surface roughness is influenced by cutting tool and workpiece properties and cutting conditions. Thus, cutting conditions form the surface texture. In general, average roughness ( $R_a$ ) which is the mean value of the vertical deviations from the nominal surface over the pre-determined cut off length ( $l$ ) (Figure 1.17), is used to determine the surface roughness in machining [1, 44].

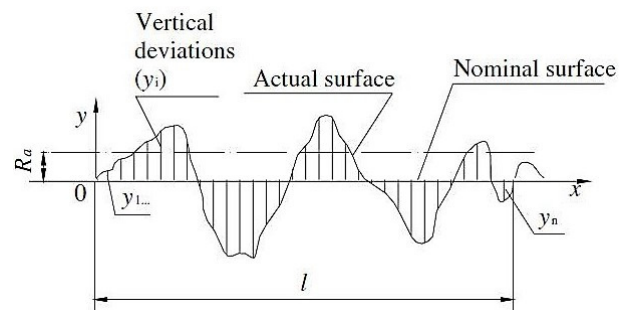


**Figure 1.17** The average surface roughness [44].

$R_a$  can be represented in mathematical form as following:

$$R_a = \frac{1}{l} \int_0^l |y| dx \quad (1.18)$$

Where,  $R_a$  ( $\mu\text{m}$ ) is arithmetic mean value of roughness values,  $l$  ( $\mu\text{m}$ ) is the determined distance over which the surface deviations are measured (cut off length), and  $|y|$  ( $\mu\text{m}$ ) is an absolute value of vertical deviation from nominal surface. An approximate value of Equation (1.18) can be expressed as follows:

$$R_a = \frac{1}{n} \sum_{i=1}^n |y_i| \quad (1.19)$$

Where,  $|y_i|$  ( $\mu\text{m}$ ) is an absolute value of vertical deviation identified by the subscript  $i$ , and  $n$  is the number of deviations included in  $l$ .

#### 1.3.1.8 Burr Formation

At the end of the machining operations, the burrs occur in especially drilling operations. Burr formation are not desired because they lead to assembly problems and a risk for handling machined parts.

Different burr types can be occurred in drilling. Generally, they have an uneven appearance. During drilling of highly ductile materials, uniform burrs with drill cap (Figure 18a) or crown burrs (Figure 18b) may occur. Modifications in drill point geometry can reduce the burr formation.

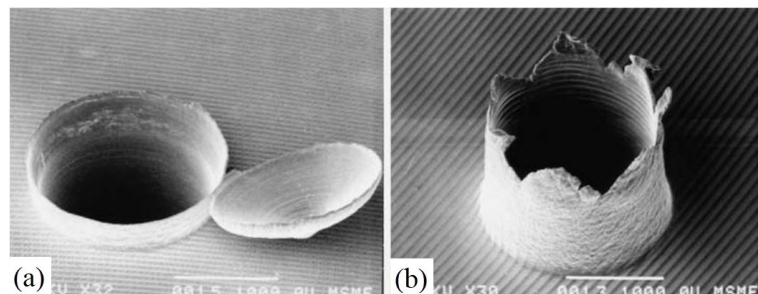


**Figure 1.18** a) uniform burr with drill cap b) crown burr [25].

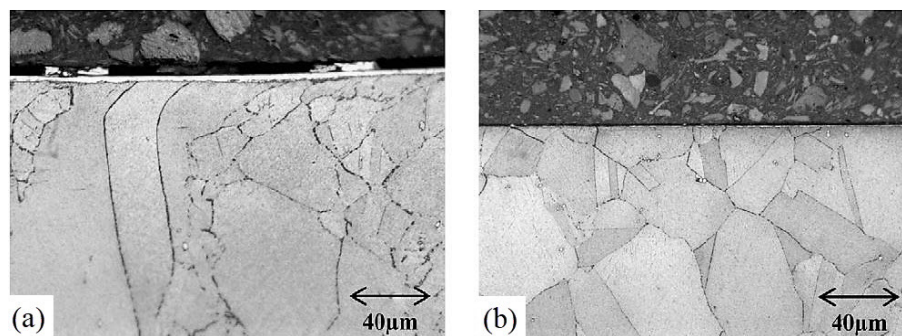


Burr formations are critical problems for worn drills because tool wear lead to higher cutting forces. Precautions that improve the tool life will thus also decrease burr formation. However, burr free machining generally is not possible in many drilling operations, thus deburring operations will often needed before assembling of the machined part [23].

## **1.4 Literature Review**

Nowadays, machinability of nickel-based superalloys is always an important research topic for researchers due to their critical application areas and machining difficulties. Several review articles can be found in the literature about the machinability of these advanced alloys. In particular, these publications are focused on superior mechanical and physical properties, machining problems and their solution proposals [2–4, 45], tool wear [46] and tool materials [47], surface integrity [11, 15] and sustainable machinability [12, 48] in machining of nickel-based superalloys. It is well-known that Inconel 718 is the most popular one within nickel-based superalloys. Although there are many studies about turning [49–53] and milling [43, 54–56] of this advanced engineering material, very few studies are related to the drilling operation.

The superior properties of Inconel 718 are also responsible for its poor machinability. Especially, some properties of Inconel 718 such as work hardening tendency, low thermal conductivity, ability to maintain its mechanical properties at elevated temperatures, chemical affinity with some of the cutting tool materials, etc. lead to insufficient tool performance, poor workpiece quality and thus, high manufacturing costs. Commercially available drills are insufficient to meet product quality desired by the aerospace industry. Drilled holes contains a white layer which is a hard structure in the microstructure. Because of that, reaming or grinding operations are required to obtain the desired surface quality [6]. Figure 1.19 shows the effects of secondary operation mill boring on subsurface microstructure quality in drilling of Inconel 718. The white layer formation and plastic deformation in grain structure (Figure 1.19a) should be minimized to provide desirable hole quality in drilling operations of Inconel 718.

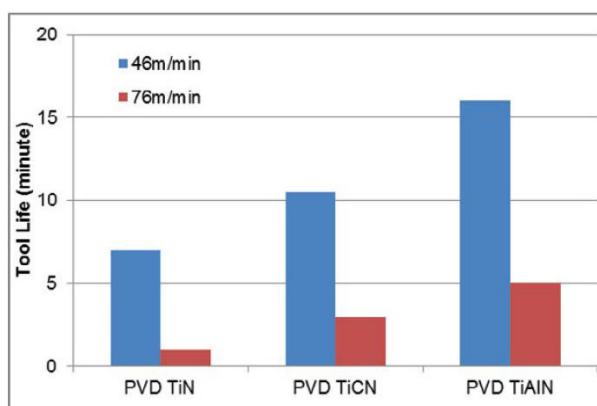


**Figure 1.19** Subsurface microstructures resulting from a) drilling b) mill boring [6].

Application of different machining conditions and innovative techniques are necessary to improve drilling performance of Inconel 718. Modification of the twist drill geometry [57], and applications of different cooling and/or lubrication techniques such as minimum quantity lubrication (MQL) [58], cryogenic cooling [29] and hybrid cooling [59, 60], are current issues for research works in drilling of Inconel 718.

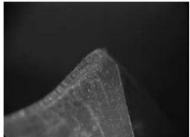
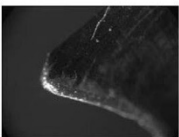
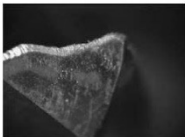
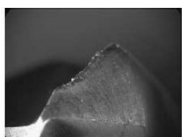
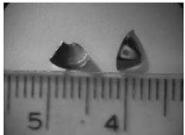


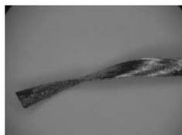
In machining operations, it is crucial to determine suitable cutting tool for the any workpiece material. The coated carbide cutting tools are superior to the uncoated ones in machining of nickel-based superalloys [47]. Lower cutting temperatures can be achieved with coated cutting tools because the friction between the workpiece and the cutting tool is reduced by application of thin film coating material on a cemented carbide substrate [61]. Besides, due to high cutting temperatures in the cutting zone, it is significant to use coating materials with lower thermal conductivity and higher hot hardness than the workpiece material and cemented carbide substrate. TiAlN coated carbide tools are commonly used due to their superior oxidation resistance and hot hardness under elevated temperatures when machining nickel-based superalloys. However, their tool life and cutting condition ranges are limited in drilling of nickel-based superalloys in comparison to other materials such as steel or iron-based alloys [62]. Figure 1.20 shows comparison of the performance of different coating materials and cutting speeds in machining of Inconel 718. As shown in the Figure 1.20, TiAlN coated cutting tool has the longer tool life than TiCN and TiN coated tools and an increase in cutting speed leads to a significant reduction in tool

life. As well-known, the cutting speed is the most effective parameter on the tool life. This study confirms this information.



**Figure 1.20** Tool life performance of different type coating materials [18].

In order to obtain the effective drilling performance for Inconel 718 the optimal drill point angle and clearance angle are determined as  $140^\circ$  and  $8^\circ$ , respectively by Chen and Liao [7]. Their investigation about wear mechanisms in drilling of Inconel 718 showed that the friction force is the most influential on tool life. Figure 1.21 shows the progress of the wear on drills after 5 holes in each stage. Fracture, flank wear, and chipping and subsurface fatigue cracks were observed as wear types.

	Stage			
	I	II	III	IV
Tool wear				
Chip types				
Descriptions	Coated layer is abraded-off segmented chips of 0.08 mm thickness; flank wear: 0.1 mm	Chipping with micro-cracks; larger segmented chips; flank wear: 0.2 mm	Breakage of cutting edge; serrated chips; flank wear: 0.3 mm	Drill failure; long chips of 0.4 mm thickness

**Figure 1.21** Wear progress in drilling Inconel 718 [18].

They also studied the effects of different cooling agents which are conventional cutting fluid and nano-modifier fluid. Figure 1.22 shows the drilling test results. According to Figure 1.22, it can be said that coated drills have longer tool life than uncoated ones under the same cutting conditions and uncoated carbide drills showed better performance under nano-modifier fluid than coated ones under conventional cutting fluid. Therefore, it can be said that TiAlN coated carbide drills exhibited better performance and nano-modifier fluid substantially affected the tool performance in drilling of Inconel 718.

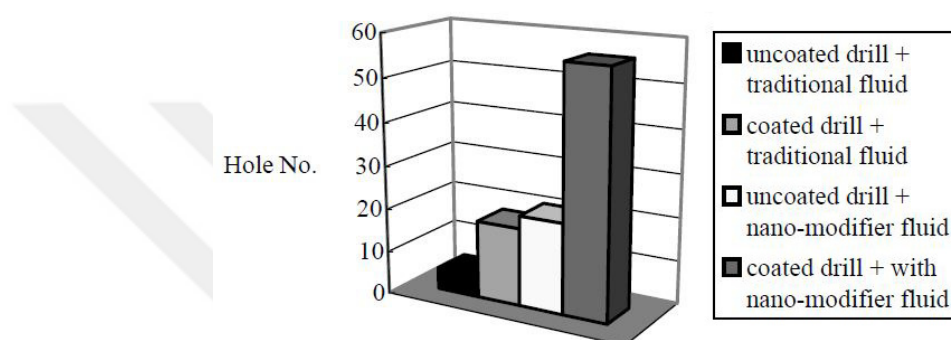


**Figure 1.22** Effects of coating material and cutting fluid on drill life in drilling of Inconel 718 [7].

Due to its critical applications in industry, surface integrity studies [57, 63] have a great importance in drilling of Inconel 718. At this point, the cutting fluids play a critical role to obtain desired product quality. According to first law of metal cutting (the Makarow's law), the most effective machining can be achieved at a specific temperature known as optimal cutting temperature [64]. And this temperature is independent from the cutting conditions and it is related to only the cutting tool and the workpiece material properties. However, considering machining of Inconel 718, it cannot be possible to achieve this optimal cutting temperature due its work hardening tendency and strength and hardness properties at elevated temperatures which cutting tools cannot withstand. Because of that the cooling action of cutting fluids would help to keep the cutting temperature closer to optimal cutting temperature to obtain an effective machining [43, 64].

Ezugwu et al. [3] reported that the most important issues during machining of nickel-based superalloys are poor surface quality and insufficient cutting tool life.

Therefore, usage of the cutting fluids is crucial, because with the reduction in the overall cutting temperature, more efficient machining can be obtained. According to Ezugwu [45], cryogenic machining technology is one of the custom designed cooling techniques to reduce cutting temperatures and thus, effective and economic machining can be achieved in machining of aero-engine materials. Because cutting tool materials do not lose their strength and hardness at higher cutting temperatures with efficient cooling.

Cryogenic machining affects the properties of the workpiece and/or the cutting tool, because of application of very low temperatures. It can be expected that extremely low temperatures could enhance the strength and hardness and decrease the elongation and toughness of the materials. Because of that cryogenic machining could be effective for materials with high cutting temperature problems [12].

In addition to its possible advantages in machinability of hard-to-cut materials, cryogenic machining also known as a one of the green manufacturing methods [65]. Nowadays, there is a growing interest in environmentally friendly manufacturing because conventional cutting fluids lead to some environmental and health problems and also undesirable manufacturing costs. Thus, cryogenic machining has a good attention in machining community [65–68].

In a review study [42], authors investigated application methods and effects of cryogens in metal cutting processes. It was pointed out that there is a need for more research works about the effects of cryogenic cooling on milling and drilling operations. When compared to cryogenic cooling with dry cutting and conventional fluids in machining operations, it can be said that cryogenic cooling enhances the dimensional accuracy, surface quality of workpiece and tool life. However, it was also mentioned by the authors that according to their review investigations, lower temperatures at cutting zone lead to harder and stronger workpiece material, as a result, this situation causes an increase in cutting forces.

One of the earlier investigations about cryogenic machining of Inconel 718 have been conducted by Shokrani et al. [43]. They analyzed the performance of TiAlN coated carbide cutting tools in cryogenic milling of Inconel 718. It was found that

cryogenic machining enhanced the surface roughness by about 33% without a significant increase in power consumption in comparison to dry machining. However significant tool life reduction occurred under cryogenic cooling condition. Chipping was observed under both machining conditions.

High temperatures and high cutting forces lead to plastic deformation of the grain structure of the machined surface when machining Inconel 718. However, cryogenic cooling can be a solution to reduce plastic deformation depth of machined surface. Aramcharoen and Chuan [69] obtained lesser plastic deformation (Figure 1.23) with the usage of cryogenic cooling in milling of Inconel 718. In addition, they obtained better tool life with a significant reduction in cutting temperature. They recommended the cryogenic cooling method in milling of Inconel 718 to increase its machinability.

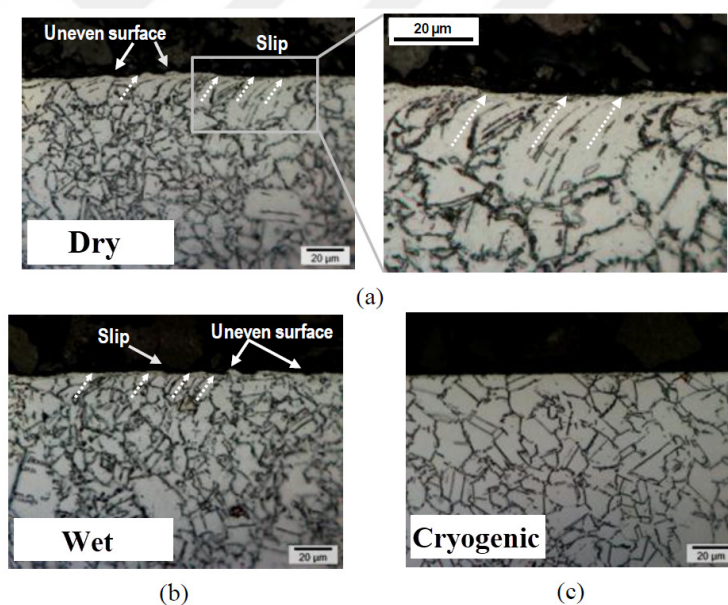


**Figure 1.23** Machined subsurface microstructures under a) dry, b) wet, and c) cryogenic milling conditions [69].

Performance comparison between cryogenic cooling and the other environmentally friendly cooling environments such as MQL, hybrid systems, and air cooling, etc. in machining is one of the current topics in the research works related to machinability of Inconel 718. Cryogenic turning performance of Inconel 718 has been compared

with dry, wet, and MQL machining conditions by Kaynak [58]. According to test results, at higher cutting speeds, the best surface quality, lower tool wear and thermal deformation were obtained under cryogenic machining condition. It was found that cryogenic cooling is very effective for high speed machining, while MQL has high machining performance at lower cutting speeds. On the other hand, surface integrity comparisons of different cooling environments in turning of Inconel 718 have been investigated by Pusavec et al. [59]. They used a hybrid system called cryo-MQL. The test results showed that cryogenic machining increased compressive residual stress, decreased surface roughness, and slightly decreased plastic deformation zone. And also surface hardness of cryogenically machined parts was lower than that in dry machining. They proposed the usage of cryogenic cooling in machining of Inconel 718 not only as a cleaner process but also a performance enhancing method. In addition to dry, wet, MQL and hybrid cooling machining conditions, performance of chilled air method was also compared to cryogenic cooling in turning of Inconel 718 by Fernandez et al. [70]. The test results showed that cryogenic machining showed better tool life (34.6% lesser tool wear) performance than the chilled air. In general, lesser tool wear results in better surface quality in machining. However, the surface roughness values were found better in chilled air condition. This case was associated with poor lubrication capacity of LN<sub>2</sub> and workpiece properties.

Although there are many studies have been conducted about cryogenic machining, cryogenic drilling studies are relatively less. One of the cryogenic drilling studies has been conducted by Ahmed and Kumar [27]. They used indexable inserts in drilling of Ti6Al4V alloy. Their cryogenic cooling application method is given in Figure 1.24. With usage of LN<sub>2</sub> as a cooling agent, cutting temperatures are reduced between 28-61% in comparison to wet drilling. Besides, significantly better surface quality, lower torque and thrust force values were also obtained with cryogenic cooling. They recommended the cryogenic cooling as the best alternative to conventional cooling in drilling of Ti6Al4V alloy.

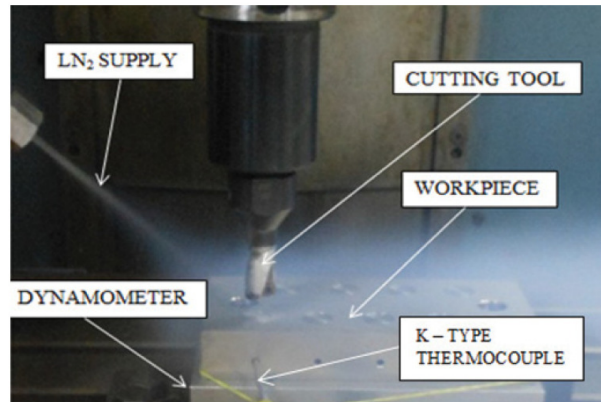


**Figure 1.24** Cryogenic cooling application of the study [27].

Burr formation occurs after the machining operations and lead to risks for injuries and affect the functionality of the machine parts. To remove these undesired excessive material, deburring operations are performed. However, these secondary operations significantly increase the costs of drilling operations [39]. Because of that research works related with minimization of burr formation in especially drilling operations are essential to improve the productivity in machining. Cryogenic cooling method can be a solution to minimize the burr formation in drilling operations because the behavior of the material would be more brittle under cryogenic cooling conditions, thus it is expected lower burr heights after drilling operations. The effects of cryogenic drilling on burr formation has been investigated by Biermann and Hartmann [39] on 34CrNiMo6 and AlMgSi materials. They used CO<sub>2</sub> as a cooling agent. The tests were conducted with indexable inserts. According to test results, cryogenic cooling reduced the burr formation but it did not affect hole diameter and roundness error values when compared to dry machining. In another study [36], the hole quality was investigated under dry, MQL and cryogenic cooling conditions in drilling of GLARE fibre metal laminates with TiAlN coated solid carbide drills. According to tests results, a reduction of 47% in exit burr formation was observed with cryogenic cooling in comparison to dry drilling. On the other hand, Xia et al. [34] studied the performance of cryogenic cooling in drilling of a CFRP composite material. According to test results, cryogenic cooling enhanced the drilling performance in terms of tool wear, surface roughness and roundness error, but delamination values are not satisfactory. In addition, torque and thrust force values



were higher in cryogenic cooling. The authors recommended the selection of wider range of cutting parameters to determine the effects of cryogenic cooling in drilling of CFRP composites for further studies.

When compared to external machining operations such as turning and milling, greater thermo-mechanical loadings occur on the cutting tool and the workpiece in drilling operations. Because of that tool life, surface integrity and hole quality are greatly influenced. The effect of cryogenic drilling on this thermo-mechanical phenomenon in drilling Inconel 718 was investigated by Outeiro et al. [29] both experimentally and using finite element method. Besides, this is the only study found in the literature about cryogenic drilling of Inconel 718. They used standard TiAlN coated solid carbide drills with a diameter of 12.015 mm, in drilling of Inconel 718 having 10 mm thickness under wet ( $v_c=10-30$  m/min,  $f=0.08-0.11$  mm) and cryogenic cooling ( $v_c=5-24$  m/min,  $f=0.08-0.11$  mm) conditions. LN<sub>2</sub>, ( $p=10$  bar) and metal cutting fluid, ( $p=20$  bar) send to the cutting zone through internal channels in the twist drill. They also measured the drilling temperature using K type thermocouples located close to cutting edges on the twist drill. Figure 1.25 shows the experimental setup of their study.



**Figure 1.25** Experimental setup of the study [29].

It was found that generally, torque and thrust force values under cryogenic drilling condition were higher than those of wet drilling. This situation was associated with the increases in the material resistance to plastic deformation under cryogenic temperatures, excessive tool wear and failure in cryogenic drilling and low lubrication properties of LN<sub>2</sub>. When the optimal cutting conditions under LN<sub>2</sub> ( $v_c=10$  m/min,  $f=0.11$  mm) and wet ( $v_c=24$  m/min,  $f=0.11$  mm) drilling were compared, cryogenic cooling led to larger tool wear. The tool wear results are given in Figure 1.26.

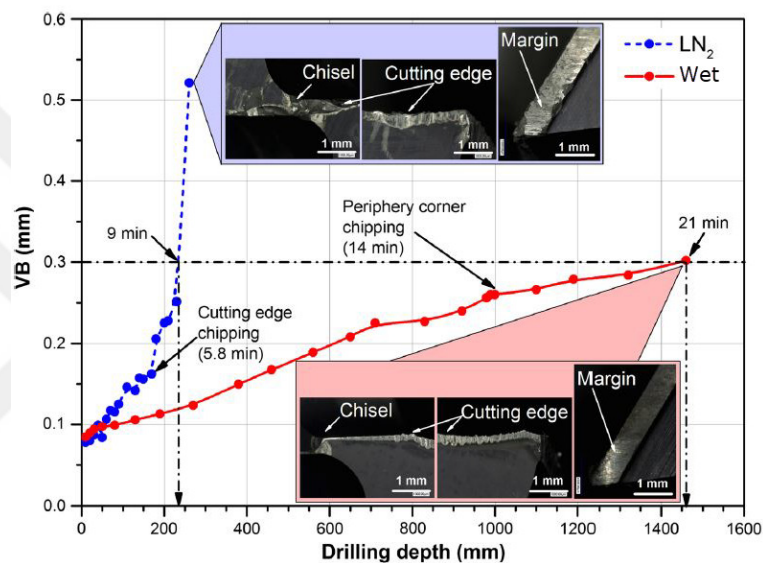


**Figure 1.26** Tool wear examination of the study [29].

It was pointed out that, drill geometry, coolant pressure and application method, location of the coolant supply have a great importance on thermo-mechanical phenomena and thus drilling performance. It was found that the main advantage of cryogenic cooling is a remarkable reduction in heat generation on the twist drill (Figure 1.27). Therefore, it is possible to achieve a reduction in drilling time, and thus an increase in productivity in cryogenic drilling of Inconel 718. The authors proposed that a modification in drill geometry can enhance the performance of cryogenic cooling.

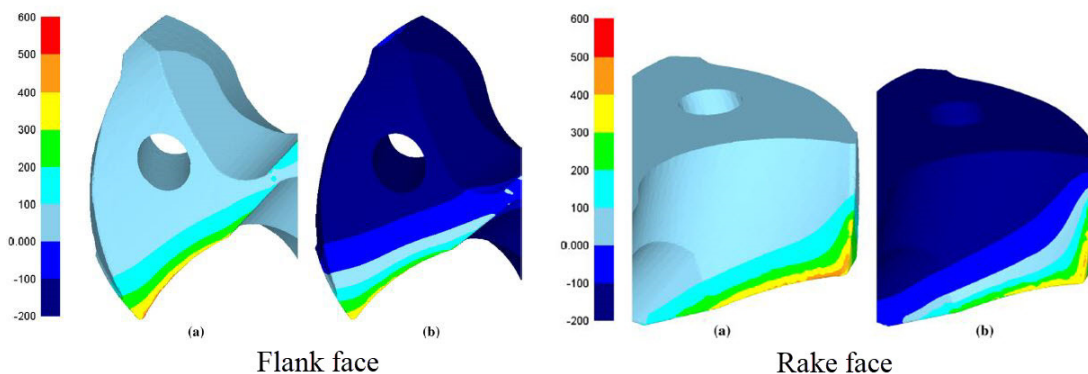


**Figure 1.27** Temperature distribution under  $v_c=10$  m/min,  $f=0.11$  mm cutting conditions a) wet , b) LN<sub>2</sub> [29].

The literature survey showed that there are relatively few studies about drilling of Inconel 718 using solid carbide drills. It is concluded that excessive temperatures in the cutting zone result in undesirable hole quality, surface integrity, and tool life. Commercial drills are not effective to obtain desirable results and therefore, new solutions are necessary. There is a need for further investigations about cryogenic drilling of Inconel 718. Cryogenic drilling can be an effective cooling method to obtain better surface quality and hole quality, tool wear, burr formation and cutting temperatures.

### 1.5 Aim of The Study

The purpose of this study is to investigate the effects of different cutting conditions on cutting temperature and drillability of Inconel 718. Different performance assessments such as the thrust force, the torque, the cutting temperature, the hole quality, the surface integrity, and the tool wear have been studied under dry, wet, and cryogenic conditions.

The novelty of this study is cutting temperature measurement method. Measurement of cutting temperature was carried out from the five different locations throughout the thickness of workpiece during the drilling tests under dry, wet, and cryogenic conditions. Thus, performance evaluations were associated with cutting temperature values.

# CHAPTER 2

## EXPERIMENTAL SETUP AND PROCEDURE

In this chapter, the experimental setup and procedure of thesis study are discussed in detail. The measurement and examination methods of outputs such as force, torque, hole diameter, roundness error, tool wear, cutting temperature, burr formation, surface roughness, microhardness and microstructure, the cooling and lubrication environments and their setups used in the tests are also introduced in the chapter. Figure 2.1 indicates a summary of the examination and measurement methods and their equipment used during/after the tests.

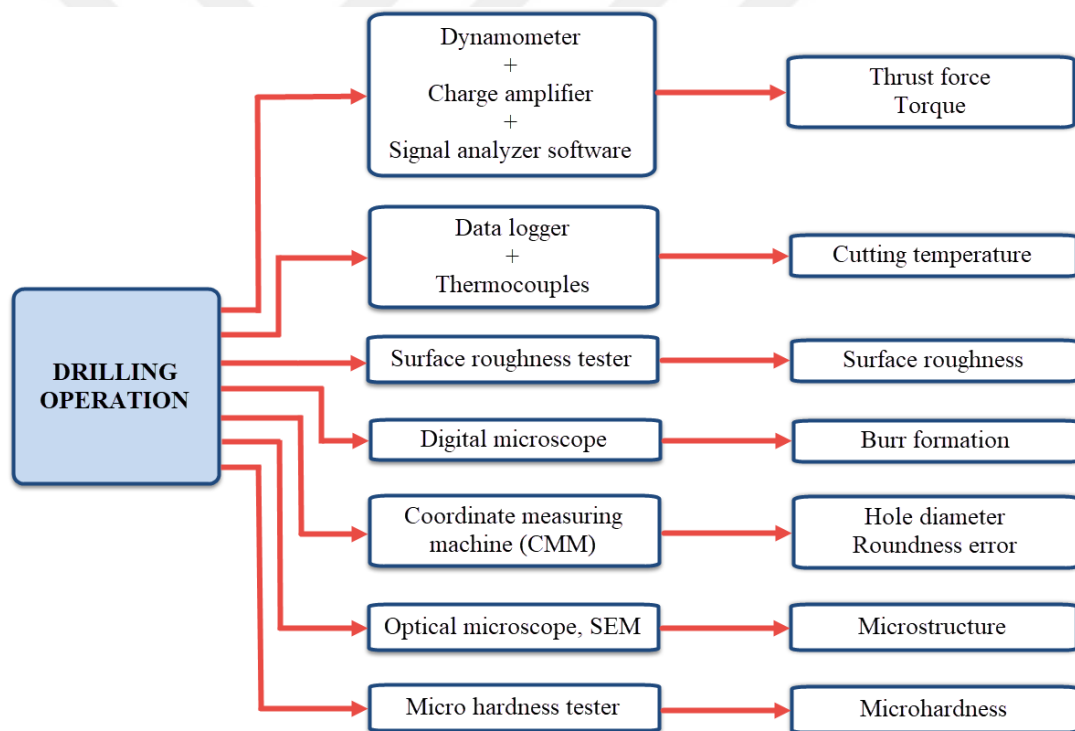


**Figure 2.1** Schematic representation of examination and measurement methods in the study.

## 2.1 Workpiece Material

In the tests, the hot rolled, descaled, and annealed Inconel 718 plates with dimensions of 100 mm x 80 mm x 15 mm were used as the workpiece material. The dimensions of the specimens are suitable to dimensions of workpiece clamping apparatus of the dynamometer. Chemical composition and some mechanical and physical properties of the Inconel 718 are given in Table 2.1 and Table 2.2, respectively

**Table 2.1** Chemical composition of the Inconel 718.

<b>Element</b>	C	Mn	Fe	S	Si	Cu	Ni	Cr
<b>wt. %</b>	0.03	0.08	17.90	0.001	0.09	0.13	53.66	18.41
<b>Element</b>	Ti	Co	Mo	Ta	B	Nb	P	
<b>wt. %</b>	0.96	0.34	2.87	0.004	0.002	4.92	0.009	

**Table 2.2** Some mechanical and physical properties of the Inconel 718.

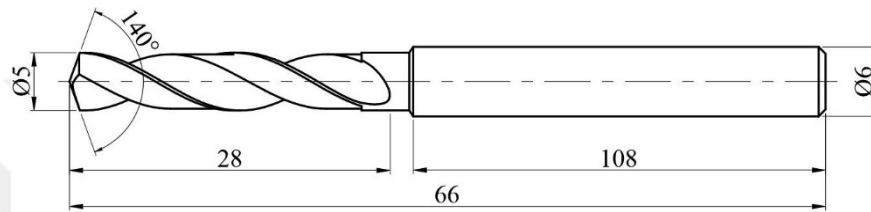
<b>Property</b>	<b>Value</b>
Tensile strength	860.47 MPa
Yield strength	368.18 MPa
Reduction of area	55.9 %
Elongation	53.4 %
Hardness	90.5 HRB
Grain size	7 (ASTM)
Density [16]	8.55 g/cm <sup>3</sup>
Thermal conductivity [6]	11.4 W/mK
Melting temperature range [16]	1260 °C – 1336 °C

## 2.2 Cutting Tools

Uncoated and TiAlN coated tungsten carbide twist drills with diameter of 5 mm were used in this study. Some geometric and dimensional properties of the twist drills are given in Table 2.3. A new twist drill was used for each machining test. Figure 2.2 indicates the dimensions of the twist drills.

**Table 2.3** Selected properties of the twist drills.

Property	Uncoated	TiAlN
Standard	DIN 6537	
Diameter	5 mm	
Point angle	140°	
Helix angle	30°	
Clearance angle	10° / 22°	
Edge chamfer	0.08 <sup>±0.03</sup>	
Shank diameter	6 mm	
Co%	10%	
Hardness	1620 HV	3300 HV

**Figure 2.2** The dimensions of the tungsten carbide twist drills.

## 2.3 Experimental Setup and Cutting Conditions

The drilling tests were conducted using a Johnford VMC-550 CNC vertical machining center at Gazi University Laboratory. Technical specifications of the CNC vertical machining center are given in Table 2.4.

**Table 2.4** Technical specifications of the CNC vertical machining center.

Property	Value
Model	VMC-550
Axis travel X-Y-Z	550-500-450 mm
Spindle motor	7.5 kW
Max. spindle speed	6000 rev/min
Accuracy	0.001 mm
Control unit	FANUC

The drilling tests were performed under dry, wet, and cryogenic cooling environments at a feed value ( $f$ ) and two different cutting speed values ( $v$ ) using uncoated and TiAlN coated twist drills. The cutting conditions for the drilling tests are given in Table 2.5. Cutting speeds and feed values were determined according to

preliminary tests results. 12 different drilling tests were conducted in the scope of the thesis. In the tests, solid carbide twist drills with a diameter of 5 mm were used to produce through holes with a depth of 15 mm on the workpiece material. Three holes were drilled in each test condition to obtain more accurate results. In addition, a number of wear tests with 50 holes were performed at cutting speed of 15 m/min to reveal the effects of coating material and cutting conditions on drill life.

**Table 2.5** Cutting conditions for the drilling tests.

Test No	Drill type	Cooling Medium	Cutting Speed, $V$ [m/min]	Feed, $f$ [mm/rev]
1	Uncoated	Cryogenic	10	0.02
2	Uncoated	Dry	10	0.02
3	Uncoated	Wet	10	0.02
4	TiAlN	Cryogenic	10	0.02
5	TiAlN	Dry	10	0.02
6	TiAlN	Wet	10	0.02
7	Uncoated	Cryogenic	15	0.02
8	Uncoated	Dry	15	0.02
9	Uncoated	Wet	15	0.02
10	TiAlN	Cryogenic	15	0.02
11	TiAlN	Dry	15	0.02
12	TiAlN	Wet	15	0.02

Drilling tests under wet cutting environment have been conducted by using an emulsion of the semi-synthetic cutting fluid and water with oil concentration of 5 % and water concentration of 95%. Cryogenic drilling tests were carried out by the aid of a cryogenic cooling setup. Liquid nitrogen ( $LN_2$ ) was used as a cooling agent. A pressure gauge and a relief valve were used to monitor and control the pressure of the cooling system to keep the  $LN_2$  supply constant for every drilling test. Besides, to provide a user-friendly utilization, the cryogenic cooling setup have been designed with  $LN_2$  on-off control system with the help of a solenoid valve.  $LN_2$  was delivered at a pressure of 1.5 bar from a  $LN_2$  tank and sprayed to the cutting zone through a nozzle with a diameter of 2 mm. The nozzle was fixed on the spindle, and thus, simultaneous motion between nozzle and twist drill was provided. During the tests, thrust force and torque values were also measured using a dynamometer, a charge amplifier, and their software. Schematic representation of the experimental setup of the study including cryogenic cooling setup is given in Figure 2.3.

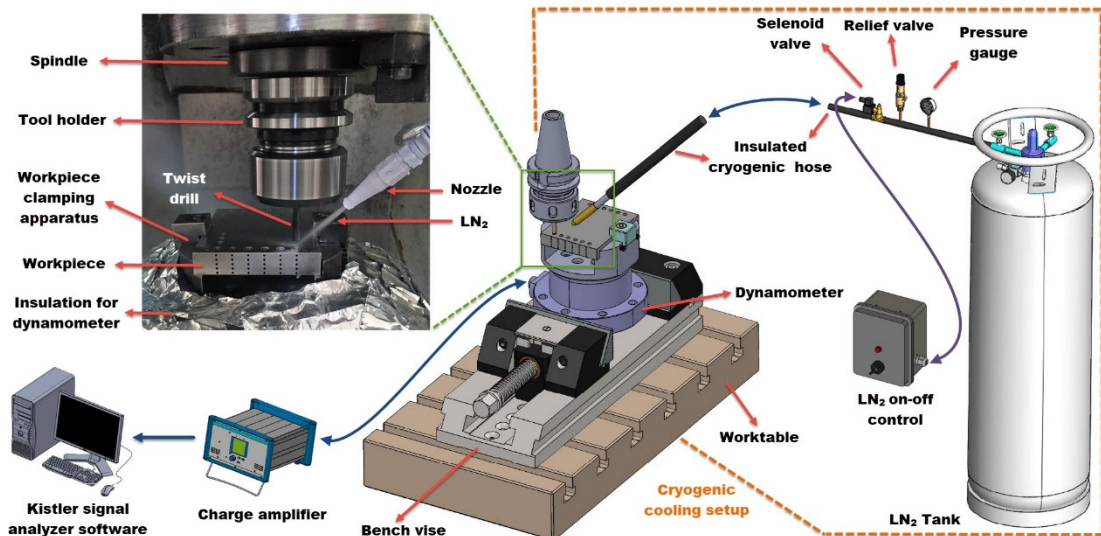


Figure 2.3 Experimental setup.

In order to provide dimensional accuracy for each specimen and to avoid surface defects, all the surfaces of the workpiece were ground to 100 mm x 80 mm x 15 mm. In the wear tests, 50 holes were drilled on a specimen. The distance between the drilled holes were taken equal and far from each other as far as possible. Thus, it was aimed to avoid the effect of work hardening around drilled holes. In order to measure cutting temperature using thermocouples, thermocouple holes with a diameter of 1.5 mm were drilled on two opposite lateral surface of each specimen for insertion of thermocouples. Positions of the test holes and thermocouple holes on a specimen are given in Figure 2.4.

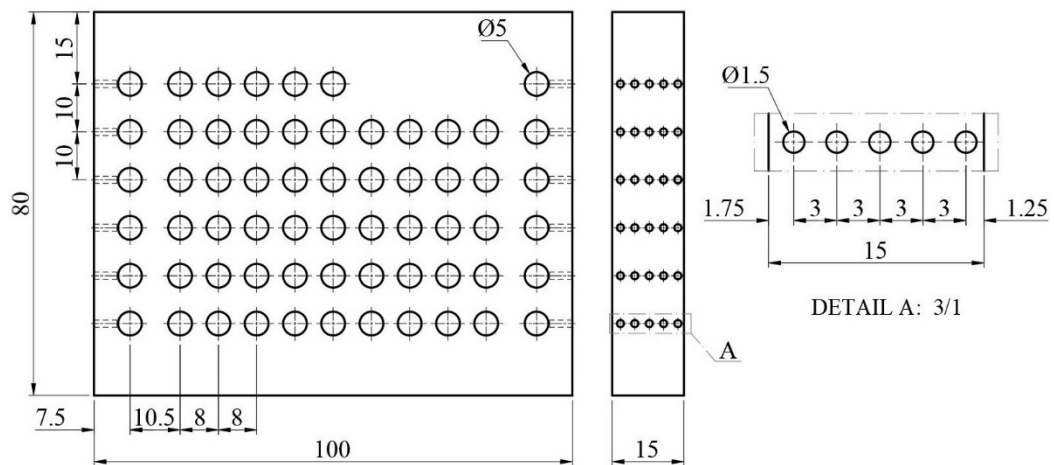


Figure 2.4 Positions of the test holes and thermocouple holes on the specimen.



## 2.4 Cutting Force and Torque

In a drilling process, the thrust force and the torque values give important information about the efficiency of the operation. An increase in the torque and the thrust force values lead to an increase in the power consumption and overall cost of the production. Also, excessive increase in these two values adversely affect the drilling performance. During the drilling tests, a Kistler 9272 4-component dynamometer and Kistler Type 5070A01100 multichannel charge amplifier were used to measure thrust force and torque values in all the test conditions. Data measured by the dynamometer were converted to numerical values through the DynoWare software. Mean values of thrust force and torque values from three drilling operations were accepted as final thrust force and torque values. Technical specifications of the dynamometer and charge amplifier are shown in Table 2.6 and 2.7, respectively. Prior to the tests, dynamometer was calibrated. A custom designed workpiece clamping apparatus was used to provide a rigid clamping of the workpiece on the dynamometer (Figure 2.3). During the tests, the distance between drill bit and tool holder was fixed to 30 mm. In this manner, it was aimed to ensure the same cutting conditions for each drilling operation.

**Table 2.6** Technical specifications of Kistler 9272 4-component dynamometer. [71]

		Technical Data		
Measuring range	$F_x, F_y$	kN	-5 ... 5	
	$F_z$	kN	-5 ... 20	
	$M_z$	N.m	-200 ... 200	
Accuracy	$F_x, F_y$	pC/N	0.02	
	$F_z$	pC/N	0.02	
	$M_z$	pC/N.m	0.02	
Natural frequency	$f_n(x,y)$	kHz	$\approx 3.1$	
	$f_n(z)$	kHz	$\approx 6.3$	
	$f_n(M_z)$	kHz	$\approx 4.2$	
Diameter		mm	100	
Height		mm	70	
Connector		Fischer flange 9-pole		
Degree of protection EN60529		IP67		
Weight		kg	4.2	



**Kistler Type 9272 4-component dynamometer**

**Table 2.7** Technical specifications of Kistler 5070A01100 multichannel charge amplifier. [72]

<b>Technical Data</b>		
Number of channels		8
Connector		Fischer flange 9-pole
Measuring range	pC	200 ... 200000
Frequency range	kHz	$\approx 0 \dots > 45$
Output voltage	V	$\pm 10$
Voltage	V AC	100 ... 240
Interface		RS-232C



**Kistler Type 5070A01100  
multichannel charge amplifier**

## 2.5 Cutting Temperature

The best way to understand the effects of different cooling environments and also cutting parameters on thermal behavior of the drilling process is measurement of the cutting temperature. In this study, cutting temperature was measured from the five different locations throughout the thickness of workpiece during the drilling tests under all cutting conditions. The detailed representation of the temperature measurement setup is schematically given in Figure 2.5. K type (NiCr-Ni) thermocouples with a diameter of 1 mm, which can be measured the temperatures in the range between  $-200\text{ }^{\circ}\text{C}$  and  $1200\text{ }^{\circ}\text{C}$ , were employed for the measurement of cutting temperatures. In order to prevent any deformation during the tests and to get more accurate and reliable measurements under cryogenic temperatures ( $-196\text{ }^{\circ}\text{C}$ ), thermocouples were insulated with Inconel 600 protecting tube. The recordings of the temperatures were monitored on a data logger (E-PR-110, Elimko Co., Turkey). Table 2.8 shows technical specifications of the data logger. A thermocouple clamping apparatus was designed and manufactured in order to position the five thermocouples properly and to firmly fix the thermocouples on the workpiece. The locations of the thermocouples on the workpiece and their clamping conditions are shown in Figure 2.5. The thermocouples were positioned in equal distance from each other (3 mm), and in distance of 1.75 mm from hole entrance (T1) and 1.25 mm from hole exit (T5). Thus, temperature changes throughout the drilled hole can be determined precisely.

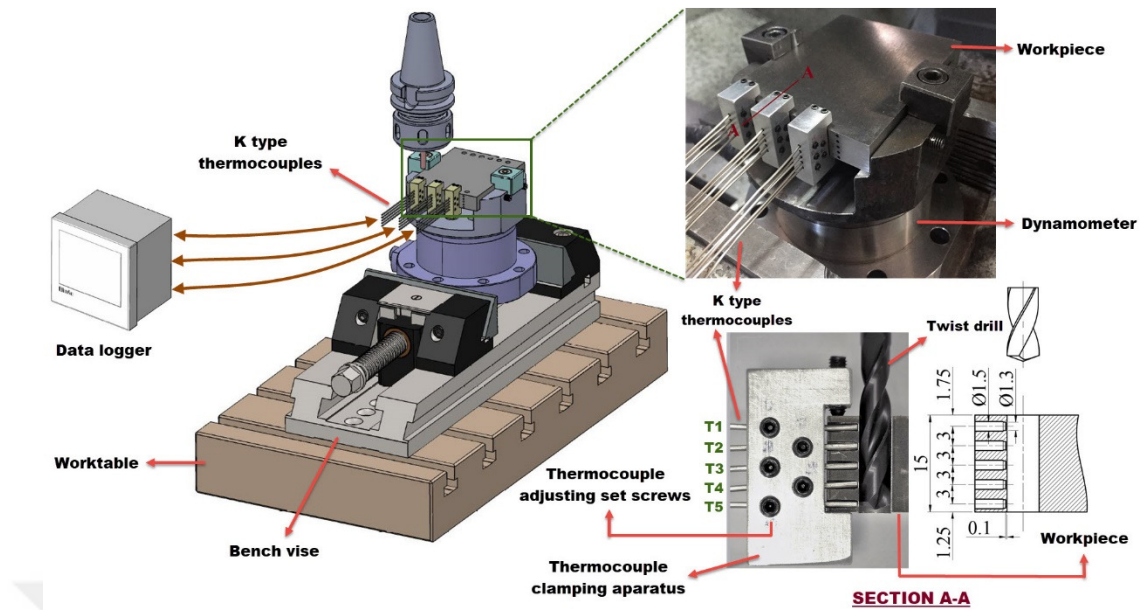
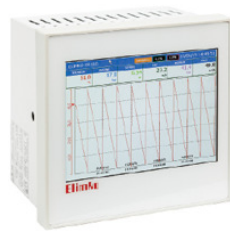


Figure 2.5 Measurement setup for cutting temperature.

Table 2.8 Technical properties of Elimko E-PR-110 data logger [73].

Technical Data		
Accuracy class	0.5	
Analog inputs	15 analog inputs	
Sampling rate	ms	100 (for all channels)
Protection class	Front panel	IP65
	Back panel	IP20
Data storage	8 GB Micro SD Flash Internal	
Voltage	V AC	85 ... 265; 50-60 Hz
Communication	Ethernet, RS-485, 1 USB Host	
Weight	kg	1.6



Elimko E-PR-110-2-2-1-0-0 data logger

The five thermocouples named from T1 to T5 were positioned at approximately a distance of 0.1 mm from the surface of the drilled hole. TiAlN coated tungsten carbide twist drills with a diameter of 1.5 mm and point angle of  $120^\circ$  were used to drill thermocouple holes. After thermocouple holes with a diameter of 1.5 mm were drilled, TiAlN coated tungsten carbide end mills with a diameter of 1.3 mm were used to flatten the bottom of the holes. In this manner, it was aimed to provide a full contact between end surfaces of thermocouples and bottom surfaces of the drilled thermocouple holes. Since it is essential to ensure full contact between thermocouple and workpiece material in the achievement of accurate and reliable results. Figure

2.6 indicates the SEM and digital microscope images of the cross section of the workpiece showing thermocouple holes.

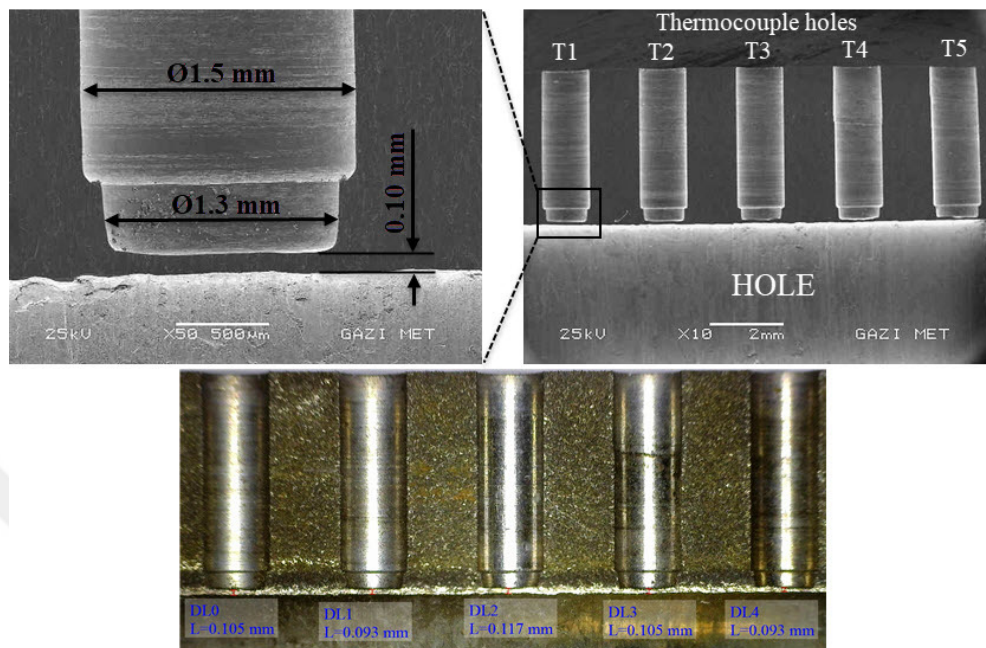


**Figure 2.6** SEM and digital microscope images of the cross section of the workpiece showing positions and dimensions of thermocouple holes.

## 2.6 Surface Roughness

In drilling operations, generally secondary operations such as reaming and grinding are used to obtain desired surface roughness value. However, this situation is time-consuming and leads to extra machining costs. Because of that, it is important to investigate different machining conditions to eliminate these secondary operations. In order to reveal the effects of cutting conditions on surface hole quality, the roughness values of the machined surfaces in each machining condition were measured using a Mitutoyo SurfTest SJ-301 surface roughness tester at Ankara Yıldırım Beyazıt University, Department of Mechanical Engineering, Design & Manufacturing Laboratories. For this purpose, drilled holes were sliced into two parts parallel to the hole axes using a wire electro discharge machine. Three measurements were taken for the both parts of the hole from different locations and their mean value was accepted as the surface roughness value of the hole. Only average surface

roughness value ( $R_a$ ) was evaluated for each measurement. Surface roughness measurement and sliced parts of the specimens are shown in Figure 2.7.

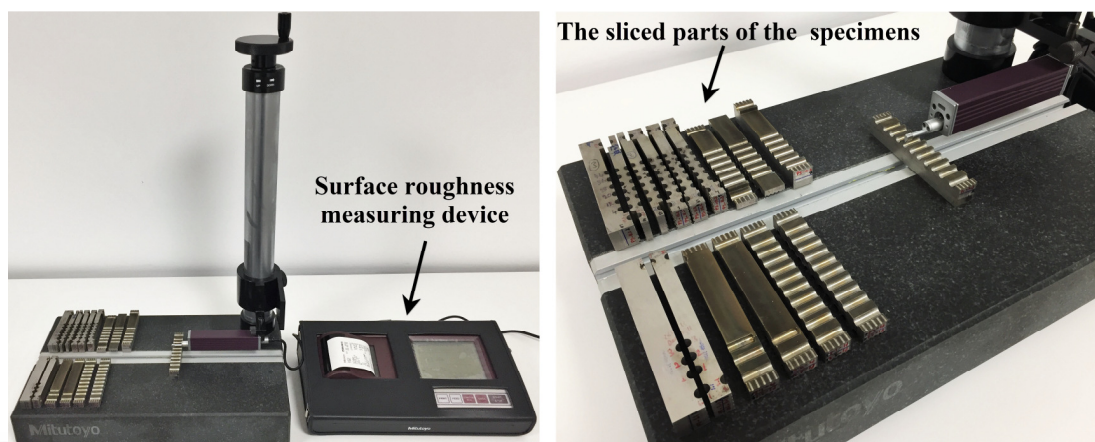


**Figure 2.7** Surface roughness measurement.

## 2.7 Hole Diameter and Roundness Error

In general, drilling is the final process of the production plan of designed parts in a production cycle. Because of that, it is important to obtain desired hole quality after the drilling operation. Hole diameter accuracy, and roundness error are two main criteria to determine the hole quality. Because of that, hole diameter and roundness error values measurements were performed in this study to reveal the effects of different cutting conditions on hole quality when drilling of Inconel 718.

Hole diameters and roundness errors were measured using a DEA Global coordinate measuring machine (CMM). Hole diameters and roundness errors were measured from five points at different depths through the hole. At each point, measurements were performed three times at different locations. Hole diameter and roundness error values were determined as mean values of these measurements, separately. The CMM employed for measurement hole diameter and roundness error is shown in Figure 2.8.

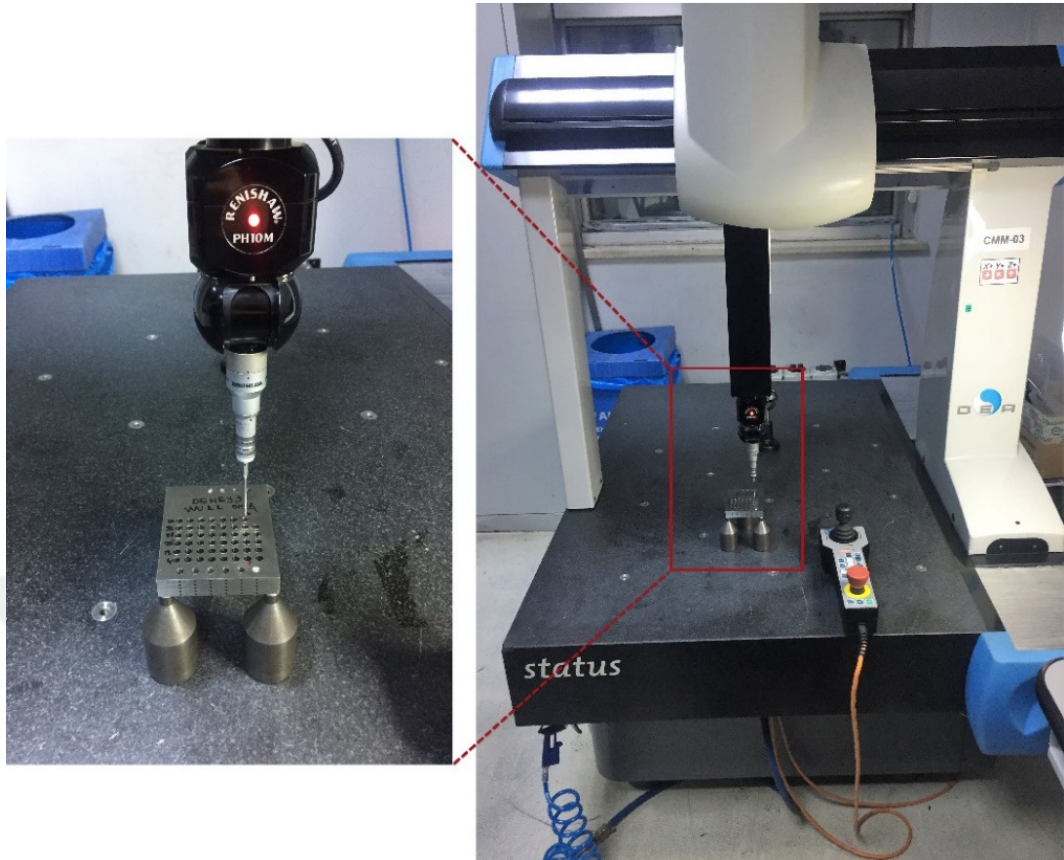


**Figure 2.8** Hole diameter and roughness error measurement.

As well known, the evaluation of the roundness error can be performed using four internationally standardized methods according to ISO 6318: Least Square Circle (LSC) Minimal Zone Circle (MZC), Minimum Circumscribed Circle (MCC) and Maximum Inscribed Circle (MIC) [74]. In this study, roundness error values of the drilled holes were obtained by CMM device using LSC technique. In this method, the theoretical reference circle is fitted inside the profile, such that the sum of the squares of radial coordinates between the circle and the profile is minimized as shown in Figure 2.9. After that, the center of the reference circle is used to draw two circles, inside and outside of the polar profile. Thus, the roundness error value would be determined as the radial separation of these circles [75, 76].

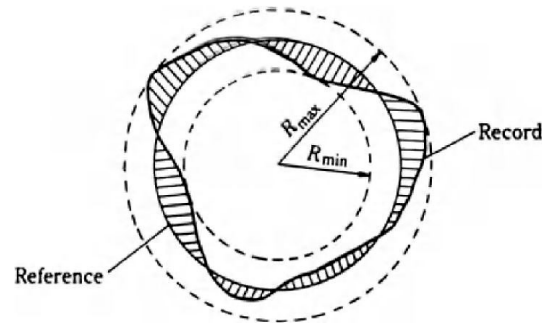


**Figure 2.9** LSC method for roundness error measurement [76].

## 2.8 Burr Formation

In particular, after the drilling operation of the ductile workpiece materials such as Inconel 718 and titanium alloys, burrs form at the entrance and the exit of the hole. Therefore, deburring which is a costly and time-consuming operation is required to obtain desirable finished product quality. Because of that, machining of the components as burr free is an important subject for both industry and academia. For this reason, in order to determine the effects of different cutting conditions on burr formation, burr heights occurred at the entrance and at the exit of the holes were measured by a digital microscope (Dino-Lite AM4113T). Six burr height measurements were taken from the both sliced parts of the workpiece, and mean value of these measurements were accepted as the burr height. This manner was conducted for both entrance and exit burr height measurements. A sample measuring image taken by digital microscope is given in Figure 2.10.

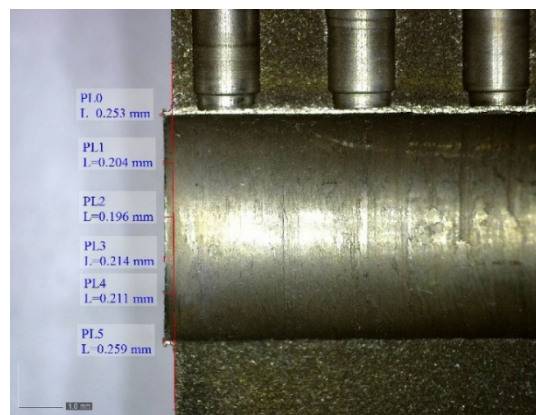


**Figure 2.10** Burr height measurement.

## 2.9 Microstructural Examination and Microhardness

It is important to obtain surface quality having aerospace industry standards in drilling of Inconel 718 with no need to secondary machining operations. Because of that investigation of the hole subsurface condition after drilling operation of Inconel 718 is a critical issue. It is desired to obtain hole subsurface microstructure without white layer formation and plastic deformation in grain structure. The changes in the microstructure of the workpiece and microhardness values beneath the hole surface were analyzed at Ankara Yıldırım Beyazıt University, Department of Materials Engineering, Metallography Laboratory. In order to perform metallographic examinations, the specimens were cut by using a metallographic sample cutting machine. After cutting operation, grinding, and polishing were performed by using a grinding and polishing equipment (Figure 2.11). Specimens were ground with silicon carbide sandpapers with mesh numbers of 320, 600, 800 and 1000, respectively. Then, polishing was performed. Diamond solution with grain size of 3  $\mu\text{m}$  is employed as polishing agent. After polishing, each specimen was etched for 5 s. The composition of the reagent was 100 ml hydrochloric acid, 100 ml water, and 40 ml hydrogen peroxide 30%. The microstructural changes beneath the hole surface were analyzed using an optical microscope (Figure 2.12). Figure 2.13 indicates 200x magnified optical microscope microstructural image of Inconel 178.



**Figure 2.11** Grinding and polishing equipment.



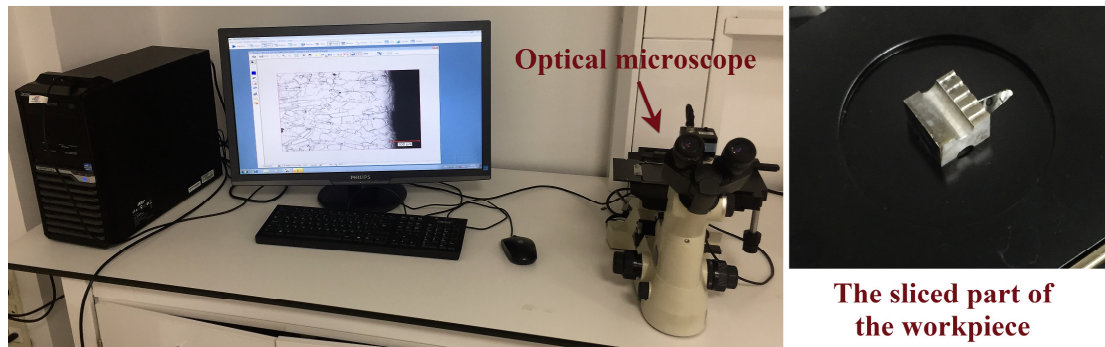


**Figure 2.12** Optical microscope.

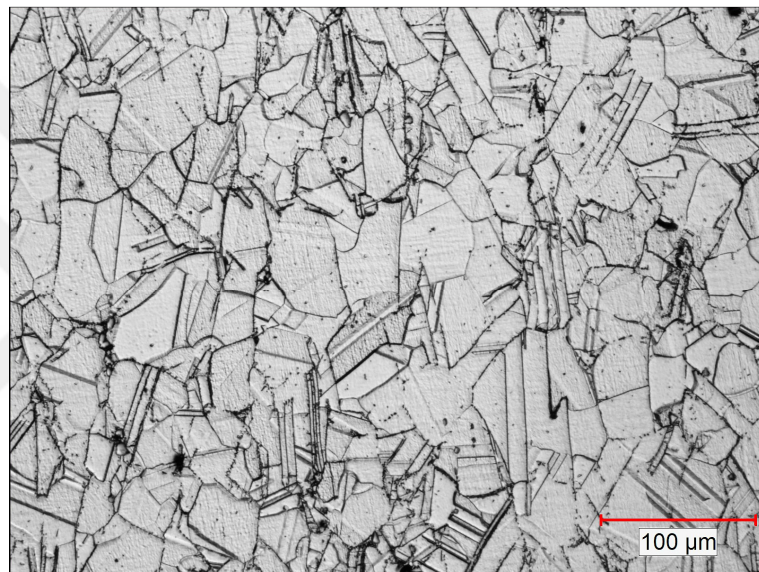


**Figure 2.13** Microstructure of Inconel 718 used in the tests.

One of the major criteria affecting the mechanical properties of Inconel 718 is hardness. Inconel 718 are subjected to high cutting temperature and pressure during machining. Therefore, work hardened layer having higher hardness value than that of bulk material is formed [11]. This formation leads to problems for industrial applications [15]. Machining conditions significantly affect the hardness values. The subsurface microhardness values of specimens were measured using a HMV-G21 Shimadzu Vickers hardness tester (Figure 2.14). The load of 50 g was applied for 10 s to workpiece materials for the hardness test. First microhardness measurements were conducted at a distance of 40 μm from the test hole surface and ten measurements were taken with a distance of 40 μm between each measurement.

These measurements were taken from the entrance, the middle and the exit of the drilled holes and mean value of these values was accepted as microhardness value of the subsurface of the test hole wall. Optical microscope image of the microhardness measurements is given in Figure 2.15.

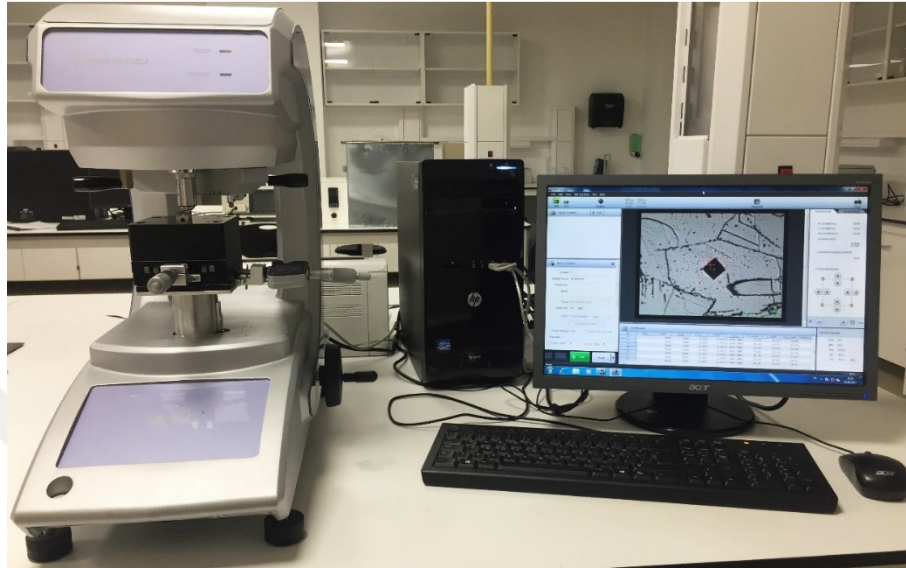


**Figure 2.14** Vickers hardness tester.

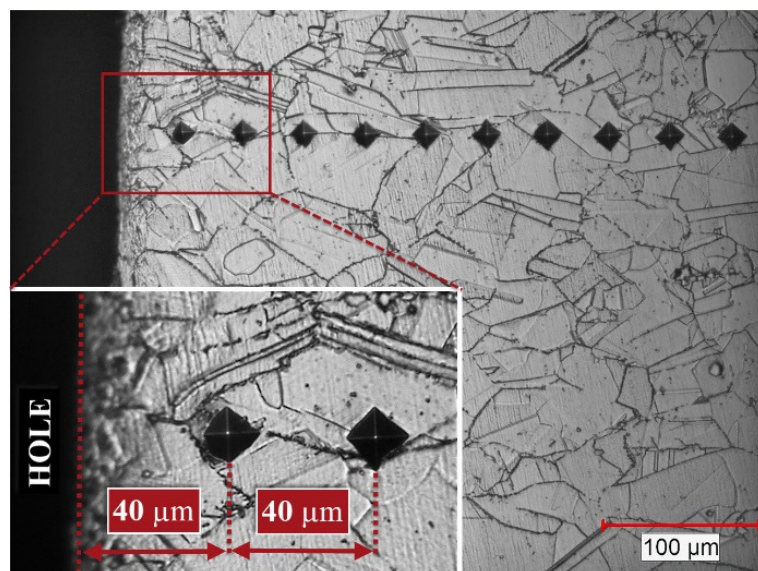


**Figure 2.15** Microhardness measurements.

## 2.10 Tool Wear

Tool wear leads to loss of original geometry of the cutting tool and results in a reduction in the cutting performance or failure of the operation. Generally, in drilling operations high thrust force values and undesirable surface finish are related with excessive wear of the drill. Because of that it is important to perform drilling operations under optimum cutting conditions to obtain desirable tool life and finish surface quality. In this study, tool wear examinations were performed on the twist drills to determine the effects of cutting conditions on the cutting tool life. A digital microscope (Dino-Lite AM4113T) was used to measure cutting tool flank wear. Figure 2.16 shows the tool wear measurement method from the flank of the twist drill. SEM analysis was also performed to determine the wear types on the drills and the relations between the performance test results and the machining conditions.

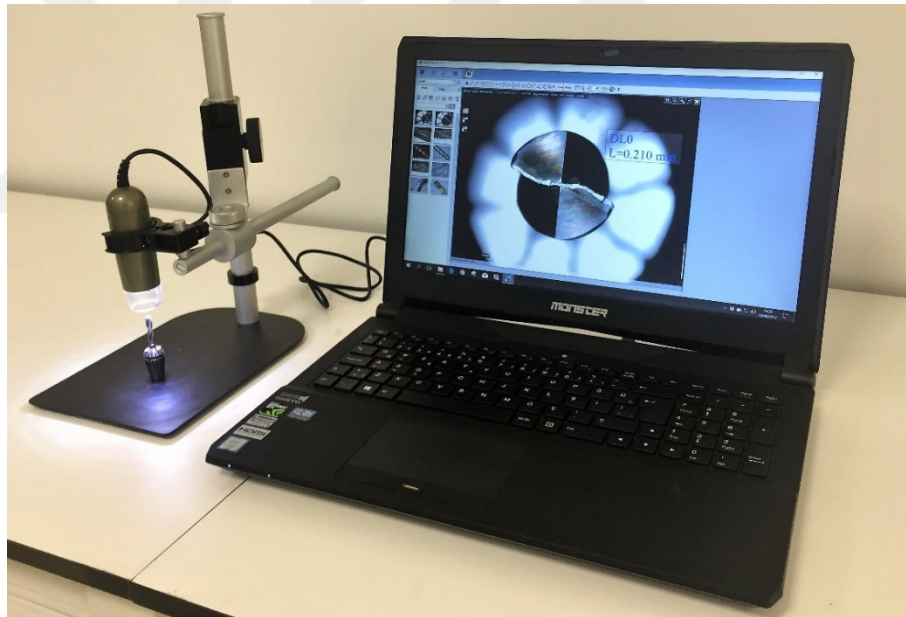


**Figure 2.16** Measurement of the tool wear on a digital microscope.

# CHAPTER 3

## RESULTS AND DISCUSSION

In this chapter, the drillability of Inconel 718 under different cutting conditions is discussed according to some performance evaluation criteria. The machinability evaluation variables are thrust force, torque, cutting temperature, surface roughness, hole diameter and roundness errors, burr formation, hole subsurface examinations, tool wear and tool life.

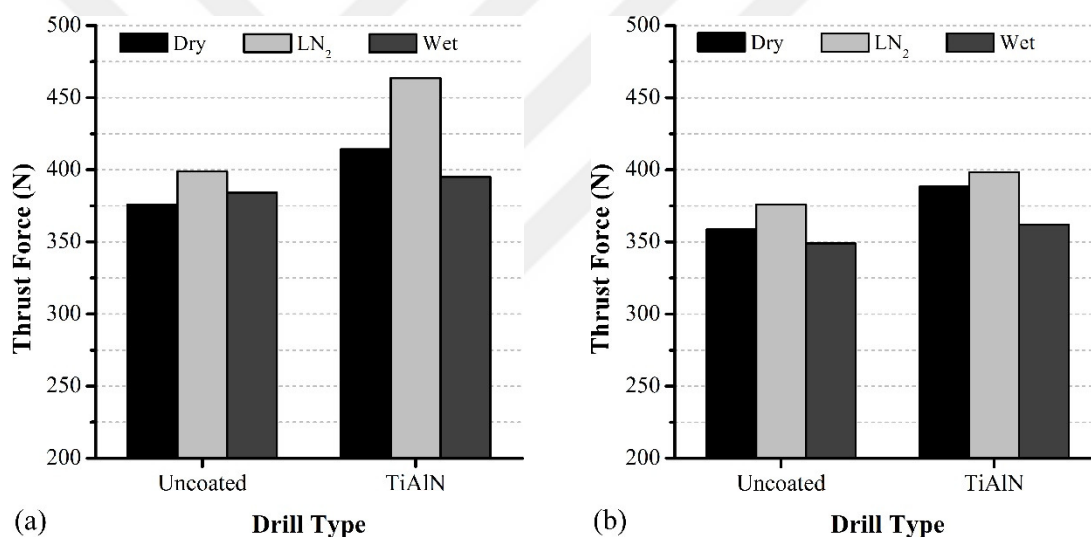
### 3.1 Cutting Force and Torque

The test results showed that the application of cooling/lubrication agents has an important influence on thrust force and torque in drilling operation. The average of thrust force values under different cutting conditions are given in Figure 3.1. Cryogenic cooling increased the thrust force between 4% and 18% at 10 m/min, and in the range of 3% and 10% at 15 m/min. In cryogenic machining, low temperatures make the workpiece material stronger and harder, thus cutting forces tend to increase [77]. Although some studies emphasize that cryogenic drilling leads to a reduction in the thrust force [27], experimental findings on cryogenic drilling of Inconel 718 showed that cryogenic conditions increase the material resistance to plastic deformation due to embrittlement at very low temperatures which result in higher thrust force values [29]. On the other hand, thrust force values under wet conditions are lower than the other machining environments almost all conditions. In general, the cutting forces and lubrication are related to each other in machining of engineering materials. During machining, adequate lubrication decreases the friction and adhesions in tool-chip and tool-workpiece interfaces. Therefore this situation usually results in a decline of the cutting forces [77, 78].

With the increase of the cutting speed from 10 m/min to 15 m/min, the thrust force values reduced at all cutting conditions as shown in Figure 3.1. The test results showed that these decreases are approximately 7% for uncoated drills and 9% for

TiAlN coated drills averagely. This reduction can be attributed to an increase in the cutting temperature with increasing cutting speed. Because higher cutting speeds lead to a reduction in the shear strength and hardness of the workpiece material in the shear zone. Besides, the frictions between the tool-chip and tool-workpiece interfaces also reduced with an increase in cutting temperature. Therefore, all these factors lead to a reduction in the thrust force values [79].

Coating material led to an increase in thrust force values in all machining conditions. According to test results, TiAlN coating increased the thrust force in the range of 3% and 16% at 10 m/min and 4% and 8% at 15 m/min. This case can be associated with the increasing cutting edge radius with application of the coating material on tungsten carbide substrate.



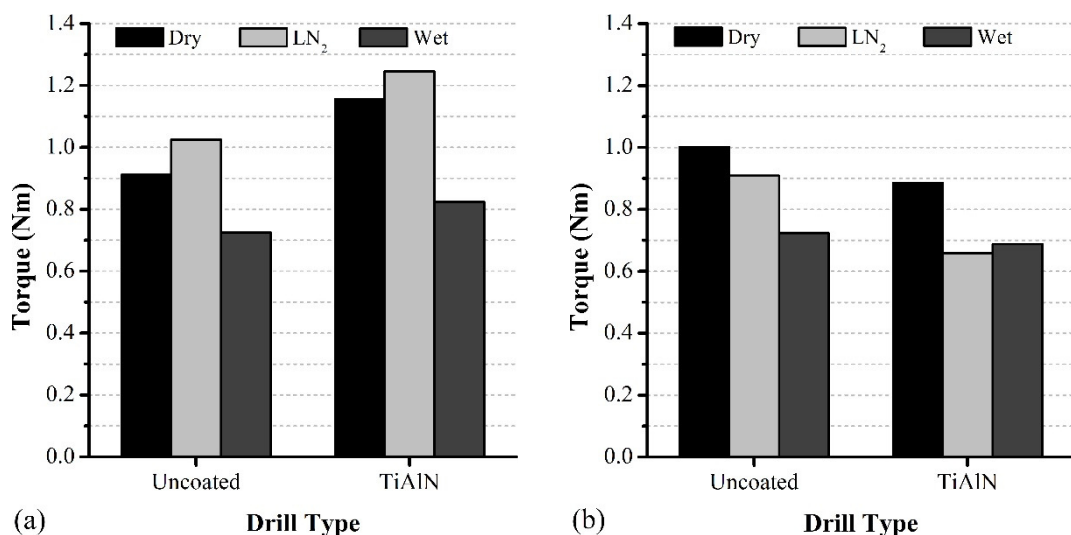
**Figure 3.1** Thrust force values at cutting speeds of a) 10 m/min, and b) 15 m/min.

Figure 3.2 shows the torque values at all cutting conditions, averagely. According to figure, the torque values were increased in the range of 8% and 51% at cutting speed of 10 m/min under cryogenic conditions in comparison to dry and wet conditions. As mentioned above, cryogenic temperatures can cause to higher torque values due to an increase in the strength and hardness of the workpiece material [34]. On the other hand, the torque values under wet cutting conditions exhibit a similar trend with the

thrust force results. Lubrication effect of the cutting fluid played a major role on lower torque values.

In addition, it was observed that increasing cutting speed dramatically decreased the torque values 11% for uncoated drill and 47% for TiAlN coated drill under cryogenic conditions. This significant reduction can be explained with increasing drilling time at the lower cutting speeds. The workpiece material is subjected to larger amount of LN<sub>2</sub> during the longer drilling process at lower cutting speeds. For this reason, workpiece material becomes harder and stronger at lower cutting speeds under cryogenic conditions. Therefore, it can be said that lower cutting speeds are not suitable for cryogenic conditions. On the other hand, torque values generally decreased under dry and wet conditions with increasing cutting speed. As discussed previously, an increase in the cutting speed means increasing cutting temperatures. Thus, it is possible to measure lower torque values at higher cutting speeds.

When TiAlN coated drills are used, the torque values increased in the range of 14% and 22% at cutting speed of 10 m/min while they decreased between %5 and 38% at cutting speed of 15 m/min.



**Figure 3.2** Torque values at a) 10 m/min, and b) 15 m/min cutting speeds.

### 3.2 Cutting Temperature

Figure 3.3 and 3.4 present the maximum cutting temperatures for each thermocouple position at cutting speeds of 10 and 15 m/min, respectively. At both cutting speeds, as the drilling depth increased, the temperature, measured by each thermocouple, also increased as expected [23].

Cryogenic cooling decreased the cutting temperatures significantly when compared to the dry and wet conditions. According to measurements, the maximum cutting temperatures were measured as by about  $-31^{\circ}\text{C}$  under cryogenic,  $62.25^{\circ}\text{C}$  under wet and  $182.85^{\circ}\text{C}$  under dry conditions at 10 m/min. The coating material also affected the cutting temperatures. As shown in Figure 3.3, lower cutting temperatures were generally recorded at all thermocouple locations when uncoated drills are used in the drilling process. This can be attributed to higher thermal conductivity of uncoated carbide drills than that of coating materials (TiAlN) at longer drilling times.

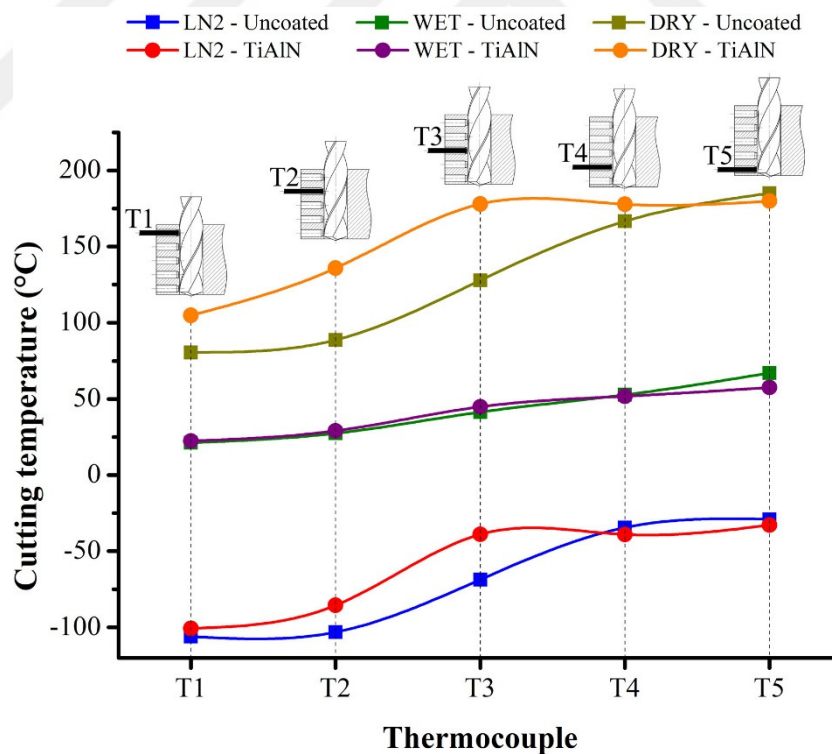
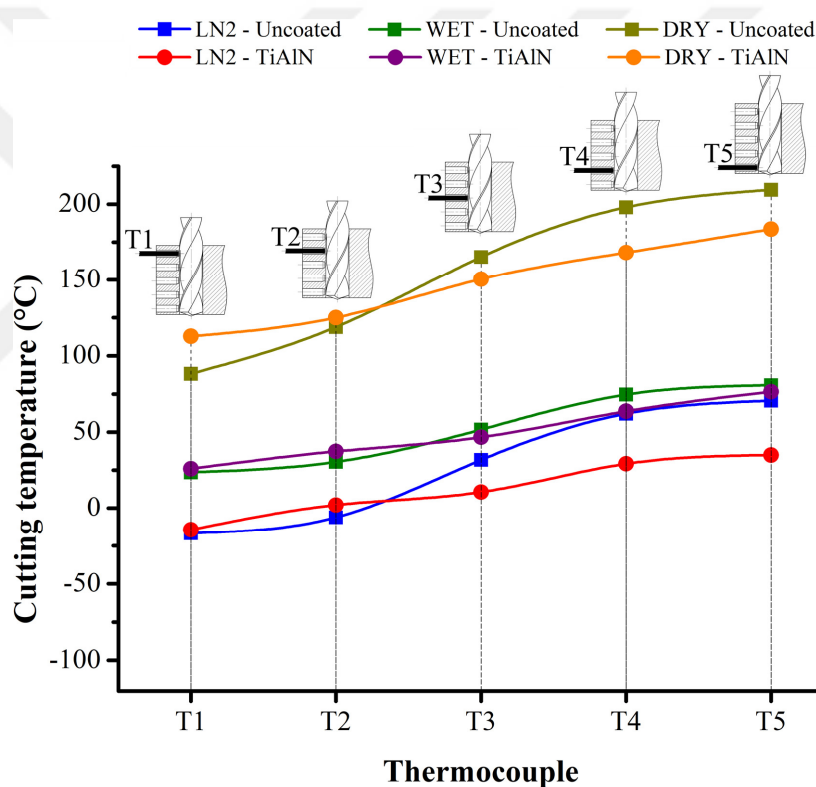


Figure 3.3 Cutting temperature values under different machining conditions at 10 m/min.

On the other hand, the cutting temperatures increased with increasing cutting speed due to an increase in strain rate of workpiece material at higher cutting speeds. As indicated in Figure 3.4, under cryogenic, wet, and dry conditions, the maximum cutting temperatures at cutting speed of 15 m/min were measured as approximately 53°C, 79 °C, and 196.55 °C, respectively. It was observed that the increases in cutting speed increased the amount of temperature rise in uncoated drills and resulted in higher cutting temperatures than TiAlN coated ones. This situation shows the superiority of TiAlN coated drills over uncoated ones at higher cutting speeds. It is due to low friction coefficient of coating material, which can help decreasing the cutting temperature by easier chip formation [47].



**Figure 3.4** Cutting temperature values under different machining conditions at 15 m/min.

The behavior of the material is affected by temperature during machining. High cutting temperatures reduce yield strength of workpiece material and thus, the cutting forces decrease [26]. Therefore, the cutting temperature records in this study are good evidences to the decreases in thrust force and torque values with increasing cutting temperatures. Besides, the subzero temperatures measured at 10 m/min under



cryogenic cooling environment are the reason of the highest thrust force and torque values.

Literature survey showed that cryogenic cooling could be applied internally [29] or externally [37] in drilling operations. Although cryogenic cooling was performed externally in this study, the recorded cutting temperatures under cryogenic conditions were always below the cutting temperatures of the other cutting conditions in each thermocouple locations.

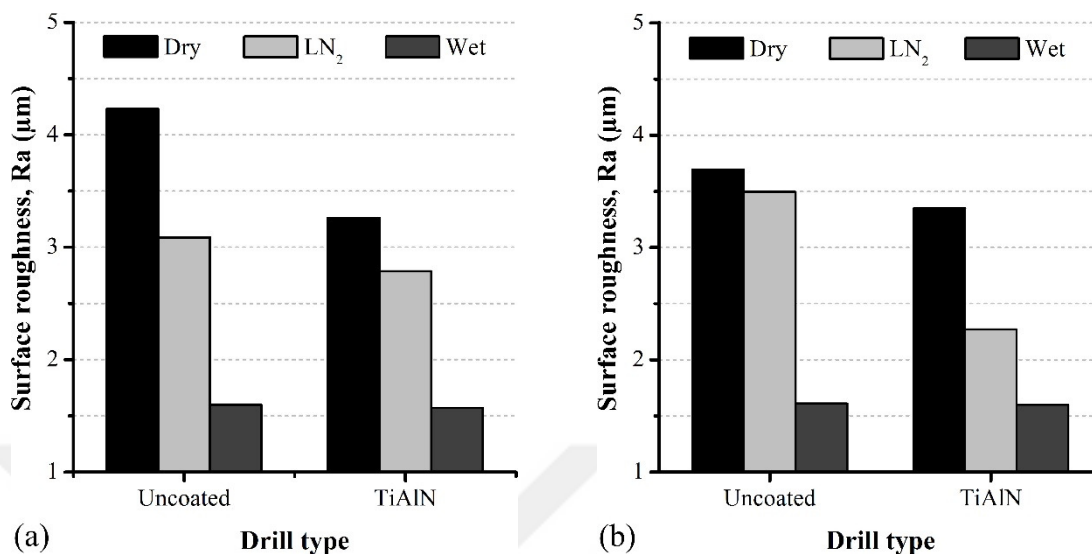
### **3.3 Surface Roughness**

Figure 3.5 shows the average surface roughness values under different cutting conditions. The lowest values were obtained under wet conditions with an improvement in the range of 178% - 265% at 10 m/min, and 142% - 229% at 15 m/min. This can be explained with sufficient cooling and lubrication effects of wet cutting conditions at the chip-tool and tool-workpiece interfaces [11]. Although surface roughness values in cryogenic drilling are better than those in dry drilling, desired surface roughness values could not be reached. Therefore, it can be concluded that the combination of cooling and lubrication effects in wet conditions rather than effective cooling in cryogenic conditions should be primary consideration to obtain desirable surface quality in drilling of Inconel 718.

In general, an increase in the cutting speed from 10 m/min to 15 m/min affected the surface roughness slightly (up to 2%) under wet machining conditions. The surface roughness values decreased up to 21% and 26%, respectively under dry and cryogenic conditions.

The coating material enhanced the surface roughness in all cutting conditions. According to test results, TiAlN coating decreased the surface roughness values between 2% and 23% at 10 m/min, and 1% and 35% at 15 m/min. One of the purposes of using the coating material is to enhance the resistance to abrasion, adhesion, diffusion, and oxidation wear mechanisms [47]. In general, lower wear amounts result in better surface roughness of the machined surface. For this reason,

achievement of smoother surfaces can be associated with increased wear resistance of drills with the coating material.



**Figure 3.5** Surface roughness values at a) 10 m/min and b) 15 m/min cutting speeds

It is well-known that higher cutting forces reduce the cutting tool life due to excessive chippings, and increase chatter, therefore rougher surface values are obtained [12]. However, test results showed that although higher thrust force values were recorded under cryogenic machining conditions, the surface roughness values are better than the dry machining conditions. It can be explained that high temperatures and lack of cooling and lubrication during drilling resulted in adhesion or welding of the chips on the hole surface and deteriorated the machined surface under dry drilling conditions, whereas smoother hole surface was obtained under cryogenic drilling conditions due to effective cooling. On the other hand, cooling and lubrication effects of wet cutting conditions provided to get better surface roughness than the others. This situation is shown on the cross-sectional SEM images of holes for these three cutting conditions in Figure 3.6. Adhered or welded chips are seen in dry conditions due to excessive BUE formation. On the other hand, scratches are clearly seen in cryogenic conditions. This can be associated with worn drill (excessive chippings), higher thrust force values [11] and hard chip evacuation because chips are more brittle under very low temperatures and they could cause to scratches on the machined surface during chip evacuation.

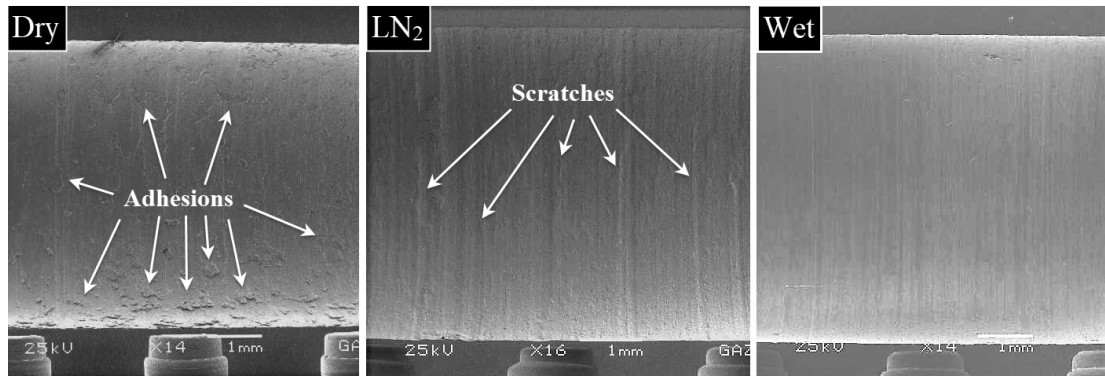


**Figure 3.6** Cross-sectional SEM images of the holes under different cutting conditions.

### 3.4 Hole Diameter and Roundness Error

Figure 3.7 shows the average hole diameter values under different cutting conditions. As shown in the figure, although there is not much difference between the measured diameters (between 5.018 – 5.035 mm), more accurate hole diameter values were obtained under cryogenic conditions. On the other side, dry conditions caused larger hole diameter values. The diameter measurement results are found parallel to the cutting temperature measurements. Higher temperatures can be a reason for larger hole diameter values under dry cutting conditions due to higher thermal expansion rates [39]. On the other hand, coating material and increasing cutting speed slightly affected the hole diameter.

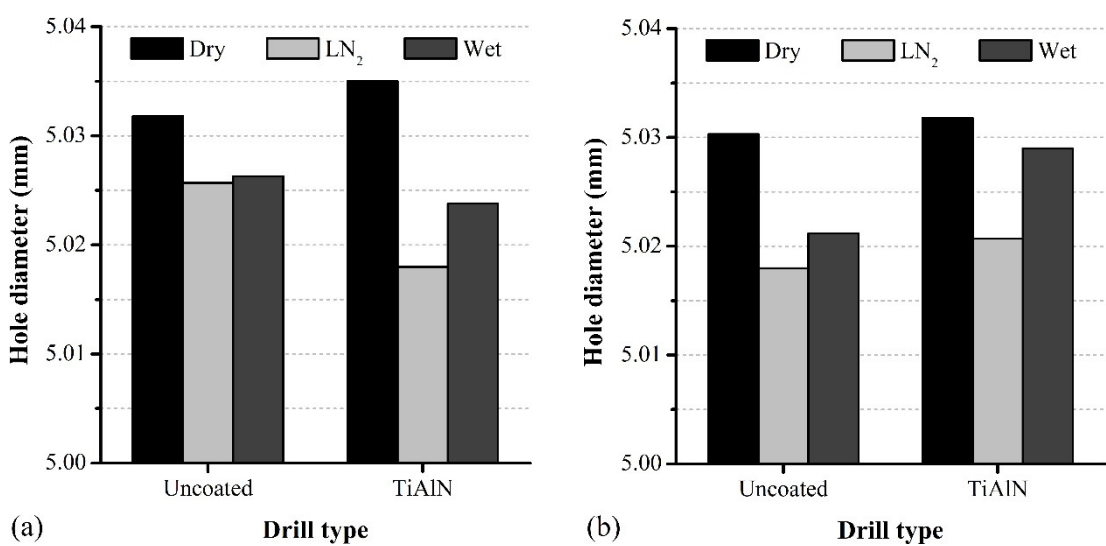


**Figure 3.7** Hole diameter values at a) 10 m/min and b) 15 m/min cutting speeds.

Figure 3.8 indicates the results of the roundness error measurements for each cutting condition, averagely. In general, cryogenic cooling led to a reduction in the roundness errors when compared to other conditions. Cryogenic conditions decreased the roundness error values in the range of 7% and 45% at 10 m/min and 20% and 70% at 15 m/min. As observed in the hole diameter measurement results, dry machining deteriorated the roundness error values at all cutting conditions. Cryogenic conditions reduce thermal expansion of the workpiece material. Therefore it is possible to reduce roundness error and also dimensional error in comparison to dry and wet conditions [37].

On the other hand, coating material enhanced the roundness accuracy between 3% and 35% at 10 m/min and 14% and 36% at 15 m/min. This could be related to improvement in the hardness and wear resistance of drill with coating material [47], because lesser tool wear will result in lower roundness errors.

Even though there is a slight increase (less than 2  $\mu\text{m}$ ) in roundness error under dry condition, the increasing cutting speed significantly reduced the roundness error under wet and cryogenic conditions by approximately 27% and 44%, respectively. This is good evidence for beneficial effects of lubrication and cooling.

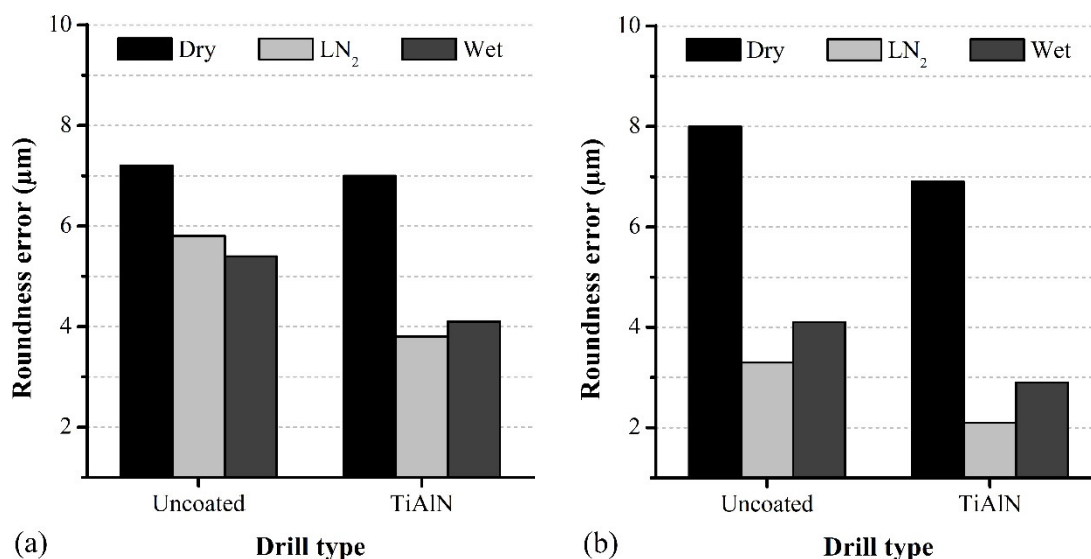


**Figure 3.8** Roundness error values at a) 10 m/min and b) 15 m/min cutting speeds.

### 3.5 Burr Formation

Figure 3.9 and 3.10 indicate the burr height values at the entrance and the exit of the holes, respectively. As indicated in the figure, higher burrs took place in the majority of the cases under dry conditions. This can be explained with increasing thermomechanical loads during the dry drilling process. As reported in the previous discussions, dry machining leads to the highest cutting temperatures and cutting forces when compared to cryogenic and wet conditions. Because of the elevated temperatures during machining, the ductility of the workpiece material increases and this case ends up with higher burr formation. On the other hand, if the burr formation area is cooled sufficiently, this causes more brittle material behavior of the workpiece material thus lower burr formation occurs [80]. Generally, cryogenic cooling caused to lower burr height at both entrance and exit of the holes due to the embrittlement at lower temperatures. According to Figure 3.9, burr height reduction at the entrance of the hole was achieved under cryogenic conditions in the range of 6% and 60 % at 10 m/min and 4% and 27% at 15 m/min. On the other hand, at cutting speed of 15 m/min, cryogenic cooling decreased the burr heights at the exit of the hole up to 54%. However, at cutting speed of 10 m/min, the highest burrs occurred under cryogenic cooling environment (burr heights increased up to 34%). This can be explained with the higher thrust force and torque values at this cutting condition. Cryogenic cooling made the workpiece material more brittle and it is expected to obtain lower burr formation. However, it is thought that high thrust force values caused to higher burr formation.

According to Figure 3.9, increasing cutting speed slightly affected the burr formation at the entrance of the hole (between 2 – 13  $\mu\text{m}$ ). However, this generally caused to a reduction in the burr heights at the exit of the hole (Figure 3.10), up to 18%, 48%, and 63% at dry, wet, and cryogenic conditions, respectively. It can be said that increasing cutting speed from 10 to 15 m/min reduced the burr heights at especially lower cutting temperature conditions.

In general, coating material hardly increased the burr formation (up to 15  $\mu\text{m}$  at 10 m/min, up to 5  $\mu\text{m}$  at 15 m/min,) at the entrance of the hole as shown in Figure 3.9.

On the other hand, TiAlN coating increased the burr formation at the exit of the hole (Figure 3.10) between 59% and 103% at 10 m/min, and 190% and 322% at 15 m/min. This result can be associated with increasing cutting edge radius with usage of coating material and higher thrust force values of coated carbide drills in comparison to uncoated ones. In addition, TiAlN coating material acts as a thermal barrier due its low thermal conductivity

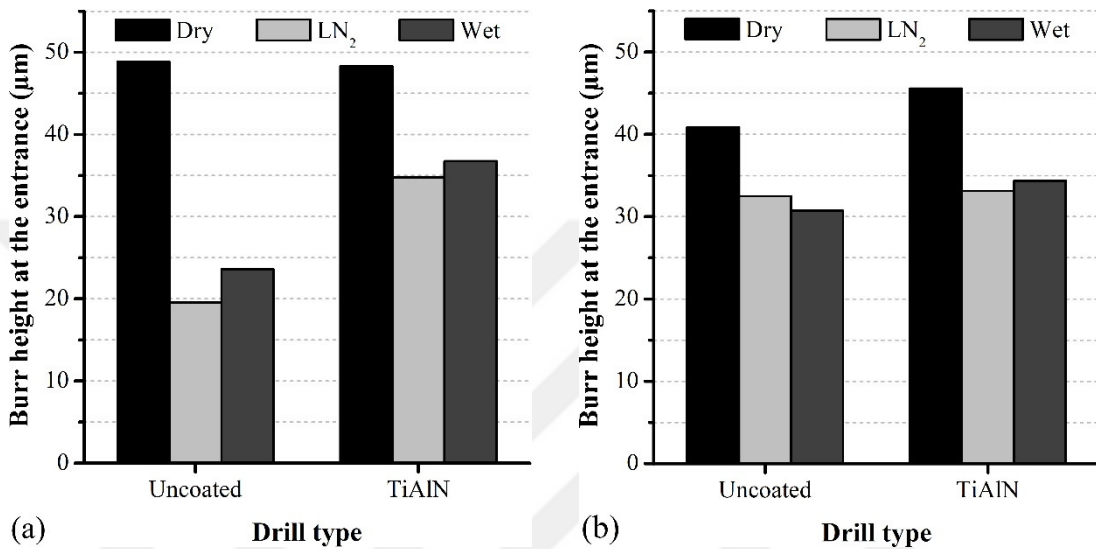


Figure 3.9 Burr height values at the entrance at a) 10 m/min and b) 15 m/min cutting speeds

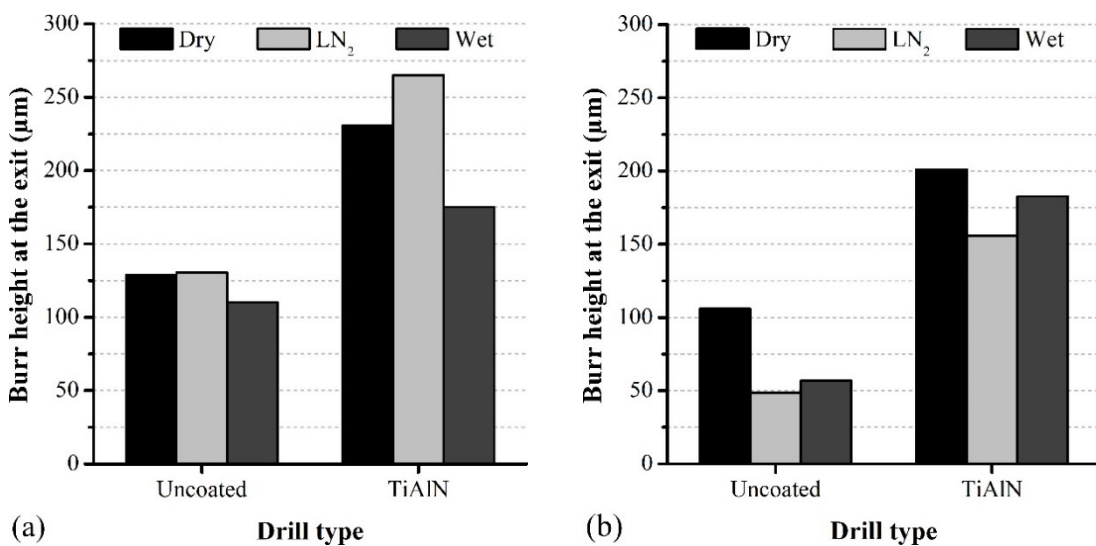
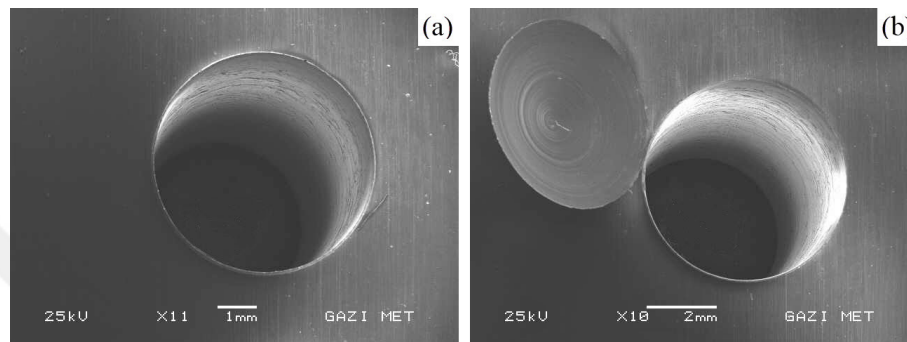


Figure 3.10 Burr height values at the exit at a) 10 m/min and b) 15 m/min cutting speeds

In order to obtain more information about burr formation at the exit of holes, SEM analysis was carried out at the end of the drilling process. According to results of the burr formation examinations, two types of burrs were observed for all conditions: uniform burr formation (Figure 3.11a) and burr with drill cap (Figure 3.11b). Although drilling performances substantially changed the burr heights under different conditions, the burr types are found to be similar. This can be due to the constant feed and low and moderate cutting speeds.



**Figure 3.11** The most common burr types at the exit surface of the holes: a) uniform burr and b) uniform burr with drill cap.

### 3.6 Microstructural Examination and Microhardness

Figure 3.12, 3.13, 3.14, and 3.15 show the microstructural changes and deformation thickness beneath the hole surface under different cutting conditions. As shown in the figures, plastic deformation depends on deformation and alteration of the grain structure beneath the machined surface of the material and occurs due to the sliding motion of the cutting tool during the drilling. Considering the occurred thickness values of the plastic deformation zone after drilling operations, the highest plastic deformation took place under dry conditions. High cutting temperatures and high thrust force values play a major role in high subsurface deformation [81]. The cutting temperature and thrust force values in this study confirm more plastic deformation under dry conditions. Under wet conditions, the measured cutting temperatures and thrust force values were lower, and therefore, a reduction in the thickness of the plastic deformation was observed. On the other hand, plastic deformation depth was minimal under cryogenic conditions (between 7 – 11  $\mu\text{m}$ ). The lesser plastic

deformation thickness was also observed in other studies about turning [48] and milling [69] of Inconel 718 under cryogenic conditions. This can be attributed with increased hardness and less sticky characteristic of the workpiece material.

When the effect of coating material on microstructural changes is investigated, it was observed that there is an increase in the thickness of the affected zone in comparison to uncoated ones. Pu et al. [82] proposed that tools with large cutting edge radius cause to more burnishing effects and alter the subsurface microstructure of the machined surface deeper. Due to this reason, lower plastic deformation depths were observed with uncoated drills. On the other hand, with increase in the cutting speed from 10 m/min to 15 m/min influenced the affected layer thickness in a small amount.

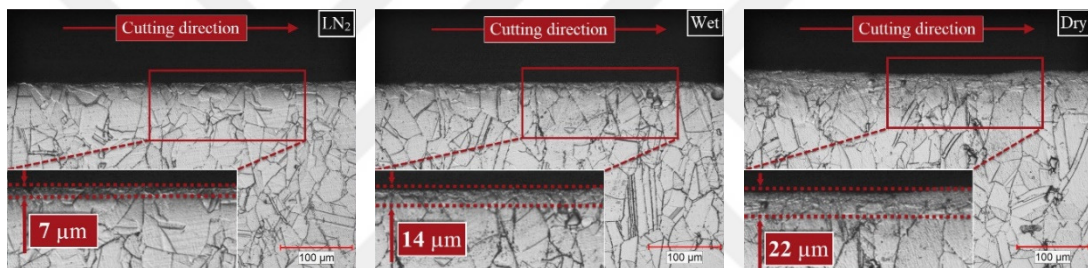


**Figure 3.12** Plastic deformation zone beneath the hole surface at 10 m/min with uncoated twist drill under different cutting environments.

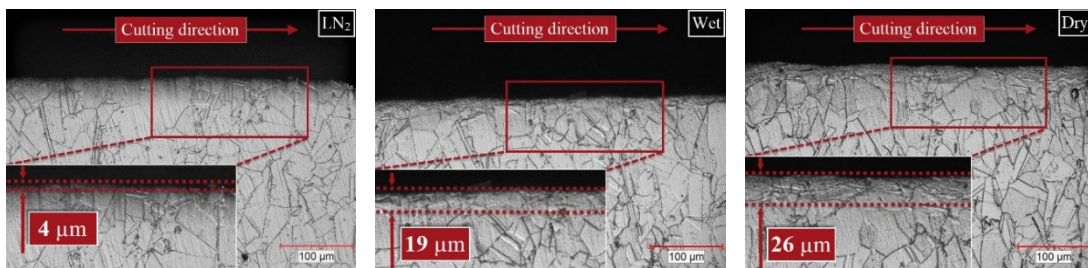


**Figure 3.13** Plastic deformation zone beneath the hole surface at 15 m/min with uncoated twist drill under different cutting environments.



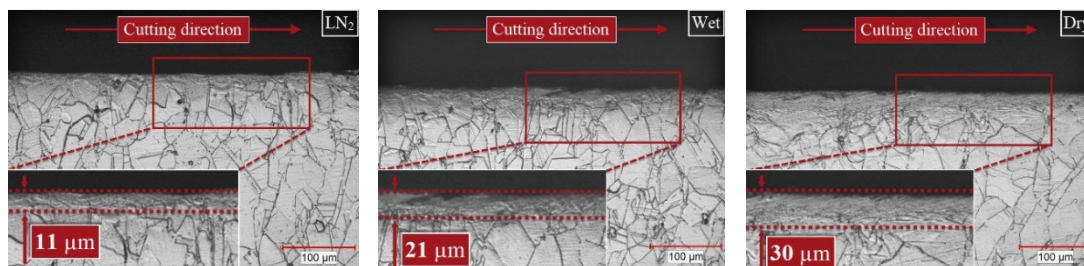


**Figure 3.14** Plastic deformation zone beneath the hole surface at 10 m/min with TiAlN coated twist drill under different cutting environments.

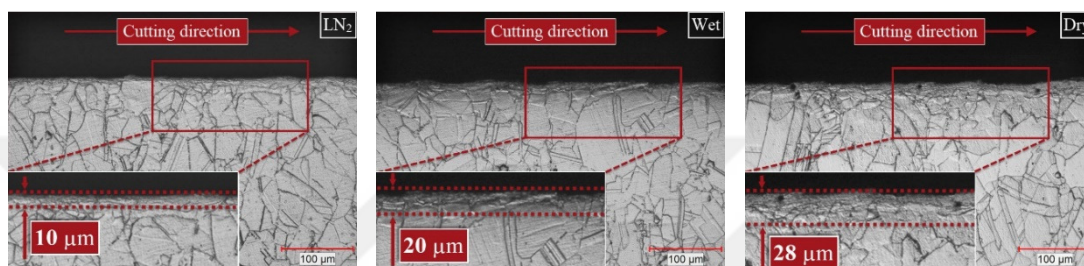


**Figure 3.15** Plastic deformation zone beneath the hole surface at 15 m/min with TiAlN coated twist drill under different cutting environments.

Inconel 718 has an austenitic structure, thus drilling operation induces to work hardening of the deformed zone under the machined surface [1]. Figure 3.16, 3.17, 3.18, and 3.19 show the microhardness values beneath the hole surface under different cutting conditions. After a particular distance from the hole surface (approximately 400  $\mu\text{m}$ ), microhardness measurements reached to the bulk material hardness by about 235 HV. The microhardness measurement results are found to be parallel to microstructure examination findings. Under cryogenic conditions, the lowest microhardness values were achieved. It is well-known that the subsurface hardness of a machined ductile material is dependent on the thickness of the plastically deformed zone [11].

A slight increase in microhardness values was observed with increasing cutting speed, and usage of the TiAlN coated drills, generally. It can be associated with low feed and low and moderate cutting speeds values of the study. Besides, Zhou et al. [81] pointed out that the effect of the cutting parameters and coating materials on the

increases in subsurface damage is significantly less than the that of the cooling conditions. The results of the microstructural examinations verified this information.

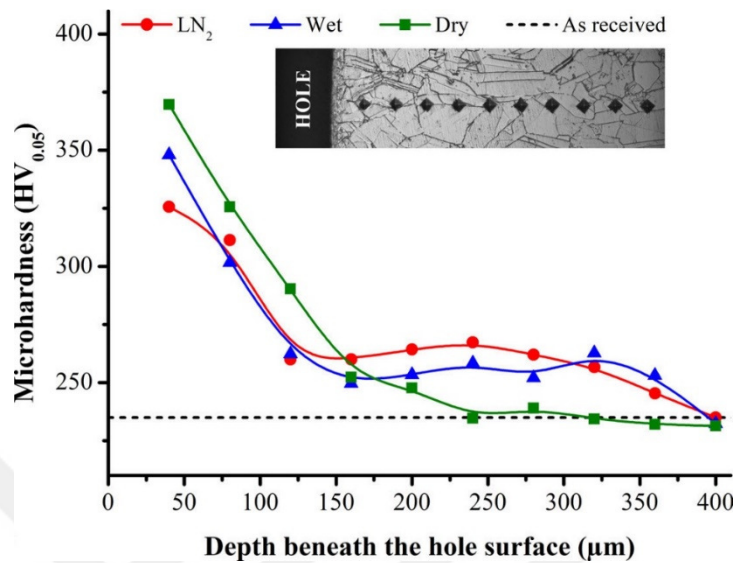


**Figure 3.16** Microhardness values beneath the hole surface under different cooling/lubricating environments with uncoated twist drill at 10 m/min.

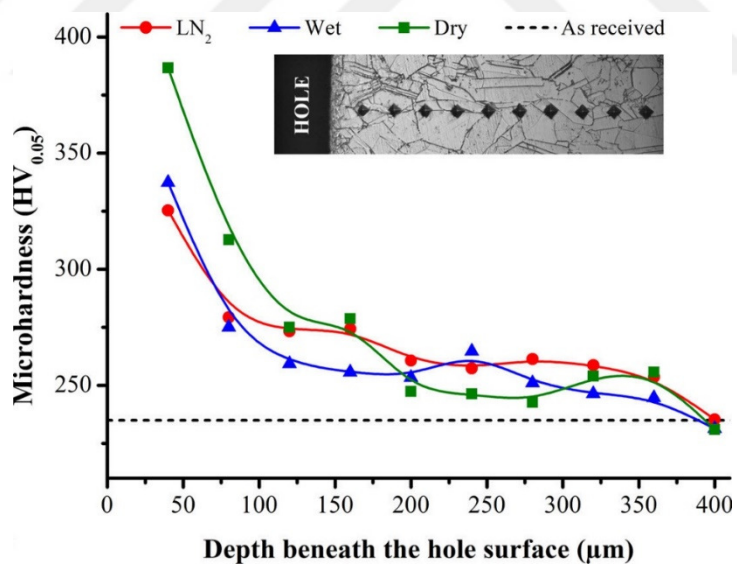


**Figure 3.17** Microhardness values beneath the hole surface under different cooling/lubricating environments with uncoated twist drill at 15 m/min.

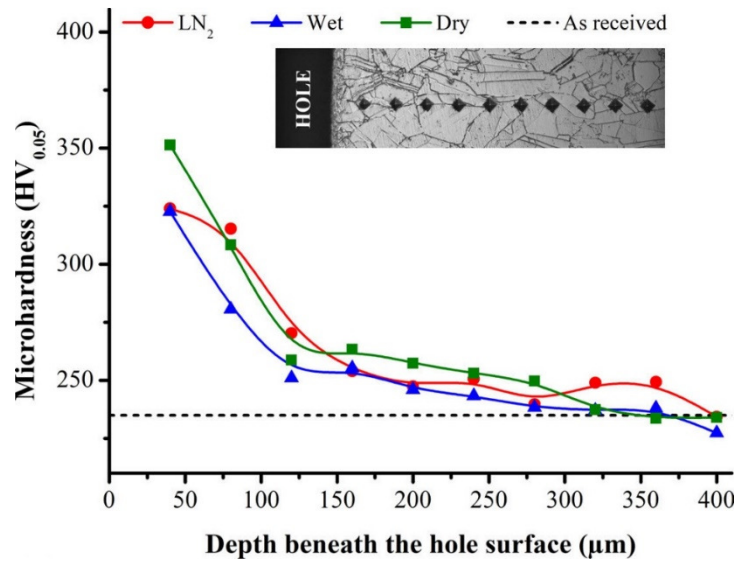


**Figure 3.18** Microhardness values beneath the hole surface under different cooling/lubricating environments with TiAlN coated twist drill at 10 m/min.

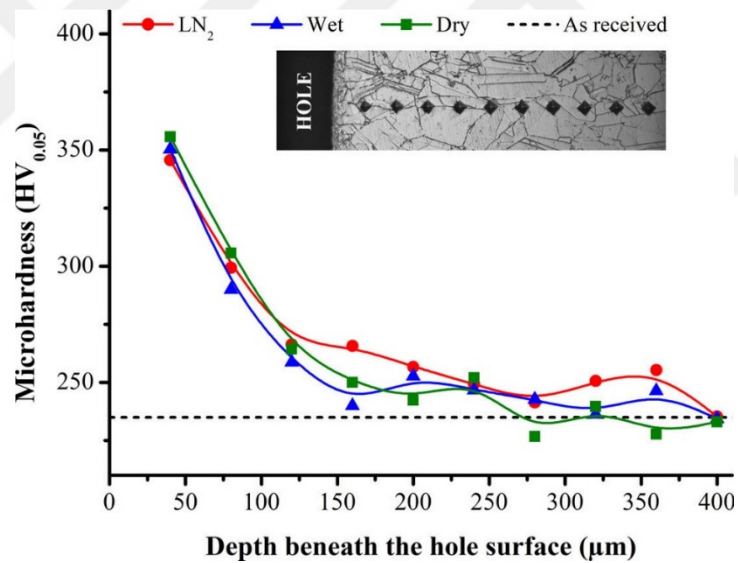


**Figure 3.19** Microhardness values beneath the hole surface under different cooling/lubricating environments with TiAlN coated twist drill at 15 m/min.

### 3.7 Tool Wear

When drilling of Inconel 718, tool wear types found on carbide drills are flank wear, BUE, chipping, corner wear, margin wear, chisel edge wear, and fracture. Figure 3.20, 3.21, and 3.22 show the SEM images of the used uncoated solid carbide twist

drills at cutting speed of 10 m/min under dry, cryogenic, and wet conditions, respectively. Under dry and wet cutting conditions, three holes were drilled, but uncoated twist drill failed without drilling three holes in cryogenic conditions, thus Figure 3.21 show the drill conditions after two drilling. The same situation also occurred for TiAlN coated drill used at 10 m/min under cryogenic cooling condition. It is associated with embrittlement of both tool and workpiece material at very low temperatures during drilling. As explained in the previous sections, high torque and thrust force values occurred under low cutting speed in cryogenic conditions. Because of that severe chipping and tool failure took place under cryogenic conditions. As a result, the desired number of holes could not be reached. Among three cutting conditions, longer tool life was obtained under wet conditions. Cryogenic and dry conditions caused to severe tool wear on the drills at 10 m/min.

In dry machining conditions, the combination of high cutting temperature and high cutting force values result in severe tool wear at 10 m/min. Adhesions of chips, corner wear, margin wear, BUE and fracture can be seen in Figure 3.20. In addition, poor surface quality under dry conditions is directly associated with these excessive tool wear.

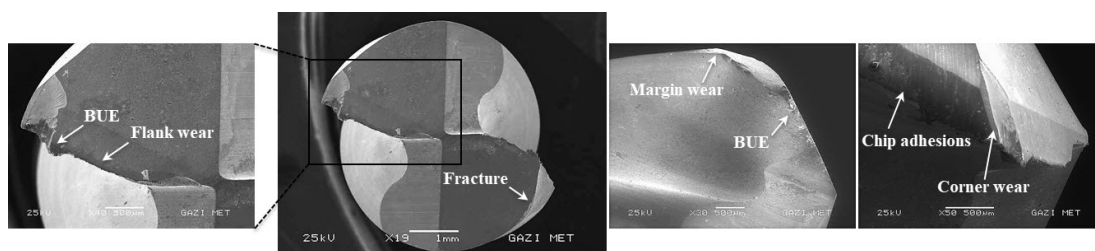


**Figure 3.20** Tool wear types on uncoated twist drill after three holes at 10 m/min under dry conditions.

In cryogenic conditions, low cutting temperatures, high thrust force and torque values led to excessive wear of the cutting tool at 10 m/min. The chippings and fractures on the cutting edges can be observed in Figure 3.21.

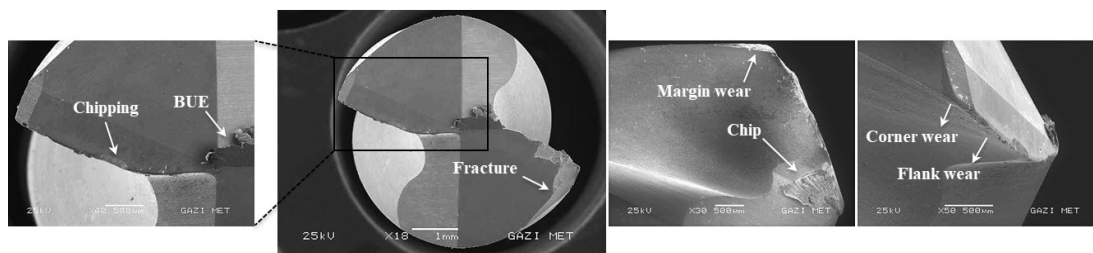


**Figure 3.21** Tool wear types on uncoated twist drill after two holes at 10 m/min under cryogenic conditions.

On the other hand, wet cutting provided the gradual wear of the cutting tool at 10 m/min as shown in Figure 3.22. This can be directly associated with not only cooling but also lubrication effects of wet conditions. Flank wear and chip adhesions occurred in small quantities.

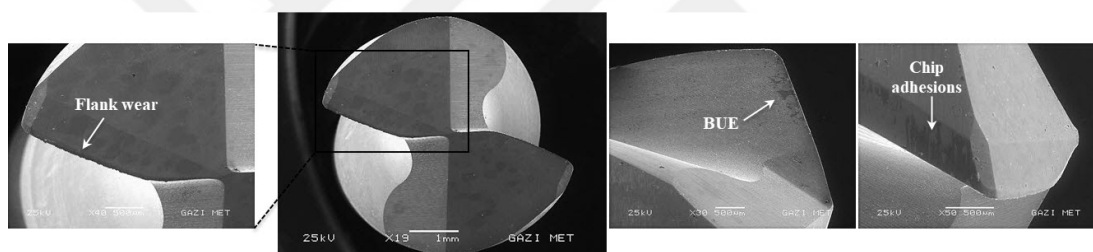


**Figure 3.22** Tool wear types on uncoated twist drill after three holes at 10 m/min under wet conditions.

Figure 3.23, 3.24, and 3.25 show the SEM images of the used TiAlN coated carbide drills after three holes at cutting speed of 15 m/min under dry, cryogenic, and wet conditions, respectively.

In dry machining conditions, higher thrust forces and cutting temperatures caused chisel edge wear, chippings, and non-uniform flank wear as can be observed from Figure 3.23. In addition, BUE and adhered chips on the rake face occurred due to high cutting temperatures, lack of cooling and lubrication and ductile characteristic of workpiece material.

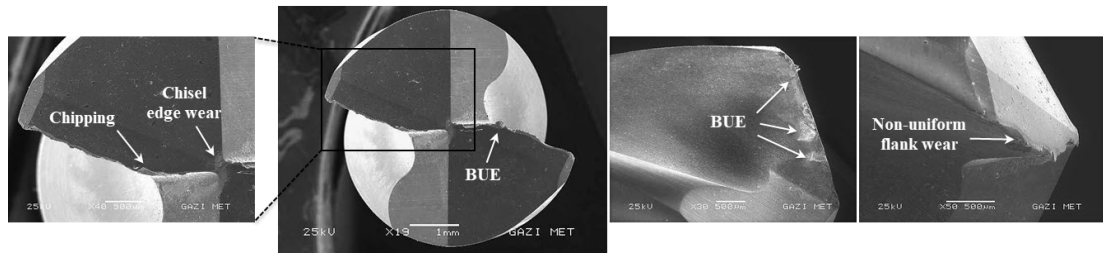


**Figure 3.23** Tool wear types on TiAlN coated twist drill after three holes at 15 m/min under dry conditions.

Chipping was the dominant wear type in cryogenic conditions as shown in Figure 3.24. This can be attributed to very low cutting temperatures under cryogenic conditions. These wear type can also be associated with formations of the scratches on the hole surfaces (Figure 3.6) which result in rougher machined surface. When compared to low cutting speed, fractures were not observed due to moderate lower thrust force and torque values at higher cutting speeds.

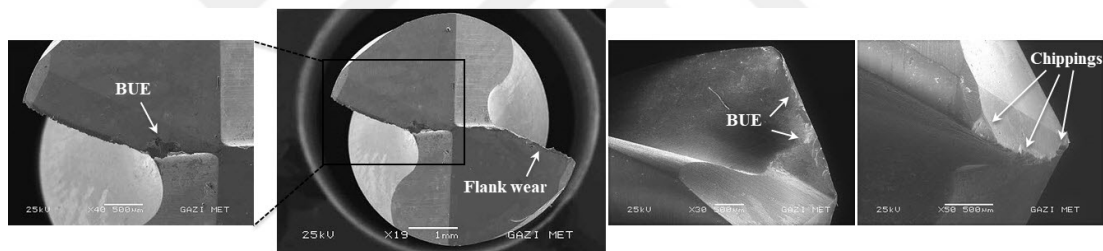


**Figure 3.24** Tool wear types on TiAlN coated twist drill after three holes at 15 m/min under cryogenic conditions.

The best tool performance was observed under wet conditions. In comparison to 10 m/min, chip adhesions and BUE increased due to higher cutting temperatures. The wear types occurred under this cutting condition are given in Figure 3.25.

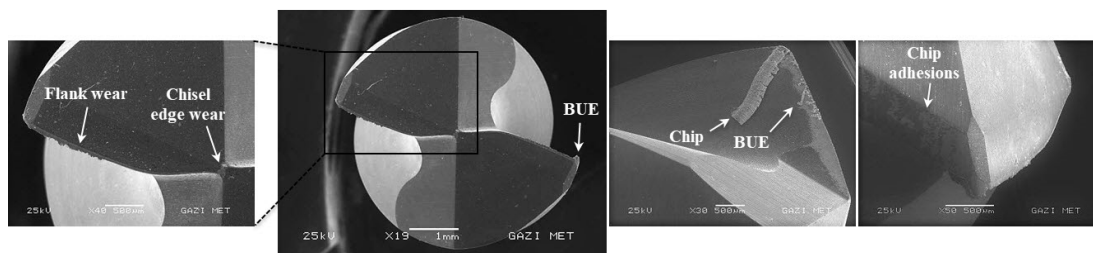


**Figure 3.25** Tool wear types on TiAlN coated twist drill after three holes at 15 m/min under wet conditions.

With the increase of cutting speed from 10 m/min to 15 m/min, the tool life improved under especially cryogenic conditions. Premature failure is observed due to excessive chippings and fractures formed with the effect of higher forces and torques under dry and cryogenic conditions whereas there are regular flank wear and small amount BUE, fractures and chisel edge wear on the twist drills under wet conditions (Figure 3.27 and 3.28). According to test results, uncoated drills failed after 4 and 6 holes under dry and cryogenic conditions, respectively. When TiAlN coated drills were used, they were subjected to catastrophic failure after 6 holes and 20 holes under dry and cryogenic conditions, respectively. On the other hand, carbide drills showed superior tool wear performance under wet conditions when compared to others. Gradual wear (GW), the desired wear mode, was observed under wet conditions without being any catastrophic failure. After fifty holes, according to flank wear measurements, flank wears of 0.21 mm and 0.16 mm formed on uncoated and TiAlN coated drills, respectively (Figure 3.26). Although tool life performances are quite inadequate when compared to wet conditions, cryogenic conditions improved the tool life with respect to dry conditions. TiAlN coated carbide drills significantly outperformed in all machining conditions when compared with uncoated ones due to high hot hardness, low thermal conductivity, good wear resistance and low friction coefficient of TiAlN coating materials. In addition, formation of micro-thin amorphous oxide layer ( $\text{Al}_2\text{O}_3$ ) takes place with the reaction between TiAlN and oxygen in the surrounding air during machining and provides thermal insulation for the cutting tool. Besides  $\text{Al}_2\text{O}_3$  layer behaves like a solid lubricant and decrease the friction between the workpiece and cutting tool. Therefore, the tool life improves [83, 84].

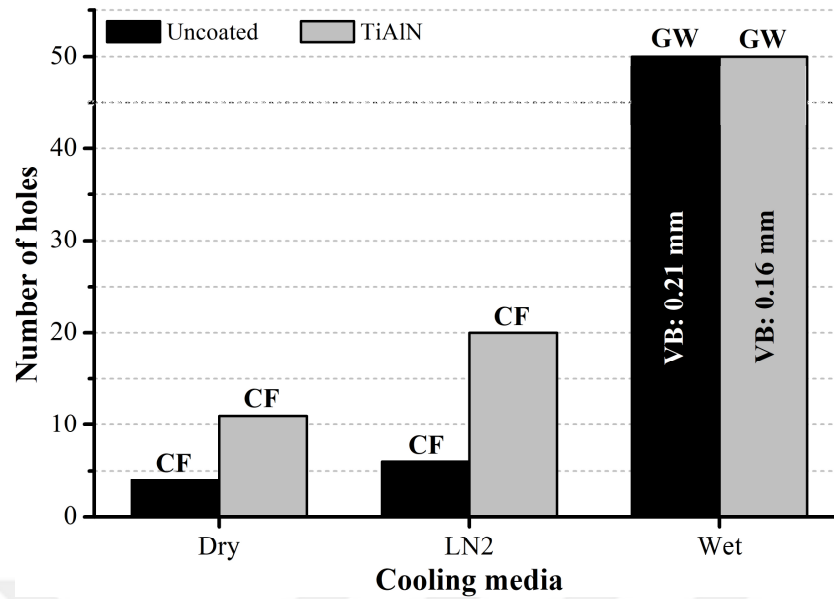


**Figure 3.26** Comparison of tool performances under different cutting conditions.

Figure 3.27, and 3.28 show the SEM images of used uncoated and TiAlN coated carbide drills after fifty holes at cutting speed of 15 m/min under wet conditions, respectively. Gradual flank wear and adhesions were observed for both cutting tools.

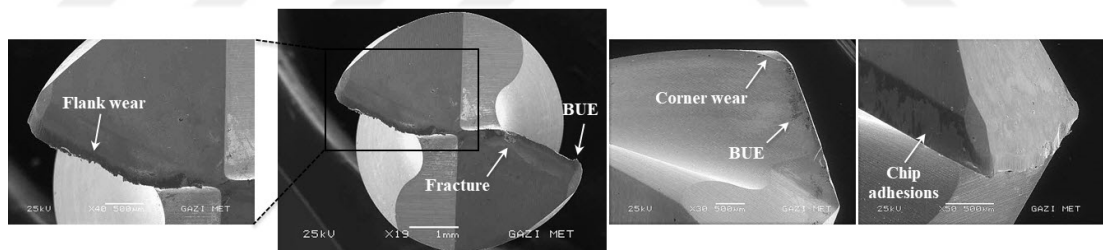


**Figure 3.27** Tool wear types on uncoated twist drill after fifty holes under wet conditions.

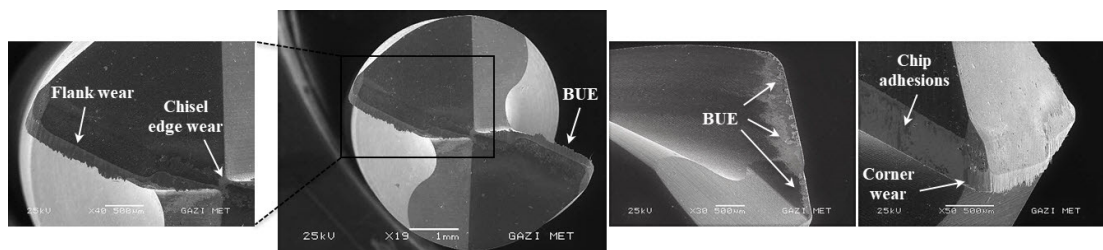


**Figure 3.28** Tool wear types on TiAlN coated twist drill after fifty holes under wet conditions.



# CHAPTER 4

## CONCLUSION AND FUTURE WORK

### 4.1 Summary of The Present Study

In this thesis study, experimental investigations on the influence of different cutting conditions (dry, wet, cryogenic), cutting parameters (cutting speeds 10, 15 m/min; feed 0.02 mm/rev), and coating material (TiAlN) on the drilling of Inconel 718, including thrust force, torque, cutting temperature, hole quality, surface integrity of the hole, tool wear, tool life, etc. have been performed. The advantages of cryogenic machining for different machining operations and engineering materials have been reported in the literature. However, cryogenic drilling of Inconel 718 was rarely investigated. In addition, cutting temperature in drilling operations plays a crucial role to determine the optimal conditions and to interpret obtained results especially for hard-to-cut materials such as Inconel 718. Therefore, these situations are the main focus of this experimental study. The findings of this research work are as follows:

- A significant reduction in cutting temperature by spraying LN<sub>2</sub> onto the tool-workpiece interface improved the hole quality in terms of burr formation, hole diameter accuracy, roundness error, and a decrease in the plastic deformation thickness and microhardness values compared with dry and wet conditions.
- In general, higher thrust force and torque values obtained under cryogenic condition due to increase in hardness and strength of the workpiece material under extremely low temperatures. This result in excessive tool wear and a reduction in the tool life especially at low cutting speed (10 m/min).
- SEM analysis showed that the dominant wear type is chipping in cryogenic machining conditions. This can be attributed with brittle characteristic properties of workpiece and tool materials at significantly low temperatures.
- Cutting temperature measurements and performance evaluation tests confirmed that in dry conditions, absence of cooling and lubrication led to

elevated temperatures in cutting zone, severe cutting tool wear, significant reduction in tool life, excessive burr formation, dimensional and roundness errors, poor surface quality, and increase in plastically deformation zone beneath the hole surface and microhardness values. Therefore, dry conditions have not any advantage in any sense compare to cryogenic and wet conditions.

- In wet conditions, better surface roughness values, lower thrust force and torque values, far better tool wear and tool life, and more stable machining conditions observed compared to dry and cryogenic conditions.
- In general, increase of cutting speed, increased the cutting temperatures, decreased the thrust force and torque values, therefore prolonged the tool life, especially for cryogenic conditions.
- Coating material enhanced the tool life significantly compared with uncoated drills.
- It can be said that significantly low and high cutting temperatures deteriorate the drilling performance in drilling of Inconel 718 at low cutting speeds. It is possible to obtain better hole quality under cryogenic conditions, however there is a need for investigations to prolong cutting tool life.

## **4.2 Future Work**

Experimental study results showed that it is possible to obtain better finish part quality under cryogenic conditions however there is a need to improve tool life performance significantly. For this reason, following suggestions can be used for future works in drilling Inconel 718 to obtain better tool performance:

- Different drill geometries can be tried in order to obtain lower thrust force and torque values under cryogenic conditions.
- Higher cutting speed values can be studied for to determine effective usage of cryogenic cooling.
- Different cooling/lubrication conditions such as cryogenic cooling with liquid CO<sub>2</sub>, or hybrid cooling setups such as cryo-MQL can be investigated to

provide lower cutting temperatures and better lubrication conditions in drilling Inconel 718.



# REFERENCES

- [1] Groover, M. *Fundamentals of Modern Manufacturing Materials, Processes and Systems* (5th ed.). NJ: John Wiley & Sons Inc.. 2010.
- [2] Ezugwu, E. O. Key improvements in the machining of difficult-to-cut aerospace superalloys. *International Journal of Machine Tools and Manufacture*, 45, 1353–1367, 2005.
- [3] Ezugwu, E. O., Wang, Z. M., & Machado, A. R. The machinability of nickel-based alloys: a review. *Journal of Materials Processing Technology*, 86, 1–16, 1999.
- [4] Arunachalam, R., & Mannan, M. A. Machinability of nickel-based high temperature alloys. *Machining Science and Technology*, 4, 127–168, 2000.
- [5] Oezkaya, E., Beer, N., & Biermann, D. Experimental studies and CFD simulation of the internal cooling conditions when drilling Inconel 718. *International Journal of Machine Tools and Manufacture*, 108, 52–65, 2016.
- [6] Sharman, A. R. C., Amarasinghe, A., & Ridgway, K. Tool life and surface integrity aspects when drilling and hole making in Inconel 718. *Journal of Materials Processing Technology*, 200, 424–432, 2008.
- [7] Chen, Y. C., & Liao, Y. S. Study on wear mechanisms in drilling of Inconel 718 superalloy. *Journal of Materials Processing Technology*, 140 (1–3) 269–273, 2003.
- [8] Geddes, B., Leon, H., & Huang, X. *Superalloys: Alloying and Performance* (1st ed.). Ohio: ASM International. 2010.
- [9] Soo, S. L., Hood, R., Aspinwall, D. K., Voice, W. E., & Sage, C. Machinability and surface integrity of RR1000 nickel based superalloy. *CIRP Annals - Manufacturing Technology*, 60, 89–92, 2011.

- [10] Reed, R. C. *The Superalloys Fundamentals and Applications* (1st ed.). New York: Cambridge University Press. (2006).
- [11] Thakur, A., & Gangopadhyay, S. State-of-the-art in surface integrity in machining of nickel-based super alloys. *International Journal of Machine Tools and Manufacture*, 100, 25–54, 2016.
- [12] Shokrani, A., Dhokia, V., & Newman, S. T. Environmentally conscious machining of difficult-to-machine materials with regard to cutting fluids. *International Journal of Machine Tools and Manufacture*, 57, 83–101, 2012.
- [13] Ezugwu, E. O., Bonney, J., & Yamane, Y. An overview of the machinability of aeroengine alloys. *Journal of Materials Processing Technology*, 134, 233–253, 2003.
- [14] M'Saoubi, R., Axinte, D., Soo, S. L., Nobel, C., Attia, H., Kappmeyer, G., et al. High performance cutting of advanced aerospace alloys and composite materials. *CIRP Annals - Manufacturing Technology*, 64, 557–580, 2015.
- [15] Ulutan, D., & Ozel, T. Machining induced surface integrity in titanium and nickel alloys: A review. *International Journal of Machine Tools and Manufacture*, 51 (3), 250–280, 2011.
- [16] Properties of Inconel Alloy 718. (n.d.). Retrieved July 11, 2017, from [http://www.specialmetals.com/assets/smc/documents/inconel\\_alloy\\_718.pdf](http://www.specialmetals.com/assets/smc/documents/inconel_alloy_718.pdf)
- [17] Grzesik, W. *Advanced Machining Processes of Metallic Materials* (1st ed.). Oxford: Elsevier. 2008.
- [18] Dudzinski, D., Devillez, A., Moufki, A., Larrouquère, D., Zerrouki, V., & Vigneau, J. A review of developments towards dry and high speed machining of Inconel 718 alloy. *International Journal of Machine Tools and Manufacture*, 44, 439–456, 2004.
- [19] Altintas, Y. *Manufacturing Automation: Metal Cutting Mechanics, Machine Tool Vibrations, and CNC Design* (2nd ed.). New York: Cambridge

University Press. 2012.

- [20] Berenji, K. R. Mechanistic modeling of drilling forces and study of residual stresses in drilling of compacted graphite iron. Master's thesis, Istanbul Technical University. 2015
- [21] Oberg, E., Jones F. D., Horton, H. L., & Ryffel H. *Machinery's Handbook: A Reference Book For The Mechanical Engineer, Designer, Manufacturing Engineer, Draftsman, Toolmaker, and Machinist* (28th ed.). New York: Industrial Press. 2008.
- [22] El-Hofy G., Abdel H. *Fundamentals of Machining Processes: Conventional and Nonconventional Processes* (2nd ed.). New York: CRC Press. 2013.
- [23] Stephenson, D. A., & Agapiou, J. S. *Metal Cutting Theory and Practice* (3rd ed.). New York: CRC Press. 2016.
- [24] Sandvik Coromat. Wear types in drilling. Retired July 11, 2017, from [http://www.sandvik.coromant.com/en-gb/knowledge/drilling/wear-and-troubleshooting/wear\\_types](http://www.sandvik.coromant.com/en-gb/knowledge/drilling/wear-and-troubleshooting/wear_types)
- [25] Dolinsek, S., Sustarsic, B., & Kopač, J. Wear mechanisms of cutting tools in high-speed cutting processes. *Wear*, 250 (1-12), 349–356, 2001.
- [26] Zeilmann, R. P., & Weingaertner, W. L. Analysis of temperature during drilling of Ti6Al4V with minimal quantity of lubricant. *Journal of Materials Processing Technology*, 179, 124–127, 2006.
- [27] Ahmed, L. S., & Kumar, M. P. Cryogenic drilling of Ti–6Al–4V alloy under liquid nitrogen cooling. *Materials and Manufacturing Processes*, 31, 951–959, 2016.
- [28] Bagci, E., & Ozcelik, B. Effects of different cooling conditions on twist drill temperature. *The International Journal of Advanced Manufacturing Technology*, 34, 867–877, 2007.

- [29] Outeiro, J. C., Lenoir, P., & Bosselut, A. Thermo-mechanical effects in drilling using metal working fluids and cryogenic cooling and their impact in tool performance. *Production Engineering*, 9, 551–562, 2015.
- [30] Cakiroglu, R., & Acir, A.: "Optimization of cutting parameters on drill bit temperature in drilling by Taguchi method". *Measurement*. 46, 3525–3531, 2013.
- [31] Blau, P., Busch, K., Dix, M., Hochmuth, C., Stoll, A., & Wertheim, R. Flushing strategies for high performance, efficient and environmentally friendly cutting. *Procedia CIRP*, 26, 361–366, 2015.
- [32] Lopez De Lacalle, L. N., Perez-Bilbatua, J., Sanchez, J. A., Llorente, J. I., Gutierrez, A., & Alboniga, J. Using high pressure coolant in the drilling and turning of low machinability alloys. *International Journal of Advanced Manufacturing Technology*, 16, 85–91, 2000.
- [33] Aslantas, K., Cicek, A., Uzun, I., Percin, M., & Hopa, H.E. Performance evaluation of a hybrid cooling-lubrication system in micro-milling of Ti6Al4V alloy. *Procedia CIRP*, 492–495, 2016.
- [34] Xia, T., Kaynak, Y., Arvin, C., & Jawahir, I. S. Cryogenic cooling-induced process performance and surface integrity in drilling CFRP composite material. *International Journal of Advanced Manufacturing Technology*, 82, 605–616, 2016.
- [35] Dix, M., Wertheim, R., Schmidt, G., & Hochmuth, C. Modeling of drilling assisted by cryogenic cooling for higher efficiency. *CIRP Annals - Manufacturing Technology*, 63, 73–76, 2014.
- [36] Giasin, K., Ayvar-Soberanis, S., & Hodzic, A. The effects of minimum quantity lubrication and cryogenic liquid nitrogen cooling on drilled hole quality in GLARE fibre metal laminates. *Materials and Design*, 89, 996–1006, 2016.

- [37] Ahmed, L. S., Govindaraju, N., & Pradeep Kumar, M. Experimental investigations on cryogenic cooling in the drilling of titanium alloy. *Materials and Manufacturing Processes*, 31, 603–607, 2016.
- [38] Kheireddine, A. H., Ammouri, A. H., Lu, T., Jawahir, I. S., & Hamade, R. F. An FEM analysis with experimental validation to study the hardness of in-process cryogenically cooled drilled holes in Mg AZ31b. *Procedia CIRP*, 8, 588–593, 2013.
- [39] Biermann, D., & Hartmann, H. Reduction of burr formation in drilling using cryogenic process cooling. *Procedia CIRP*, 3, 85–90, 2012.
- [40] Aramcharoen, A.: "Influence of Cryogenic Cooling on Tool Wear and Chip Formation in Turning of Titanium Alloy". In: *Procedia CIRP*. pp. 83–86 (2016).
- [41] Hong, S. Y., & Zhao, Z. Thermal aspects, material considerations and cooling strategies in cryogenic machining. *Clean Technologies and Environmental Policy*, 1, 107–116, 1999.
- [42] Yildiz, Y., & Nalbant, M. "A review of cryogenic cooling in machining processes. *International Journal of Advanced Manufacturing Technology* , 48, (9), 947-964, 2008.
- [43] Shokrani, A., Dhokia, V., Newman, S. T., & Imani-Asrai, R. An initial study of the effect of using liquid nitrogen coolant on the surface roughness of inconel 718 nickel-based alloy in CNC milling. *Procedia CIRP*, 3, 121–125 2012.
- [44] Boljanovic, V. *Metal Shaping Processes: Casting and Molding, Particulate Processing, Deformation Processes, and Metal Removal* (1st ed.). New York: Industrial Press. 2010.
- [45] Ezugwu, E.O. High speed machining of aero-engine alloys. *Journal of the Brazilian Society of Mechanical Sciences and Engineering*, 26, 1–11, 2004.




- [46] Zhu, D., Zhang, X., & Ding, H. Tool wear characteristics in machining of nickel-based superalloys. *International Journal of Machine Tools and Manufacture*, 64, 60–77, 2013.
- [47] Pervaiz, S., Rashid, A., Deiab, I., & Nicolescu, M. Influence of tool materials on machinability of titanium- and nickel-based alloys: A Review". *Materials and Manufacturing Processes*, 29, 219–252, 2014.
- [48] Pusavec, F., Deshpande, A., Yang, S., M'Saoubi, R., Kopac, J., Dillon, O. W., & Jawahir, I.S.: "Sustainable machining of high temperature nickel alloy - Inconel 718: Part 1 - Predictive performance models. *Journal of Cleaner Production*, 81, 255–269, 2014.
- [49] Sharman, A. R. C., Hughes, J. I., & Ridgway, K. Workpiece surface integrity and tool life issues when turning inconel 718 nickel based superalloy". *Machining Science and Technology*, 8, 399–414, 2004.
- [50] Thakur, D. G., Ramamoorthy, B., & Vijayaraghavan, L. Study on the machinability characteristics of superalloy Inconel 718 during high speed turning. *Materials and Design*, 30, 1718–1725, 2009.
- [51] Li, L., He, N., Wang, M., & Wang, Z. G. High speed cutting of Inconel 718 with coated carbide and ceramic inserts. *Journal of Materials Processing Technology*, 1, (3), 127–130 2002.
- [52] Pawade, R. S., & Joshi, S. S. Multi-objective optimization of surface roughness and cutting forces in high-speed turning of Inconel 718 using Taguchi grey relational analysis (TGRA). *International Journal of Advanced Manufacturing Technology*, 56, 47–62, 2011.
- [53] Thakur, D. G., Ramamoorthy, B., & Vijayaraghavan, L. Effect of cutting parameters on the degree of work hardening and tool life during high-speed machining of Inconel 718. *The International Journal of Advanced Manufacturing Technology*, 59, 483–489, 2012.

- [54] Ma, J., Wang, F. Jia, Z., Xu, Q., & Yang, Y. Y. Study of machining parameter optimization in high speed milling of Inconel 718 curved surface based on cutting force. *International Journal of Advanced Manufacturing Technology*, 75, 269–277, 2014.
- [55] Liao, Y.S., Lin, H.M., & Wang, J.H.: "Behaviors of end milling Inconel 718 superalloy by cemented carbide tools". *Journal of Materials Processing Technology*. 201, 460–465, 2008.
- [56] Kasim, M. S., Che Haron, C. H., Ghani, J. A., Sulaiman, M. A., & Yazid, M. Z. A. Wear mechanism and notch wear location prediction model in ball nose end milling of Inconel 718. *Wear*, 302, 1171–1179, 2013.
- [57] Beer, N., Özkaya, E., & Biermann, D. Drilling of Inconel 718 with geometry-modified twist drills. *Procedia CIRP*, 24, 49–55, 2014.
- [58] Kaynak, Y. Evaluation of machining performance in cryogenic machining of Inconel 718 and comparison with dry and MQL machining". *International Journal of Advanced Manufacturing Technology*, 72, 919–933, 2014.
- [59] Pusavec, F., Hamdi, H., Kopac, J., & Jawahir, I. S. Surface integrity in cryogenic machining of nickel based alloy-Inconel 718. *Journal of Materials Processing Technology*, 211, 773–783, 2011.
- [60] Park, K. H., Yang, G. D., Suhaimi, M. A., Lee, D. Y., Kim, T.G., Kim, D., et al. The effect of cryogenic cooling and minimum quantity lubrication on end milling of titanium alloy Ti-6Al-4V. *Journal of Mechanical Science and Technology*, 29, 5121–5126, 2015.
- [61] M'Saoubi, R., Outeiro, J. C., Changeux, B., Lebrun, J. L., & Morão Dias, A.: "Residual stress analysis in orthogonal machining of standard and resulfurized AISI 316L steels". *Journal of Materials Processing Technology*, 96, 225–233, 1999.
- [62] Zhang, L. J., Wanger. T. & Bierman, D. Optimization of cutting parameters

for drilling Nickel-based alloys using statistical experimental design techniques. Hinduja, S. and Li, L. (eds.) Proceedings of the 37th International MATADOR Conference. 25-27.2012, 123–126. Manchester, England, 2013.

- [63] Rahim, E. A., & Sasahara, H. An analysis of surface integrity when drilling inconel 718 using palm oil and synthetic ester under mql condition. *Machining Science and Technology*, 15, 76–90, 2011.
- [64] Astakhov, V. P. *Tribology of Metal Cutting. Tribology of Metal Cutting* (1st ed., 52). Oxford: Elsevier. 2006.
- [65] Debnath, S., Reddy, M. M., & Yi, Q. S. Environmental friendly cutting fluids and cooling techniques in machining: a review. *Journal of Cleaner Production*, 82, 33–47, 2014.
- [66] Jawahir, I. S., Attia, H., Biermann, D., Duflou, J., Klocke, F., Meyer, D., et. al. Cryogenic manufacturing processes. *CIRP Annals - Manufacturing Technology*, 65, 713–736, 2016.
- [67] Pusavec, F., Stoic, A., & Kopac, J. The role of cryogenics in machining processes. *Tehnicka Gazeta*, 16 (4), 3–9, 2009.
- [68] Hong, S.Y.: "Lubrication mechanisms of Ln<sub>2</sub> in ecological cryogenic machining. *Machining Science and Technology*, 10, 133–155, 2006.
- [69] Aramcharoen, A., & Chuan, S. K. An experimental investigation on cryogenic milling of inconel 718 and its sustainability assessment. *Procedia CIRP*, 14, 529–534, 2014.
- [70] Fernandez, D., Garcia Navas, V., Sanda, A., & Bengoetxea, I. Comparison of machining inconel 718 with conventional and sustainable coolant. *MM Science Journal*, 04, 506–510, 2014.
- [71] Kistler 4-Component Dynamometer. (n.d.). Retrieved July 11, 2017, from <https://www.kistler.com/?type=669&fid=60755>.

- [72] Kistler Multichannel Charge Amplifier 5070A. (n.d.). Retrieved July 11, 2017, from <https://www.kistler.com/?type=669&fid=55772>.
- [73] Elimko, E-PR-110 series data logger. (n.d.). Retrieved July 11, 2017, from [http://www.elimko.com.tr/files/E\\_PR\\_110\\_TR.pdf](http://www.elimko.com.tr/files/E_PR_110_TR.pdf).
- [74] Gapinski, B., & Rucki, M. The roundness deviation measurement with CMM. IEEE Workshop on Advanced Methods for Uncertainty Estimation Measurement (AMUEM), 26, 108–111, 2008.
- [75] Sui, W., & Zhang, D. Four Methods for Roundness Evaluation. *Physics Procedia*, 24, 2159–2164, 2012.
- [76] Dornfeld, D., & Lee, D. E. *Precision manufacturing* (1st ed.). New York: Springer. 2008.
- [77] Hong, S. Y., Ding, Y., & Jeong, W. Jeong. Friction and cutting forces in cryogenic machining of Ti-6Al-4V. *International Journal of Machine Tools and Manufacture*, 41, 2271–2285, 2001.
- [78] Kaynak, Y., Karaca, H. E., Noebe, R. D., & Jawahir, I. S. Analysis of tool-wear and cutting force components in dry, preheated, and cryogenic machining of NiTi shape memory alloys. *Procedia CIRP*, 8, 498–503, 2013.
- [79] Tian, X., Zhao, J., Zhao, J., Gong, Z., & Dong, Y. Effect of cutting speed on cutting forces and wear mechanisms in high-speed face milling of Inconel 718 with Sialon ceramic tools. *The International Journal of Advanced Manufacturing Technology*, 69, 2669–2678, 2013.
- [80] Biermann, D., & Heilmann, M. Burr Minimization Strategies in Machining Operations. *Proceedings of CIRP International Conference on Burrs*. 13–20. Berlin, 2010.
- [81] Zhou, J. M., Bushlya, V., & Stahl, J. E. An investigation of surface damage in the high speed turning of Inconel 718 with use of whisker reinforced ceramic tools. *Journal of Materials Processing Technology*, 212, 372–384, 2012.

- [82] Pu, Z., Outeiro, J. C., Batista, A. C., Dillon, O. W., Puleo, D. A., & Jawahir, I. S. Enhanced surface integrity of AZ31B Mg alloy by cryogenic machining towards improved functional performance of machined components. *International Journal of Machine Tools and Manufacture*, 56, 17–27, 2012.
- [83] Sharif, S., & Rahim, E.A. Performance of coated- and uncoated-carbide tools when drilling titanium alloy-Ti-6Al4V. *Journal of Materials Processing Technology*, 185, 72–76, 2007.
- [84] Cselle, T., & Barimani, A. Today's applications and future developments of coatings for drills and rotating cutting tools. *Surface and Coatings Technology*, 76–77, 712–718, 1995.
- 

# APPENDIX

**Appendix A:** Certificate of the workpiece material Inconel 718.



# Appendix A – Certificate of the workpiece material Inconel 718



**HUNTINGTON ALLOYS CORPORATION**  
 3200 Riverside Drive, Huntington, West Virginia 25706-1771 USA  
 Tel: +1.304.626.6100 Toll-Free in the USA: 1.800.334.4626  
 Fax: +1.304.626.5643 info@specialmetals.com

CERTIFICATE NO. N61224-00

Dated 19-APR-16

**CERTIFIED MATERIALS TEST REPORT** Page No. 1 / 5

NOTE: The recording of false, fictitious or fraudulent statements on copies of this document may be punishable as a felony under Federal statute. This report relates only to the item(s) tested and may not be reproduced except in full.

**Customer:**  
 ROLLED ALLOYS INC  
 125 W STERNS RD  
 TEMPERANCE  
 MI  
 48182-0310

**Ship To:**  
 ROLLED ALLOYS INC  
 125 W STERNS RD  
 TEMPERANCE  
 MI  
 48182-0310

<b>Sales Order Number</b>	<b>Purchase Order Number</b>	<b>Mark Order Number</b>	<b>Material Heat / Lot Identity</b>
100065377 / 1.1	0135529-TEM	0135529-TEM	HT5618EK12
			<b>UNS Number</b>
			N07718

**Material Description**

INCONEL alloy 718, VACUUM INDUCTION MELTED-ELECTROSLAG REMELTED, HOT ROLLED PLATE, DESCALED, ANNEALED, .6250, 48.0000, 240.0000-280.0000, IN 1 PC PLATE# P98590 2611 LBS

**Specifications**

SAB AMS 5596K/ ASTM B 670-07 (2013)/ GE B50TF14 S22 CL A & E - CL B & F CAPABILITY/ GE S-400 (5-18-15)/ GE S-1000 (5-29-15)/ NACE MR0175-ISO 15156-3 (2015) & NACE MR0103-2012 (ANNEALED) AS SHIPPED CONDITION ONLY / WERKSTOFF 2.4668. MARK PER ORDER.

TRACER # 19620T

HEAT # HT5618EK12  
  
 TRACER # 0478587US

**ANALYSIS**

	C %	MN %	FE %	S %	SI %	CO %	NI %	CR %	AL %
H	.03	.08	17.90	.001	.09	.13	53.66	18.41	.50
Method	C/S	XR26	XR26	C/S	DES	XR26	XR26	XR26	XR26
	TI %	CO %	MO %	TA %	B %	NB %	P %		
H	.96	.34	2.87	.004	.002	4.92	.000		

INCOLOY®, INCONEL®, MONEL®, NILO®, NIMONIC®, NI-SPAN-C®, UDIMET®, DURANICKEL®, 601GC®, 625LC®, 718SPF®, 740H®, 800HT®, 945®, and 945X® are trademarks of the Special Metals group of companies. EF595

**VARZENE METAL**  
 SAN. VE TIC. A.S.  
 Beşir Topraklar - Tuzla - İSTANBUL  
 Tel: +90 216 444 5555

**HUNTINGTON ALLOYS CORPORATION**  
 3200 Riverside Drive, Huntington, West Virginia 25705-1771 USA  
 Tel: +1.304.526.5100 Toll-Free in the USA: 1.800.334.4826  
 Fax: +1.304.526.6543 Info@specialmetals.com

CERTIFICATE NO. N61224-00

Dated 19-APR-16

**CERTIFIED MATERIALS TEST REPORT**

Page No. 2 / 5

Method XR26 XR26 XR26 OES OES XR26 OES

NB+TA  
 H 4.92  
 Method

**ANALYSIS METHOD LEGEND**

OES - Optical Emission Spectroscopy  
 C/S - Carbon/Sulfur  
 XR26 - X-Ray Fluorescence 2600

**TENSILE TEST**

**HIGH TEMP TENSILE - TRANS|LAB|MECHANICAL**

TEST TEMPER TEST TEMP F TENSILE KSI .2% YIELD KSI EFF GA LNTH IN RED OF AREA% ELONG% ORIENT

TEST TEMPER	TEST TEMP F	TENSILE KSI	.2% YIELD KSI	EFF GA	LNTH IN RED OF AREA%	ELONG%	ORIENT
AG	1200	154.5	129.7	1.000	39.4	25.4	TRANS
MG	1200	160.3	140.3	1.000	24.6	18.7	TRANS

**ROOM TEMP TENSILE - TRANS|LAB|MECHANICAL**

PIECE TEST TEMPER TENSILE KSI .2% YIELD KSI EFF GA LNTH IN RED OF AREA% ELONG% ORIENT

PIECE	TEST TEMPER	TENSILE KSI	.2% YIELD KSI	EFF GA	LNTH IN RED OF AREA%	ELONG%	ORIENT
P98590	AN	124.8	59.0	1.4	55.9	53.4	TRANS
P98590	MG	198.6	169.0	1.4	37.4	21.1	TRANS
P98590	AG	200.9	173.1	1.4	37.8	21.1	TRANS

**HARDNESS TEST**

**HARDNESS - STANDARD|LAB|MECHANICAL**

TEST TEMPER HRD SCALE VALUE 1 VALUE 2 VALUE 3 HRD AVG

TEST TEMPER	HRD SCALE	VALUE 1	VALUE 2	VALUE 3	HRD AVG
AG	HRC	42.6	42.7	42.7	42.7
AN	HRB	91.1	90.3	90.0	90.5
MG	HRC	42.9	43.5	42.6	43.0

**CREEP TEST**

**STRESS RUPTURE - TRANS|LAB|MECHANICAL**

TEST TEMPER TEMPERATURE F INITIAL STRESS PSI TEST ORIENT RUPTURE LIFE HRS ELONGATION%

TEST TEMPER	TEMPERATURE F	INITIAL STRESS PSI	TEST ORIENT	RUPTURE LIFE HRS	ELONGATION%
AG	1200	100000	TRANS	102.4	25.9

RED OF AREA%

41.4

**VARZENE METAL**  
 SAN. VS. TIC. AS.  
 ITOSH 3 Div. 86.10 Perugia Italia - 15740000  
 Telex V.D. 320400073 Tel. No. 645113

INCOLOY®, INCONEL®, MONEL®, NIOLO®, NIMONIC®, NI-SPAN-C®, UDIMET®, DURANICKEL®, 601GC®, 625LCP®, 718SPF®, 740H®, 800HT®, 945®, and 945X® are trademarks of the Special Metals group of companies EF595



**HUNTINGTON ALLOYS CORPORATION**  
 3200 Riverside Drive, Huntington, West Virginia 25708-1771 USA  
 Tel: +1.304.628.6100 Toll-Free in the USA: 1.800.334.4828  
 Fax: +1.304.628.6643 Info@specialmetals.com

CERTIFICATE NO. N61224-00

Dated 19-APR-16

**CERTIFIED MATERIALS TEST REPORT**

Page No. 3 / 5

TEST TEMPER	TEMPERATURE F	INITIAL STRESS PSI	TEST ORIENT	RUPTURE LIFE HRS	ELONGATION%
MG	1200	100000	TRANS	44.9	4.1

RED OF AREA%

2.6

**HEAT TREATMENT**

TREATMENT	FURNACE	TEMP SCALE	TEMP 1 F	TEMP 1 HOLD	HOLO 1 UNITS	CHANGE 1
ANNEAL	SPF	F	1775	1	HR	WQ

**HEAT TREATMENT|LAB|HEAT TREAT**

TEST TEMPER	TEMP 1 F	TEMP 1 HOLD	HOLO 1 UNITS	CHANGE 1	CHANGE RATE 1	CHNG UNITS 1	TEMP 2 F
AG	1325	8	hr	FC	100	hr	1150
TEMP 2 HOLD	HOLD 2 UNITS	CHANGE 2					

8 hr AC

TEST TEMPER	TEMP 1 F	TEMP 1 HOLD	HOLO 1 UNITS	CHANGE 1
MG	1750	1	hr	AC

TEST TEMPER	TEMP 1 F	TEMP 1 HOLD	HOLO 1 UNITS	CHANGE 1	CHANGE RATE 1	CHNG UNITS 1	TEMP 2 F
MG	1325	8.25	hr	FC	100	hr	1150
TEMP 2 HOLD	HOLD 2 UNITS	CHANGE 2					

8.25 hr AC

**OTHER TESTS**

**GRAIN SIZE MEASUREMENT|LAB|METALLOGRAPHY**

PIECE ID	TEST TEMPER	TEST ORIENT	AV GS ASTM	OCC GS ALA ASTM	NRM or DUP
P98590	AN	LONGITUDINAL	7	3	NORMAL

**MICROSTRUCTURE TEST|LAB|METALLOGRAPHY**

PIECE	TEST VERDICT	AREA EVAL	METHOD	E50TF133	STRUCTURE E50TF133	AGS

INCOLOY®, INCONEL®, MONEL®, NILO®, NIMONIC®, NI-SPAN-C®, UDIMET®, DURANICKEL®, 6016C®, 625LCP®, 7185PF®, 740H®, 800HT®, 945®, and 945X® are trademarks of the Special Metals group of companies

EF595

**VAZENE METAL**  
 10000 W. 13th St. S.  
 Tukwila, WA 98148  
 Tel: 206.835.4400  
 Fax: 206.835.4401  
 Email: info@vazene.com

**HUNTINGTON ALLOYS CORPORATION**  
 3200 Riverside Drive, Huntington, West Virginia 25705-1771 USA  
 Tel: +1.304.526.6100 Toll-Free in the USA: 1.800.334.4626  
 Fax: +1.304.526.6643 info@specialmetals.com

CERTIFICATE NO. N61224-00

Dated 19-APR-16

**CERTIFIED MATERIALS TEST REPORT**

Page No. 4 / 5

P98590	P	X SECTION	GE-E50TF133	NON-UNIFORM	6
E50TF133 ALA	E50TF133 PCT FINE GRAIN	E50TF133 AGS COARSE	E50TF133 AGS FINE	MAGNIFICATION	
3	30	6	9	100X	

SNC-NA WAS THE TESTING FACILITY

NO WELDING OR WELD REPAIR WAS PERFORMED.

PLATE DIMS: .625 X 48.000 X 280.000

LOCATION LEGEND: B = BACK C = CENTER F = FRONT H = HEAD M = MIDDLE T = TOE

TEST VERDICT LEGEND: P = PASS W = WAIVER

TEST TEMPER LEGEND

AG - Annealed + age hardened

AN - Annealed

MG - Mill solution anneal+ lab solution anneal + aged

ALL TEST RESULTS ARE REPORTED TO AT LEAST THE REQUIRED PRECISION BY THE ROUNDING METHOD OF ASTM E 29

UNLESS OTHERWISE REQUIRED BY PURCHASE ORDER OR SPECIFICATION.

COUNTRY OF ORIGIN: MELTED AND MANUFACTURED IN THE USA. DFARS PART 252.225.7014 AND 252.225.7008 COMPLIANT.

THIS CERTIFICATION AFFIRMS THAT THE CONTENTS OF THIS REPORT ARE CORRECT AND ACCURATE AND THAT ALL TEST RESULTS AND OPERATIONS PERFORMED BY SPECIAL METALS CORPORATION, INC. OR ITS SUBCONTRACTORS ARE IN COMPLIANCE WITH THE MATERIAL SPECIFICATIONS.

QUALITY SYSTEM MEETS REQUIREMENTS OF DIRECTIVE 97-23/EC (PRESSURE EQUIPMENT DIRECTIVE),

ANNEX 1, CHAPTER 4.3 PER ABS GROUP LTD CERTIFICATE 41734 (EXPIRES JULY 28, 2017).

HUNTINGTON ALLOYS CORPORATION IS AN ACCREDITED INDEPENDENT NADCAP MATERIALS TESTING LABORATORY VIA CERTIFICATE NUMBER 3200165734 (EXPIRES APRIL 30, 2018) FOR ALL TESTING SPECIFIED IN THE SCOPE OF ACCREDITATION.

MATERIAL PRODUCED UNDER QA SYSTEM DOCUMENTED IN HUNTINGTON ALLOYS CORE QA MANUAL REV. 51, DATED 10/17/2014

QA MANUAL NOT TO IMPLY COMPLIANCE TO ASME SECTION III. COMPLIANCE MUST BE OTHERWISE STATED ON CMTR.

QUALITY SYSTEM CERTIFICATION: ISO 9001:2008 (ABS-QE CERT. 30125); EN 10 204/DIN 50049 (TYPE 3.1)

LABORATORY IS ACCREDITED TO ISO/IEC 17025:2005 FOR MECHANICAL TESTING AND CHEMICAL ANALYSIS.

VISUAL AND DIMENSIONAL EXAMINATION SATISFACTORY.

MATERIAL, WHEN SHIPPED, IS FREE FROM CONTAMINATION BY MERCURY, RADIUM, ALPHA SOURCE, AND LOW MELTING ELEMENTS.

INCOLOY®, INCONEL®, MONEL®, NIOLO®, NIMONIC®, NI-SPAN-C®, UDIMET®, DURANICKEL®, 601GC®, 625LCP®, 718SPF®, 740H®, 800HT®, 945®, and 945X® are trademarks of the Special Metals group of companies EF535

**SPECIAL METALS**  
 17039 S. L. ...  
 Train P.O. : 9240467377  
 Tel: 304.526.6100 Fax: 304.526.6643

HUNTINGTON ALLOYS CORPORATION  
3200 Riverside Drive, Huntington, West Virginia 25705-1771 USA  
Tel: +1.304.528.8100 Toll-Free in the USA: 1.800.334.4628  
Fax: +1.304.528.8643 Info@specialmetals.com

CERTIFICATE NO. N61224-00

Dated 19-APR-16

CERTIFIED MATERIALS TEST REPORT

Page No. 5 / 5

CHEMICAL ANALYSIS AS REQUIRED FOR CARBON, SULFUR, NITROGEN, OR OXYGEN IS PERFORMED BY COMBUSTION TECHNIQUES.  
ALL OTHER REPORTED ELEMENTS ARE ANALYZED BY X-RAY AND/OR EMISSION SPECTROSCOPY."

AUTHORIZED QUALITY CERTIFICATION REPRESENTATIVES:

W.F. SOLEN, D.K. MILLER, K.R. SMITH, V.A. POWELL, S.E. LEHR, K.BORSODI, ROBERT D. DILLE, ROBERT SMITHSON

CERTIFIED TESTING LABORATORY DATA SOURCE IS: AARG VENDOR NO. 47150 M. R. B. CASE RECORD NO. : NONE

AUTHORIZED VENDOR SIGNATURE [Signature] DATE 4-19-16

RECEIVED  
METALS  
LABORATORY

Receiving Inspection  
By: [Signature]  
Date: 4-27-16

End Of Certificate

This is to certify that all required sampling inspections and tests have been performed in accordance with the order and specification requirements. The test report represents the actual attributes of the material furnished and the values shown are correct and true. The material described by this certificate is in full compliance with all order and inspection requirements. We hereby certify that the figures given are in accordance with the specified contract requirements.

Signed  
[Signature]  
For and on behalf of HUNTINGTON ALLOYS CORPORATION  
Authorized Signature

INCOLOY®, INCONEL®, MONEL®, NILO®, NIMONIC®, NI-SPAN-C®, UDIMET®, DURANICKEL®, 601GC®, 625LC®, 7185PF®, 740H®, 800HT®, 945®, and 945X® are trademarks of the Special Metals group of companies

SPECIAL METALS  
S.A.S. - S.p.A.  
TTC: A.S.  
Tosco S.p.A. - Toschem - Tosin - ISTRASER  
Tosco S.p.A. - Toschem - Tosin - ISTRASER  
Tosco S.p.A. - Toschem - Tosin - ISTRASER

## CURRICULUM VITAE

### PERSONAL INFORMATION

**Name Surname** : Necati UÇAK  
**Date of Birth** : 08.01.1990  
**E-mail** : nucak@ybu.edu.tr



### EDUCATION

**High School** : Mustafa Kemal High School / ANKARA (2003-2008)  
(4.35 / 5)  
**Bachelor** : Süleyman Demirel University / ISPARTA (2008-2012)  
(3.46 / 4)  
**Master Degree** : Ankara Yıldırım Beyazıt University / (2014-continued)

### WORK EXPERIENCE

**R & D Engineer** : Ermaksan Dişli Co. (2012 - 2014)  
**Research Assistant** : Ankara Yıldırım Beyazıt University / (2014 - continued)

### PUBLICATIONS

1) Çetin, A., Çakır, G., **Uçak, N.**, Çiçek, A., Performance evaluation of cryogenically treated Cu-Cr-Zr alloy electrodes in electro discharge machining of AISI P20 tool steel. 3rd International Symposium on Innovative Technologies in Engineering and Science (ISITES), 3-5 June 2015, Valencia, Spain.

2) Usta, T., Çiçek, A., **Uçak, N.**, Çelik, V., Ağca, S., Performance Evaluation of S700MC and ST52 Steels in Terms of Mechanical Properties and Fatigue Life. 25th International Conference on Metallurgy and Materials (Metal 2016), 25-27 May 2016, Brno, Czech Republic.

3) A. Çetin, G. Çakır, K. Aslantaş, **N. Uçak**, A. Çiçek. Performance of cryo-treated Cu and CuCrZr electrodes in an EDM process. Kovove Materialy - Metallic Materials, Accepted for Publication, 2017.

### TOPICS OF INTEREST

- Manufacturing, Machinability, Material Science, CAD, CAM.